EFFECTS OF UTERINE DISEASE ON THE OVARY OF DAIRY COWS

By

RACHEL LIMA FRANÇA PIERSANTI

A DISSERTATION PRESENTED TO THE GRADUATE SCHOOL
OF THE UNIVERSITY OF FLORIDA IN PARTIAL FULFILLMENT
OF THE REQUIREMENTS FOR THE DEGREE OF
DOCTOR OF PHILOSOPHY

UNIVERSITY OF FLORIDA

2018

To my parents, Lea Lima Piersanti and Alexandre França Piersanti.

ACKNOWLEDGMENTS

I first have to thank my family who have always been my biggest supporters and without them I would not have been able to conclude my PhD. My parents who do everything for me, even more than I dream. I am lucky to be part of a family that supports me, cheer for me and go beyond their ways to make me happy. My sister, my grandparents, uncles and aunts are also an important part of this achievement, each of them play a role in keeping me focused and made sure I would be able to finish this PhD. I want to specially thank my uncle Vladmir for more than once being a great mentor during my graduate life.

During the past 5 years I also started a family and I will never be able to thank my husband Thiago enough for everything he has done for me. He not only has been extremely helpful during trials and analysis, but has also been by my side for the good and the bad times. I am happy to share my life with him and with our son Oliver.

I would also like to thank my advisor, Dr Bromfield for accepting me into his lab when I had no skills to offer and was about to quit my PhD. I appreciate his patience and dedication in taking the time to teach and guide me through all these years and consider myself extremely lucky to be a part of the "Republica de Bromfield". I hope I can be as dedicated and enthusiastic about science as he is and always keep the respect and friendship towards the students.

I appreciate the dedication and patience from all my committee members during the past 5 years, all the discussions, inputs and care made me a better scientist and a better person. I would kile to specially thank Dr Hansen for guiding me during difficult times, when he wasn't even part of my committee or anything. Without his help I wouldn't have joined Bromfield's lab and wouldn't finish this PhD.

I am lucky that I made amazing friends along the way, friends that became my support system and part of my family. I would like to thank Francine, Darren, Marta, Veronica, Sossi,

Fernanda, Eduardo, Tania, Mackenzie, Paula, Laila and Jason. Old friends and new friends who have been part of this journey.

I have been around the Department of Animal Sciences for a long time and I would like to thank everyone that works there. Everyone has always been extremely nice to me and help me throughout the years.

TABLE OF CONTENTS

page

LIST OF TABLES

LIST OF FIGURES

LIST OF ABBREVIATIONS

AI	Artificial insemination
BMP15	Bone morphogenic protein 15
COC	Cumulus oocyte complex
ESC	Embryonic stem cells
GDF9	Growth differentiation factor 9
HK	Housekeeper
IFC	Integrated fluidic circuit
IL	Interleukin
IVF	In vitro fertilization
IVM	In vitro maturation
LB	Luria Bertani
LPS	Lipopolysaccharide
NFκB	Nuclear factor kappa-light-chain-enhancer of activated B cells
PAMP	Pathogen associated molecular pattern
PCR	Polymerase chain reaction
PG	Prostaglandins
PGE_2	Prostaglandin E2
$PGF_{2\alpha}$	Prostaglandin F2α
PLO	Pyolysin
PMNs	Polymorphonuclear neutrophils
PRR	Pattern recognition receptors
TLRs	Toll-like receptors
TNFα	Tumor necrosis factor alpha
TZP	Transzonal projections

Abstract of Dissertation Presented to the Graduate School
of the University of Florida in Partial Fulfillment of the
Requirements for the Degree of Doctor of Philosophy

EFFECTS OF UTERINE DISEASE ON THE OVARY OF DAIRY COWS

By

Rachel Lima França Piersanti

December 2018

Chair: John J. Bromfield
Major: Animal Sciences

Uterine disease affects 20 to 40% of postpartum dairy cows and cost the US dairy industry near $900 million annually. In part, this cost is associated with a decline in cow fertility after the resolution of uterine disease. Cows that develop uterine disease display reduced follicle growth and decreased estradiol synthesis; in parallel the Gram-negative bacterial cell wall component, lipopolysaccharide (LPS), accumulates within the follicular fluid of the dominant follicle. Exposure of oocytes to LPS in culture increases meiotic failure during *in vitro* maturation (IVM) and causes a subsequent reduction in embryo development. The changes to ovarian function described above occur during active uterine infection; it is unclear if enduring changes to the follicular environment at the time of breeding persist from uterine disease in the early postpartum period. If persistent changes to the follicular environment occur as a result of uterine infection, this may in part explain the reduced pregnancy rates observed in dairy cows after resolution of disease. To better understand the mechanisms of uterine disease associated subfertility in dairy cows we performed three experiments: 1) to assess the follicular environment at the time of breeding in cows that had resolved metritis; 2) determine the effect of LPS or tumor necrosis factor alpha (TNFalpha) exposure on cumulus-oocyte complex (COC) gene transcription; and 3) to develop a model of induced uterine disease in virgin Holstein

heifers in an attempt to better understand the mechanisms of infection induced subfertility in the absence of confounding effects (lactation, disease) observed in postpartum cows.

Combined, the studies described here demonstrate the enduring impact of uterine infection on the follicular environment well after the clearance of infection, in both induced and spontaneous uterine infection. In addition, our *in vitro* analysis of oocyte gene expression following exposure to bacterial LPS, suggest possible molecular mechanisms by which uterine infection reduces fertility in the high producing dairy cow.

CHAPTER 1
LITERATURE REVIEW

Introduction

Postpartum bacterial contamination of the uterus occurs in nearly all dairy cows. While the majority of the cows are able to control this contamination without developing uterine disease, it is estimated that 20 to 40% go on to develop uterine disease (Sheldon et al., 2006). Risk factors for the development of postpartum uterine disease include retained fetal membranes, stillbirth, dystocia and twin birth (Potter et al., 2010). These risk factors suggest an association between tissue damage and establishment of a pathogenic bacterial infection after parturition (Potter et al., 2010).

Numerous bacterial species are associated with the development of postpartum uterine disease, the most commonly isolated species include *Escherichia coli, Trueperella pyogenes* and anaerobic species such as *Fusobacterium necrophorum* (Bonnett et al., 1991). *E. coli* infects the uterus within the first week after parturition and it is highly associated with the development of uterine disease. *T. pyogenes* is noted to cause greater tissue damage and it is correlated to severity of disease (Bonnett et al., 1991; Williams et al., 2007).

The economic cost associated with uterine disease is a consequence of reduced milk production, disease treatment, reduced fertility, and premature culling. Combined, these factors contribute to the $358 cost for each diagnosed case of uterine disease in the dairy cow (Overton and Fetrow, 2008). According to the USDA, there were 9.4 million cows in the U.S. dairy herd in January 2018, applying a conservative 25% incidence of uterine disease, the annual cost to the US dairy industry is over $841 million.

In order to maintain productivity and profitability, dairy cows need to become pregnant during an optimal interval after calving. The largest cost associated with uterine disease arises

from the decrease in fertility and the culling of cows due to their inability to become pregnant. The impact of uterine disease on reproductive performance of the dairy cow has been extensively reported (Dubuc et al., 2010; Ribeiro et al., 2013; Ribeiro et al., 2016). In brief, cows with endometritis (clinical or subclinical) have an increased latency between calving and pregnancy compared to healthy cows (Dubuc et al., 2010), while metritis reduces pregnancy per service at day 45, reduces calving rates and increases pregnancy loss (Ribeiro et al., 2016). Uterine disease also affects ovarian function by disrupting the estrous cycle and prolonging the luteal phase (Opsomer et al., 2000), slowing the growth of the dominant follicle, and reducing estradiol secretion during the first two weeks postpartum (Sheldon et al., 2002). It is important to emphasize that uterine disease occurs during the early postpartum period and is generally resolved before the first attempt to inseminate cows. Here we will discuss the potential mechanisms by which uterine disease affects the reproductive tract of dairy cows, focusing on the consequences to fertility, the ovary and female germline.

Uterine Infection

Uterine Disease Development and Classification

The transition from late pregnancy to early lactation presents new metabolic and immune challenges for the dairy cow. Periparturient metabolic disorders are important risk factors for the development of metritis, endometritis and subclinical endometritis (Kim and Kang, 2003; Lima et al., 2014). Feed intake fails to meet the increasing energy demand associated with lactation, and the cow faces a period of negative energy balance (Roche et al., 2009). The nutrient shortage encountered during this period is associated with the development of postpartum clinical pathologies, including retained fetal membranes and hypocalcemia, which have been correlated to the development of postpartum uterine disease (Potter et al., 2010; Martinez et al., 2012).

Postpartum uterine diseases are classified by the severity and persistence of uterine inflammation. Metritis is classified as inflammation of the uterine wall during the first 21 days after parturition, and is clinically diagnosed by an enlarged uterus and the presence of a fetid red-brown watery vaginal discharge. The presence of additional systemic signs of illness including fever, dullness and reduced milk yield, are used to grade the intensity of metritis (Sheldon et al., 2009). The main identified risk factors associated with the development of metritis are retained fetal membranes, dystocia, stillbirth and twin birth (Potter et al., 2010). Antimicrobial treatment can be used to attenuate the clinical signs of metritis but show no improvement of subsequent fertility (Galvão et al., 2009). On average, 36% of cows with metritis will self-cure in the first 14 days after calving (Haimerl and Heuwieser, 2014).

Endometritis is defined as inflammation of the endometrial layer of the uterus occurring 21 days after calving and is clinically diagnosed by a mucopurulent discharge in the vagina with no systemic signs of illness. A diagnosis for endometritis can be obtained by evaluation of the uterine discharge in the vagina. Evaluation of uterine cytology to analyze the concentration of polymorphonuclear neutrophils (PMNs) in the uterine lumen, and transrectal ultrasonography to visualize the presence of fluid in the uterus are useful tools to eliminate the possibility of diagnosing cervicitis or vaginitis (Sheldon et al., 2006; Gilbert, 2016). Vaginal mucus content can be further evaluated to categorize clinical endometritis as grade 1, mucus containing flecks of white or off-white pus; grade 2, discharge containing ≤ 50% white or off-white mucopurulent material; or grade 3, discharge containing > 50% purulent material (Figure 1-1) (Sheldon et al., 2009).

Subclinical endometritis is the inflammation of the endometrial tissue with no purulent discharge and no clinical signs of disease. Subclinical endometritis is identified using cytology to

evaluate an increased concentration of PMN within the uterus between 21 and 47 days postpartum (Sheldon et al., 2006). There is debate regarding the parameters for diagnosis of subclinical endometritis, specifically defining days postpartum at diagnosis and number of PMN present in the uterus. Subclinical endometritis has been defined as the presence of PMNs exceeding 10% of cells collected from uterine lumen between 34 and 47 days postpartum (Sheldon et al., 2009), while others define subclinical endometritis using a stricter PMN cutoff of 5% of cells collected between 40 and 60 days postpartum (Gilbert et al., 2005). The treatment of subclinical endometritis can prove difficult due to inadequate on-farm diagnosis as cows present no systemic signs of disease (Sheldon et al., 2006).

Pathogens Associated with Uterine Disease

During the postpartum period the cow must undergo uterine involution, recover from endometrial tissue damage, and resume ovarian cyclicity in order to conceive again. In addition, the cow must eliminate microbial contamination of the uterine lumen that occurs around the time of calving (Sheldon et al., 2006). While the majority of cows undergo these processes efficiently during the postpartum period, many succumb to infection of the uterus with pathogenic bacteria. Culture-based methods have been used for decades to identify the bacteria associated with the development of uterine disease, and the most prevalent pathogenic bacteria as *E. coli, T. pyogenes*, *Prevotella sp.*, *Fusobacterium necrophorum*, and *Fusobacterium nucleatum* (Sheldon et al., 2002; Williams et al., 2005). The use of new sequencing techniques has facilitated the identification of bacteria that cannot be cultured and can help advance our knowledge of the uterine microbiome. Clone library sequencing, for example, allows the sequencing of large regions of the bacterial 16S rRNA but with low sequence depth, whereas metagenomics sequencing and pyrosequencing can provide better sequencing coverage but with low specificity at the species level. Sequence-based studies have been able to show that the bacterial population

in the uterus changes shortly after parturition, and that some bacterial genera and species are correlated with good uterine health, while others are related with the development of uterine infections (Santos and Bicalho, 2012). Also, during the first week after parturition, bacterial species richness is reduced in the uterus of cows that develop uterine infection in comparison with cows that remain healthy (Jeon et al., 2015). Sequencing techniques are reporting conflicting results regarding the bacterial species associated with the development of uterine disease compared to those previously reported by cultured-based studies (Santos and Bicalho, 2012; Jeon et al., 2015). Due to the microbiome diversity and the ability of sequencing studies to detect a higher number of bacteria, the identification of previously unknown correlations between bacterial genus and disease are possible, that might explain the conflicting results mentioned above. A discussion about how to best identify the pathogens associated with uterine disease is ongoing. However, it is important to emphasize that associations between pathogens and uterine disease made by sequencing technology are at the phylum and genus level, and are mostly not species or strain specific. The identification of the uterine pathogenic bacterial species including their strains and virulence factors is an important tool for better understanding the development of uterine disease. Different strains of the same species of bacteria can have opposing associations with the development of uterine disease, and can differ in disease severity and consequences to reproductive performance (Sheldon et al., 2010; Bicalho et al., 2016). In the study from Jeon et al.,2015, the genera *Escherichia* was associated with uterine health. Genotyping of *E. coli* isolates demonstrated that different clonal groups from unaffected animals clustered together and that the same is true for the uterine pathogenic *E. coli,* reiterating the importance of specific factors for bacteria pathogenicity (Sheldon et al., 2010). Pathogenic bacteria carry various molecules that aid in their goal of replicating and disseminating

throughout the host, and avoiding host defense mechanisms. These molecules, including virulence factors and toxins, can significantly impact the pathogenicity of bacteria, consequently influencing disease establishment, severity and duration.

Escherichia coli

Escherichia coli are Gram-negative bacteria characterized by two phospholipid membrane layers containing the endotoxin, LPS in the outer membrane. When LPS is released from the bacterial membrane it is recognized by the host innate immune system to initiate an inflammatory response (Raetz, 1990). *E. coli* are widely distributed in the environment and different pathogenic strains can cause a variety of intestinal and non-intestinal diseases. *E. coli* is present in the uterus of animals that develop uterine infection in the first days after calving and their abundance decreases later in the postpartum period (Williams et al., 2007). When *E. coli* is present in the uterus during the first week (days 1 to 7) following parturition, cows have an increased incidence of metritis (Kassé et al., 2016). Also, when *E. coli* is identified in the uterus at day 10 ± 1 postpartum, cows present a higher chance of developing uterine disease (Werner et al., 2012). However, when *E. coli* is present in the uterus at day 10 postpartum, there is no influence on the development of subclinical endometritis (Sens and Heuwieser, 2013). Metagenomics sequencing demonstrates the genera *Escherichia* to be in higher abundance in the uterus of healthy cows compared to cows with metritis during the first week after calving (Jeon et al., 2015). Pyrosequencing of *E. coli* isolated from the uterus of postpartum cows describe unique *E. coli* strains isolated from cows with uterine disease compared to the uterine *E. coli* of healthy cows, or *E. coli* isolated from environmental or intestinal locations (Sheldon et al., 2010; Goldstone et al., 2014b). This finding demonstrates that specific endometrial pathogenic *E. coli* (EnPEC) may be more important than simple abundance of *E. coli* for the establishment of uterine disease.

Exposure of endometrial cells to the LPS from EnPEC induces a greater expression of inflammatory mediators (prostaglandin E2 and interleukin (IL)-8) than LPS derived from non-pathogenic endometrial *E. coli* isolated from the uterus of healthy cows (Sheldon et al., 2010). Endometrial pathogenic *E. coli* strains also express the virulence factor encoding ferric yersiniabactin uptake receptor (*fyuA*), but lack the common virulence factors associated with fecal and environmental *E. coli* (Sheldon et al., 2010). The virulence factor *fyuA* is involved in the uptake of iron by bacteria and is reported to influence the formation of biofilm during the establishment of bacterial urinary infection in humans (Hancock et al., 2008). The presence of uterine *E. coli* carrying the *fimH* virulence factor is associated with a 4-times greater odds of uterine infection, compared to the presence of uterine *fimH* negative *E. coli* (Bicalho et al., 2012). The virulence factor *fimH* is a mannose binding protein that has a role in bacterial adhesion to host cells (Schembri et al., 2001). Cows carrying uterine *fimH* positive *E.coli* 1 to 3 days after calving, are 2.1-times less likely to become pregnant than *fimH* negative cows (Bicalho et al., 2012).

Strains of *E. coli* are resistant to a large number of antimicrobials, but only a small number of isolates are resistant to treatment with ceftiofur (Santos et al., 2010b). The use of ceftiofur improves the cure rates of cows with metritis, measured by fever and discharge reduction (Drillich et al., 2001), but antimicrobial treatment does not improve the subsequent reproductive performance of the cow (Haimerl and Heuwieser, 2014).

Trueperella pyogenes

Trueperella pyogenes was previously classified as *Arcanobacterium pyogenes.* This Gram-positive bacteria species is an opportunistic pathogen and can be found in the mammary gland, gastrointestinal, and respiratory tracts of livestock animals. The main virulence factor of *T. pyogenes* is pyolysin (PLO), a cholesterol-depended cytolysin that binds to cholesterol to form

pores in the host cell membrane, causing cell lysis and death (Jost and Billington, 2005). The presence of *T. pyogenes* during uterine disease has been associated with increased uterine lesions and disease severity (Bonnett et al., 1991). Endometrial stromal cells have a higher cholesterol content and therefore are more sensitive to PLO damage compared to endometrial epithelial cells (Amos et al., 2014). This finding corroborates the idea that *T. pyogenes* takes advantage of the tissue damage caused to the endometrial epithelial layer during parturition in order to establish uterine infection and also, why *T. pyogenes* is associated with a more severe disease presentation (Amos et al., 2014). *T. pyogenes* encoding the virulence factors *plo* and *fimA* have been associated with metritis development when detected from days 1 to 3 after parturition (Kassé et al., 2016), while isolation between days 8 to 10 and 34 to 36 after parturition are associated with the development of endometritis (Bicalho et al., 2012). The isolation of *T. pyogenes* from the uterus at 10 ± 1 DIM is associated with an increase in the number of days to pregnancy, while detection at 24 ± 1 DIM is associated with an increased number of days to the first artificial insemination (AI) (Werner et al., 2012). Uterine disease mediated by *T. pyogenes* has been associated to negative effects on fertility (Williams et al., 2005). Cows positive for *T. pyogenes* in the uterus have a longer interval from calving to conception (Bicalho et al., 2016). Antimicrobial treatment is inefficient against a large number of *T. pyogenes* strains isolated from cows with postpartum uterine infection (Santos et al., 2010a), and alternative treatments using bacteriophage do not improve uterine health or fertility in these animals (Machado et al., 2012a).

Fusobacterium sp.

Fusobacterium is a genus of obligatory anaerobic Gram-negative bacteria that are known be present in the oral cavity, gut and vagina of animals and humans, and acts as an opportunistic pathogen (Bennett and Eley, 1993). Virulence factors for *Fusobacterium* include the endotoxins,

LPS and leukotoxin. Leukotoxin is a cytotoxic protein that protects the bacteria from phagocytosis by neutrophils and macrophages, and induces host cell death (Nagaraja et al., 2005). *Fusobacterium necrophorum* has been reported to be present in the uterus of cows with uterine disease and is correlated with the presence of *T. pyogenes* (Bonnett et al., 1991). In agreement with earlier reports, sequencing studies have shown anaerobic bacteria to be abundant in the uterus of cows with uterine disease (Machado et al., 2012b; Santos and Bicalho, 2012). The presence of the genus *Fusobacterium* has been associated with metritis and increasing severity of vaginal mucus scores in cows during the first week following parturition (Jeon et al., 2015). Cows with endometritis have a higher abundance of *Fusobacterium* compared with healthy cows (Machado et al., 2012b). While a decrease in reproductive performance is not associated to the presence of *Fusobacterium* in the uterus (Bicalho et al., 2012), cows with higher relative abundance of intrauterine *Fusobacterium* present a reduction in reproductive performance (Machado et al., 2012b).

Endometrial Response to Bacterial Contamination

During microbial infection, an inflammatory response is initiated when pathogen associated molecular patterns (PAMPs) bind to specific pattern recognition receptors (PRR) on host cells. These receptors are classically expressed by hematopoietic immune cells in addition to non-immune cells of the endometrium (Davies et al., 2008). Of the PPRs, the Toll-like receptor (TLR) family is comprised of 10 cellular receptors that have distinct affinity for specific PAMPs. The *Toll* gene was first identified as essential for embryonic development of *Drosophila melanogaster*, and later shown to play a role in the immune response against fungal infections (Lemaitre et al., 1996).

When the bovine uterus is contaminated with bacteria, PAMPs are recognized by specific TLRs expressed by endometrial cells that initiate an innate immune response. *In vitro* studies

have successfully demonstrated that bovine endometrial epithelial and stromal cells increase expression of proinflammatory cytokines after exposure to bacterial PAMPs, and that this response is mediated by TLRs (Herath et al., 2009; Turner et al., 2014). The TLR response by endometrial cells acts through intracellular mitogen-activated protein kinase (MAPK) and nuclear factor-kappaB (NFκB) signaling (Turner et al., 2014). As part of the innate inflammatory response to bacterial PAMPs, cultured endometrial cells secrete the cytokines interleukin (IL)-6 and IL-8 (Cronin et al., 2012; Turner et al., 2014). The role of IL-8 in inflammation is to attract neutrophils from the peripheral circulation to the site of infection and enhance their ability to kill pathogens (Kobayashi and DeLeo, 2009). Neutrophils secret more pro-inflammatory cytokines, further activating the immune response in the endometrium (Herath et al., 2006). During acute inflammation IL-6 helps control neutrophil accumulation at the site of infection to prevent excessive tissue damage by recruitment of mononuclear cells, guiding the immune response away from neutrophils (Scheller et al., 2011). Additionally, IL-6 stimulates hepatocytes to secrete acute phase proteins that act to destroy and inhibit pathogen growth, modulating the inflammatory response and also aiding in the reestablishment of tissue homeostasis (Heinrich et al., 1990; Baumann and Gauldie, 1994). The concentration of acute phase proteins in cow blood increases in response to the degree of uterine bacterial contamination (Sheldon et al., 2001).

The expression of IL-1β by endometrial stromal cells increases after *in vitro* stimulation with LPS (Cronin et al., 2012). IL-1β is a pro-inflammatory cytokine, secreted in response to TLR signaling through NFκB activation (Akira et al., 2006). IL-1β is initially translated as pro-IL1β, which has no biological activity. Pro-IL1β requires cleavage by caspase-1 to become the active form of IL-1β and elicit biological activity (Akira et al., 2006; Akdis et al., 2016). The

concentration of IL-1β increased in the supernatant of endometrial tissue cultured in the presence of PAMPs (Amos et al., 2014).

Another cytokine secreted in response to TLR signaling is TNFα. TNFα is involved in the initiation of inflammation and also has an additional role limiting the duration of the inflammatory response (Akdis et al., 2016). *In vitro*, endometrial epithelial and stromal cells increase mRNA expression of *TNF* in response to LPS, but TNFα is not detected in culture supernatants (Herath et al., 2006; Cronin et al., 2012). The lack of detection of TNFα in the culture supernatants can be explained by the fact that TNFα is a potent molecule and only a small amount might be necessary to activate its pathways, and the concentration may be under the assay's limit of detection. However, TNFα is detected in peripheral plasma and demonstrated to be increased in cows with uterine disease (Williams et al., 2007).

Prostaglandins (PG) are also secreted during the endometrial inflammatory response to pathogens. Prostaglandins are involved in the establishment of acute inflammation, by facilitating edema and pain, in addition to regulating the immune response to pathogens (Ricciotti and FitzGerald, 2011). Prostaglandins also regulate ovarian function; prostaglandin E_2 (PGE_2) is luteotropic and prostaglandin F2α ($PGF_{2\alpha}$) is luteolytic, and their secretion is modulated by oxytocin binding to its receptor in the endometrium (Asselin et al., 1997). Endometrial cells alter the secretion of PG in response to LPS or *E.coli* (Herath et al., 2006), increasing the secretion of PGE_2 and reducing secretion of $PGF_{2\alpha}$. This profile of PG secretion may explain why some cows with uterine disease have a prolonged luteal phase (Williams et al., 2007).

Effects of Postpartum Uterine Disease on Neuroendocrine Function

Cows with postpartum uterine disease have increased concentration of LPS in blood (Peter et al., 1989; Mateus et al., 2003). The exposure of different organs and tissues to bacterial

LPS can trigger immune responses no longer restricted to the uterus. Intravenous, intrauterine or intramammary infusion of LPS has been used to model the impacts of bacterial infection on the neuroendocrine system in species such as cattle and sheep (Battaglia et al., 1999; Suzuki et al., 2001; Deori et al., 2004; Lavon et al., 2008; Williams et al., 2008; Moraes et al., 2017). Alterations caused by bacterial infection to the neuroendocrine system can possibly impact hormone secretion, control of estrous cycle and ultimately reduce fertility. Intravenous infusion of LPS in cattle reduces circulating estradiol and alters luteinizing hormone (LH) pulse frequency (Suzuki et al., 2001; Lavon et al., 2008). Intravenous infusion of LPS in ewes blocked the preovulatory surge of LH (Battaglia et al., 1999), while the intravenous or intramammary infusion of LPS in cows suppressed LH surge and resulted in delayed ovulation (Lavon et al., 2010). The response of the brain to the LPS can also be mediated by inflammation. Cytokines involved in the innate immune response to LPS, such as IL-1β, also have physiological roles as modulators of the central nervous system. Intracerebroventricular injection of IL-1β in ewes causes a decrease in *GNRH1* gene expression in the pre-optic area and decreased anterior pituitary *GNRHR*, resulting in reduced cerebrospinal fluid gonadotropin-releasing hormone (GnRH) concentration (Herman et al., 2012). This results exemplify the complex cooperation between cytokines and the neuroendocrine system, and how the immune response to bacterial components can have consequences to the neuroendocrine signaling.

Impact of Uterine Disease on Reproductive Performance

The negative effects of uterine disease on reproductive performance are well established. Reproductive efficiency in dairy cows is often evaluated by markers such as calving to conception interval, pregnancy per AI, pregnancy rates, calving rates and incidence of pregnancy loss. A meta-analysis revealed that cows with metritis have higher calving to conception interval and reduced conception rates by 20%, compared to healthy cows (Fourichon et al., 2000).

Occurrence of retained fetal membranes and/or metritis within the first 10 days after calving results in a decrease in pregnancy at day 45, reduced calving rates and increased pregnancy loss (Ribeiro et al., 2016). Clinical endometritis diagnosed by purulent vaginal discharge is associated with reduced pregnancy rates (LeBlanc et al., 2002). Differences in diagnostic techniques can alter the degree of reproductive impairment reported by individual studies, but the primary outcome is a decline in fertility. Cytological evaluation of endometritis prevalence demonstrated a variation of 37 to 74% in disease incidence among 5 different farms; however cows with endometritis had a consistent reduction in pregnancy rates, an increase in the number of days open and fewer cows pregnant at the first AI (Gilbert et al., 2005). Subclinical endometritis also reduces pregnancy per AI at days 30 and 65 after insemination (Ribeiro et al., 2013). The presence of specific bacteria in the uterus has also been correlated to decreased reproductive performance, as is the case for cows positive for *T. pyogenes* or anaerobic bacteria (Bonnett et al., 1993).

Treatment of uterine disease with antimicrobial drugs such as ceftiofur does not improve pregnancy per AI at days 38 and 180 after insemination, and also does not reduce pregnancy loss at days 38 and 180 after AI (Galvão et al., 2009). Similarly treatments with 1 or 2 doses of $PGF_{2\alpha}$ in an attempt to reduce the prevalence of subclinical endometritis; administration of $PGF_{2\alpha}$ does not improve pregnancy per AI or reduce pregnancy loss (Lima et al., 2013).

Ovarian Response to Infection and Inflammation

The impact of uterine disease on the ovary may be a contributing factor in disease associated subfertility of the dairy cow. Bacterial LPS is present in the follicular fluid of cows with uterine disease, and is positively associated with the severity of uterine inflammation (Herath et al., 2007); however, the mechanisms that facilitate the concentration of bacterial components in follicular fluid during uterine disease are yet to be elucidated. Interestingly,

concentrations of bacterial LPS in follicular fluid are higher in non-ovulatory cows compared to ovulatory cows (Cheong et al., 2017). Additionally, cows with uterine disease have slower growing dominant follicles postpartum and reduced plasma estradiol concentration (Sheldon et al., 2002).

The ovarian follicle is composed of theca and granulosa cells that are essential for follicle growth, steroidogenesis and sustenance of the oocyte. Among these functions, granulosa cells also have immune cell-like properties when challenged with bacterial components. Specifically, bovine granulosa cells express mRNA for all 10 known TLRs, and when stimulated with various PAMPs *in vitro*, granulosa cells increase secretion of inflammatory mediators including IL-1β, IL-6, and IL-8. In addition, granulosa cells challenged with LPS *in vitro* reduce expression of *CYP19A1* and subsequent estradiol and progesterone secretion (Bromfield and Sheldon, 2011; Price et al., 2013). *In vivo* the concentration of estradiol is also lower in the follicular fluid of buffalo with endometritis compared to healthy controls (Boby et al., 2017). Furthermore, cows with subclinical mastitis have lower concentrations of estradiol and androstenedione in the follicular fluid (Lavon et al., 2011).

The consequences of LPS accumulation within the follicle is not constrained to impacts on granulosa cells. Culturing COCs in the presence of LPS increases secretion of IL-6 and promotes COC expansion in the absence of follicle stimulating hormone (FSH). Ultimately, maturation of COCs in the presence of LPS results in oocytes with higher rates of meiotic failure (Bromfield and Sheldon, 2011), but does not affect zygote cleavage following fertilization (Soto et al., 2003a). However, when COCs are exposed to LPS during IVM the proportion of oocytes that progress to the blastocyst stage is reduced (Soto et al., 2003a). In addition, cows with bacterial infection of the mammary gland also present altered folliculogenesis and oocyte

development. Oocytes from cows with chronic mastitis present lower levels of growth differentiation factor (GDF)-9 (Rahman et al., 2012). Oocytes recovered from cows with mastitis and submitted to IVF have lower blastocyst rates at day 7 and 8 compared to oocytes from control cows (Roth et al., 2013). The use of follicular fluid from cows infused with bacteria in the mammary gland as IVM medium results in a decrease in the number of cleaved oocytes and decrease in blastocyst rates at day 7 following IVF (Asaf et al., 2014).

The negative effect of LPS exposure on oocytes begins to explain the observed reduction in fertility of cows with active infection, but it does not justify why cows have difficulty conceiving after infection and inflammation are resolved. It is possible that the negative effect of LPS on the oocyte is not restricted to the antral follicles, and that uterine disease also impacts the follicles from the primordial stage onward that will be recruited after the resolution of disease. As observed in the case of bacterial infection of the mammary gland, the number of large follicles (> 8 mm) and secondary follicles is reduced in cows with infection (Rahman et al., 2012). *In vitro* culture of ovarian explants in the presence of LPS increase the secretion of inflammatory mediators and increases spontaneous activation of primordial follicles, subsequently depleting the ovarian reserve (Bromfield and Sheldon, 2013). However, culture of preantral follicles individually in the presence of LPS does not alter follicle diameter or estradiol secretion compared to control follicles (Bromfield and Sheldon, 2013).

Many inflammatory mediators have been reported to play a physiological role in ovarian function, including follicle growth, ovulation, oocyte maturation and luteinization (Espey, 1980; Field et al., 2014). Members of the transforming growth factor beta (TGFβ) family of cytokines, bone morphogenetic protein 15 (BMP-15) and GDF-9 are oocyte secreted factors that control folliculogenesis (Dong et al., 1996) and growth, proliferation and differentiation of granulosa

cells (Spicer et al., 2006; Gilchrist et al., 2008). Additionally, molecules such as hyaluronic acid can activate TLRs, increasing synthesis of IL-6 (Termeer et al., 2002). IL-6 is present in the follicular fluid and influence steroidogenesis in small and large follicles (Spicer and Alpizar, 1994). In rodents, increased IL-6 expression in response to physiological activation of cumulus cell TLR4, mediates COC expansion and migration of the COC through the oviduct (Shimada et al., 2006; Liu et al., 2008; Richards et al., 2008). Cytokines including TNFα and IL-8 are involved in ovulation, remodeling of the ovarian extracellular matrix and luteinization; while IL-1β mediates changes in the vascular endothelium and IL-6 affects granulosa cell survival and cumulus expansion (reviewed by Field et al., 2014). *In vitro,* TNFα inhibits steroidogenesis in bovine granulosa and theca cells (Spicer, 1998), while the expression of IL-8 and IL-1β is stimulated by angiogenic factors involved in regulation of ovarian blood flow (Murayama et al., 2010).

Due to the fundamental roles played by cytokines in basic ovarian functions, the potential for disruption of fertility occurs when there is an inappropriate accumulation, or temporal expression of cytokines that could occur in the presence of LPS and pathological inflammation. *In vitro* and *in vivo* studies have accessed the effects of inappropriate accumulation of cytokines on ovarian function. Specifically, theca and granulosa cells cultured in the presence of TNFα reduce androstenedione and estradiol production, respectively (Williams et al., 2008) *In vivo,* uterine infusion of TNFα reduces the number of cows that ultimately ovulate compared to control animals infused with vehicle (Williams et al., 2008). Exposure of oocytes to TNFα during IVM does not alter the proportion of oocytes that cleaved after fertilization, but reduces the proportion of oocytes that progress to the blastocyst stage of development (Soto et al.,

2003b). Intravenous infusion of low dose TNFα induces luteolysis and shortens the estrous cycle in cattle, while high dose infusion of TNFα prolongs the luteal phase (Skarzynski et al., 2003).

Although bacterial components have been shown to impact the ovary and the oocyte, it is possible that the reduction in fertility observed in cows following uterine disease is also mediated by inappropriate expression of cytokines mediated by intra-follicular or intra-ovarian inflammation in response to bacterial components originating from the uterus (Figure 1-2).

This dissertation will focus on the impacts of uterine disease to the ovary of dairy cows in an attempt to distinguish the underling mechanisms involved in the subfertility that arises after the development of uterine disease. The following chapters encompass experiments evaluating the impacts of uterine disease on granulosa cells and the oocyte, using natural occurring disease, *in vitro* culture and an experimental model of induced uterine disease in virgin heifers. These experiments focus on the long term effects of uterine disease on the ovary, 50-70 days postpartum after the resolution of disease at the time of breeding.

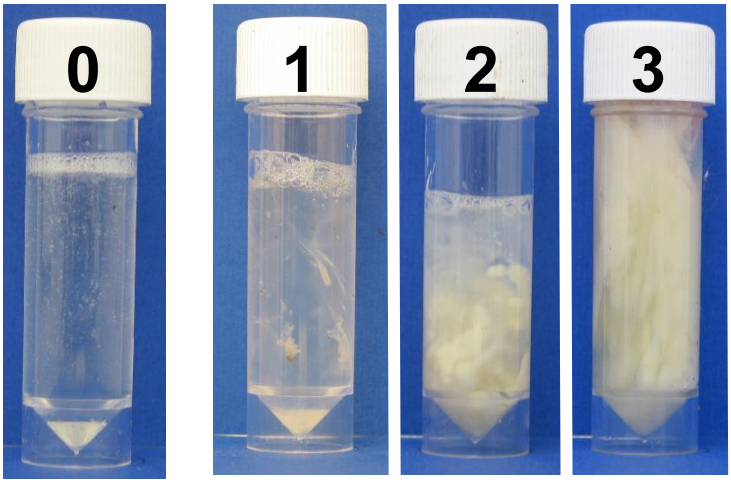

Figure 1-1. Example of vaginal mucus grading for classification of clinical endometritis. Grade 1, mucus containing flecks of white or off-white pus; grade 2, discharge containing ≤ 50% white or off-white mucopurulent material; and grade 3, discharge containing > 50% purulent material Adapted from (Sheldon et al., 2009).

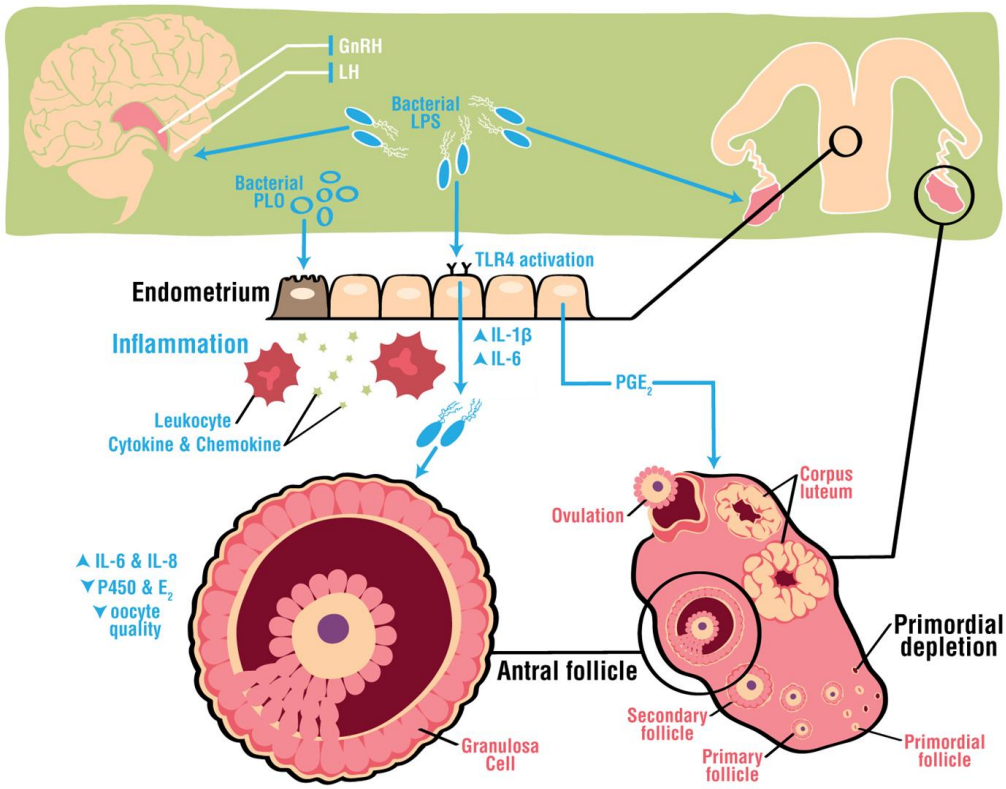

Figure 1-2. Schematic figure of the impacts of uterine disease to the endometrium, the brain and ovary. Impacts of PAMPs and inflammatory mediators to the hypothalamus and pituitary altering GnRH and LH pulsatility; endometrial cells responding to PAMPs by increasing cytokine and chemokine secretion; granulosa cell response to PAMPs in the ovary increasing local accumulation of inflammatory mediators potentially disrupting the oocyte (Bromfield et al., 2015).

CHAPTER 2
LONG LASTING EFFECTS OF METRITIS ON GRANULOSA CELL TRANSCRIPTOME AFTER THE RESOLUTION OF METRITIS

Introduction

Cows that had metritis within the first 10 days after parturition have a reduced pregnancy rate at day 45 after insemination, reduced calving rates and increased pregnancy loss (Ribeiro et al., 2016). Metritis results in an increased interval from calving to conception and a 20% reduction in pregnancy (Fourichon et al., 2000). Postpartum uterine disease impacts reproductive physiology of the dairy cow beyond uterine tissue damage. Bacterial components are present in the uterus as well as in the peripheral circulation (Mateus et al., 2003), and activate an inflammatory response and alter pituitary LH surge and pulsatility (Suzuki et al., 2001; Lavon et al., 2010). Uterine disease also impacts ovarian function, as cows with uterine disease have delayed growth of the dominant follicle, and reduced estradiol secretion (Sheldon et al., 2002). Interestingly, the Gram-negative bacterial cell wall component, LPS is concentrated in the follicular fluid of the dominant follicle in cows during active uterine infection (Herath et al., 2007). Granulosa cells respond to LPS through TLR activation, increasing the accumulation of proinflammatory cytokines, and reducing the expression of *CYP19A1* and subsequent secretion of estradiol (Price et al., 2013). The relationship between the granulosa cells and the oocyte is key for proper follicle growth, oocyte maturation and development, as the granulosa cells support oocyte growth and regulate meiotic maturation (Coticchio et al., 2014). Additionally, uterine disease may negatively affect the oocyte, as COCs cultured in the presence of LPS display increased oocyte meiotic failure (Bromfield and Sheldon, 2011), and decrease blastocyst formation following IVF (Soto et al., 2003a). The consequences of uterine disease and subsequent bacterial components on ovarian function, the follicle microenvironment and the oocyte may contribute to the subfertility observed in cows following uterine disease.

Metritis is resolved during the first 3 weeks after calving, while the first attempt to breed dairy cows will only occur after the voluntary waiting period (50 to 70 days), after the resolution of disease. The reason why cows that had metritis remain subfertile after disease resolution is unknown. We hypothesize that metritis causes a long term impact to the granulosa cells transcriptome, ultimately resulting in impaired follicular quality that may compromise the oocyte, recuing fertility. Here we evaluate the long lasting impacts of metritis on the granulosa cell transcriptome at the time of breeding, in an attempt to understand how changes to the microenvironment of the follicle may impair fertility as a result of previous disease.

Materials and Methods

The University of Florida Institutional Animal Care and Use Committee approved all procedures with cows under the protocol number 201508884. The experiment was conducted from June 2016 to February 2017 at the University of Florida Dairy Unit.

Study Design and Disease Evaluation

A total of 45 Holstein cows were enrolled in the study. Cows were evaluated every other day following parturition for signs of clinical metritis by a single researcher. Cows with a fetid, red-brown to purulent vaginal discharge within 21 days of calving were characterized as having metritis. All other postpartum diseases, including mastitis, ketosis, displaced abomasum and laminitis, were classified according to clinical diagnosis of disease by onsite veterinary staff within 21 days of calving (Table 2-1). Cows with vaginal discharge after 21 DIM or subclinical endometritis at 63 DIM (as determined by endometrial cytology) were excluded from the study. Postpartum cows were fed a total mixed ration twice daily, housed in free stall barns and milked twice daily. Milk parameters (yield and components) were collected by the AfiLab milk analyzer (Kibbutz Afikim, Israel) at each milking and compiled using AfiFarm software. Cow weight was collected daily as cows exited the milking parlor. Milk parameters and cow weight were

collected until 305 DIM. Following the voluntary waiting period (53 days), cows were enrolled in a double Ovsynch protocol for breeding. On 53 ± 1 DIM cows received 100 mg i.m. of GnRH (gonadorelin diacetate tetrahydrate; Ovacyst, Bayer) followed by 25 mg i.m. of $PGF_{2\alpha}$ (dinoprost tromethamine; Prostamate, Bayer) 7 days later. Cows received a second GnRH injection 72 h after $PGF_{2\alpha}$ at which time the dominant follicle was sampled by transvaginal ultrasound guided follicle aspiration on day 63 ± 1 postpartum. Cows received a third GnRH injection 7 days following follicle aspiration, $PGF_{2\alpha}$ 7 days later, followed by a final GnRH injection 48 h later and artificial insemination as part of routine farm practice using sires selected by farm staff. Pregnancy was confirmed by rectal palpation and ultrasound on day 32 following insemination.

Granulosa Cell Isolation by Ultrasound Guided Transvaginal Follicle Aspiration

The dominant follicle was sampled on the day of the second GnRH administration of the double Ovsynch protocol. Briefly, cows received a caudal epidural injection of 60 mg of lidocaine hydrochloride 2% (Aspen Veterinary Resources, Greely CO). The vagina was flushed using 100 mL of sterile saline containing 0.5% Virkon S (Lanxess, Germany), followed by two 100 mL flushes of sterile 0.9% saline. The perineum and vulva were cleaned and disinfected with povidone iodine followed by 70% ethanol. An oocyte pick-up handle including a 5 MHz convex ultrasound probe (Choice Medical Systems, St. Petersburg, FL) was covered in a sanitary cover sleeve (TNB, Sao Paulo, Brazil) and introduced into the vagina with sterile lubricant (Therio-gel, Agtech, Manhattan, KS). Using rectal palpation the ovary was placed toward the ultrasound probe and visualized using an Aloka ultrasound (Aloka SSD-500, Hitachi Healthcare Americas, Twinsburg, OH). A cross sectional image of the dominant follicle was collected and two perpendicular measurements of the internal diameter were made to estimate follicle size. An 18 G needle attached to a double mandrel guide and a vacuum pump was introduced into the oocyte pick-up handle, and by ultrasound guidance the dominant follicle was aspirated into a 50

mL tube containing 5 mL collection medium (all medium is presented in Appendix B). The needle was maintained inside the follicle while 10 mL of collection medium was infused through the mandrels second opening and used to flush the follicle twice with the help of a syringe. The total volume of the aspirate was determined prior to centrifugation. Aspiration contents were centrifuged at 500 x *g* for 5 min to separate granulosa cells and diluted follicular fluid. After removal of follicular fluid, granulosa cells were re-suspended in collection medium and submitted to a red blood cell lysis protocol to eliminate possible contamination by red blood cells. Briefly, contents were incubated with distilled water for 10 seconds and then 10x PBS was added quickly to restore osmolality. Granulosa cells were washed twice in sterile PBS by centrifugation. Both granulosa cells and follicular fluid were stored at -80°C.

Blood Sampling

Blood was collected from the coccygeal vessels into evacuated tubes (Vacutainer, Becton Dickson, Franklin Lakes NJ) containing sodium heparin for plasma separation at days 7, 21, 35 and 50 after calving. Blood was placed on ice prior to centrifugation at 2000 x *g* for 10 min to collect plasma. Plasma was aliquoted and stored at -20°C.

ELISA

Follicular fluid estradiol and serum progesterone were measured using commercially available ELISA kits (DRG International, Inc., Springfield, NJ) according to the manufacturer's instructions. Both ELISA kits are human specific and were validated before use. Progesterone was validated using spike-in/recovery performance based on actual and expected recovery of progesterone supplied as standard with the kit. Intra-assay CV was calculated at 6.5%, while recovery of spike-in progesterone was 89% to 101.8% of expected progesterone. Estradiol was validated using spike-in/recovery performance based on actual and expected recovery of

estradiol supplied as standard with the kit. Intra-assay CV was calculated at 7.4%, while recovery of spike-in estradiol was 88.9% to 107.4% of expected estradiol.

Isolation, Purification and RNA Sequencing Of Granulosa Cell Transcriptome

Granulosa cells were thawed and resuspended in RLT buffer for total RNA extraction using the RNeasy Micro kit (Qiagen, Valencia, CA) according to the manufacturer's instructions. Total RNA concentration was determined using a Qubit® 2.0 Fluorometer (ThermoFisher, Grand Island, NY) and RNA quality was assessed using an Agilent 2100 Bioanalyzer (Agilent Technologies, Santa Clara CA). Total RNA with a 28S to 18S ration > 1 and RNA integrity number (RIN) ≥ 7 were used for RNAseq library construction.

To produce RNAseq libraries, 200 ng of total RNA was used to isolate mRNA using NEBNext Poly(A) mRNA magnetic isolation module (New England Biolabs, Ipswich, MA) and RNA library construction with NEBNext Ultra RNA Library Prep Kit for Illumina (New England Biolabs) according to the manufacturer's instructions. Briefly, extracted mRNA was fragmented in NEBNext First Strand Synthesis Buffer by heating at 94 °C, followed by first strand cDNA synthesis using reverse transcriptase and random primers. Synthesis of double-stranded cDNA was performed using the 2nd strand master mix provided with the kit. The resulting double-stranded cDNA was end-repaired, dA-tailing and ligated with NEBNext adaptors. Finally, libraries were enriched by 12 cycles of amplification and purified by Meg-Bind RxnPure Plus beads (Omega Biotek, Norcross, GA).

Barcoded libraries were sized on a bioanalyzer, quantitated by QUBIT and qPCR (Kapa Biosystems Wilmington, MA). Eighteen individual libraries were pooled at equal molar concentrations (20 nM), and a total of 4 lanes of 2 x 100 base pair reads were run on an Illumina HiSeq3000 (Illumina, San Diego, CA).

RNA library construction and sequencing was performed at the Interdisciplinary Center for Biotechnology Research (ICBR), University of Florida.

Read Mapping, Gene Expression Analysis and Pathway Analysis of Differentially Expressed Genes

Reads acquired from the sequencing platform were cleaned with the Cutadapt program (Martin, 2011) to trim off sequencing adaptors, low quality bases, and potential errors introduced during sequencing or library preparation. Reads with a quality Phred-like score < 20 and read length < 40 bases were excluded from RNAseq analysis.

The transcripts of Bos taurus (80,896 sequences) retrieved from the NCBI RefSeq database were used as reference sequences for RNAseq analysis. The cleaned reads of each sample were mapped individually to the reference sequences using the bowtie2 mapper (v. 2.2.3) with a '3 mismatches a read' allowance (Langmead and Salzberg, 2013). The mapping results were processed with the samtools and scripts developed in house at the University of Florida ICBR to remove potential PCR duplicates and choose uniquely mapped reads for gene expression analysis. Gene expression between the control and treatment groups was assessed by counting the number of mapped reads for each transcript (Yao and Yu, 2011). Significant up and down regulated genes were selected using the *P*-value and fold-change. Adjusted *P*-values were all above the 0.1 cut-off, as such all data presented for differentially expressed genes are non-adjusted *P*-values.

Pathway analysis was performed using Ingenuity Pathway Analysis (Qiagen). Differentially expressed genes with a P-value ≤ 0.05 and $\log_2$ fold change > 2 were used for analysis. Represented canonical pathways with a –log P-value > 1.3 were determined with corresponding z-scores to describe predicted activation status. Represented gene networks were determined by assessing the number of differentially expressed genes in a given gene network.

Upstream regulators of specific gene networks and upstream regulators of differentially expressed genes were predicted using IPA algorithms. Predicted upstream regulators of differentially expressed genes were assigned an activation z-score to predict the appropriate upregulation or down regulation of various downstream differentially regulated genes. A z-score ≥ 2 or ≤ -2 was assumed to be a significant prediction of activation or inhibition, respectively.

Statistical Analysis

Data on disease incidence, milk yield, body weight, dominant follicle diameter, serum progesterone and follicular fluid estradiol were analyzed using SAS v. 9.4 (SAS Institute, Cary, NC). Disease incidence was analyzed using the GLIMMIX procedure of SAS and the model included the fixed effect of disease (metritis). Serum progesterone concentration was used to determine cyclicity. Each cow was considered as an individual observation and cyclicity considered as a binary variable when progesterone was detected ≥ 1 ng/mL (0 = did not occur; 1 = occurred). Dominant follicle size was analyzed using the GLM procedure of SAS and the model included the fixed effect of disease (metritis). Milk yield, body weight, and estradiol concentration were analyzed using the MIXED procedure of SAS and the models included the fixed effects of treatment (metritis), day (repeated measure), and their interaction. Body weight was used as a covariate to evaluate milk yield. Cow nested within disease was considered as a random effect. First order autoregressive covariance structure AR (1) was used as the covariate structure. Values are reported as LSM ± SEM for all parameters except for the RNAseq gene expression analysis. Differences with $P \leq 0.05$ were considered statistically significant.

Results

Fertility, Milk Production and Disease Incidence

A total of 45 cows were enrolled in the study with an average parity of 2.2 ± 0.2 (Table 2-1). Within 21 days of calving, 17 cows (37.8%) were diagnosed with metritis. The incidence of

other postpartum conditions including dystocia, laminitis and displaced abomasum were equally distributed between the metritis and non-metritis cows. There was an increased ($P < 0.01$) incidence of ketosis within the metritis group, with 21.4% of non-metritis and 70.6% of metritis cows displaying ketosis within the first 21 following parturition (Table 2-1). The pregnancy per AI at day 32 was not different between cows with metritis compared to non-metritis cows (28.9% and 39.7%, respectively. $P = 0.43$).

During the first 280 DIM, average body weight of cows with metritis was 21 kg lighter ($P < 0.05$) than non-metritis cows. In addition, average daily milk yield was reduced ($P < 0.05$) by 4.6 kg/d in cows with metritis. Milk fat, milk protein and milk lactose were reduced *(*$P <$ 0.05) in cows with metritis compared to non-metritis cows (0.1, 0.1 and 0.2 kg/d, respectively) (Table 2-2).

Dominant Follicle Size and Follicular Fluid Estradiol Concentration

At the time of follicle aspiration there was no difference in the diameter of dominant follicles of non-metritis or metritis cows (15.8 ± 0.9 vs 14.7 ± 0.7 mm, respectively). Follicular fluid estradiol was also comparable between non-metritis and metritis cows (556.9 ± 154.8 vs 742.1 ± 205.8 ng/mL, respectively) (Figure 2-1).

Ovarian Cyclicity

Cows with a serum progesterone concentration ≥ 1 ng/mL on days 7, 21, 35 or 50 after calving were considered to have an active estrous cycle. Survival analysis suggested that metritis cows had an increased time to cyclicity compared to non-metritis cows ($P < 0.02$) The median number of days to return to cyclicity was 35 for non-metritis cows and 50 for metritis cows (Figure 2-1).

Overview of RNA Sequencing Results

Abundance of transcript and differential gene expression was evaluated in granulosa cells of the dominant follicle from non-metritis (n = 9) and metritis (n = 7) cows. An average of 1.5 ± 0.5 μg of RNA was isolated from each follicle. All RNA samples had an RNA integrity number (RIN) greater than 7.5 (average 9.0 ± 0.2) prior to library construction. Following RNAseq and read processing a total of 574,407,346 high quality reads were used for analysis (approximately 26 million reads per sample). An average of 34% of high quality reads were aligned to the reference genome. A total of 23,308 Genebank identifiers were detected in at least one sample. A volcano plot represents the distribution of expression for all identified genes (Figure 2-2). The highest expressed genes in all samples were identified as *INHBA*, *SERPINE2*, *GSTA3*, *LRP8* and *CYP19A1* (Table 2-3).

Following analysis, a total of 177 genes were differentially expressed by 2-$\log_2$ fold change (FC) ($P \leq 0.05$) in granulosa cells from metritis cows (144 upregulated, 33 down regulated). The five highest upregulated genes in granulosa cells from cows with metritis included *ITLN1*, *NCF2*, *CLRN3*, *FSIP2* and *ANKRD17* (9.5, 7.9, 5.0, 4.9, 4.8 FC, respectively; $P \leq 0.05$) (Table 2-4). The five most downregulated genes in granulosa cells from cows with metritis included *ACSM1*, *NR4A2*, *GHITM*, *CBARP* and *NR1I3* (-5.1, -4.7, -4.5, -4.4, -4.3 FC, respectively; $P \leq 0.05$) (Table 2-4).

Selectively assessing the expression of genes involved in inflammation and steroid hormone synthesis was performed independently of statistical analysis (Figure 2-3). Selective analysis of inflammatory cytokines showed that expression of *IL18* was increased 3.1 FC ($P = 0.037$) and expression of *CXCL2* and *IL1A* were increased in metritis cows by 6.7 and 2.7 FC ($P < 0.1$). Analysis of genes involved in steroid hormone synthesis revealed that cows with metritis

had increased expression of *HSD17B2* by 2.3 FC ($P = 0.048$) and decreased expression of *CYP11A1*, *CYP19A1*, and *STAR* by -0.5, -0.8 and -1.3 FC, respectively ($P > 0.05$; Figure 2-3).

Annotation and Pathway Analysis of Differentially Expressed Genes

Significantly affected canonical pathways enriched by genes differentially expressed in granulosa cells of cows with metritis are shown in Figure 2-4. Of the 39 significantly affected canonical pathways, 8 pathways had significant positive z-scores suggesting an upregulation of the pathway due to the distinct pattern of differentially regulated genes. These pathways included Th1 pathway, cholecystokinin/gastrin-mediated signaling, neuro-inflammation signaling, thrombin signaling, actin cytoskeleton signaling, phospholipase C signaling, CXCR4 signaling, and signaling by Rho family GTPases. Of the significantly affected canonical pathways, 18 canonical pathways are involved in immunity or inflammation.

Analysis using differentially regulated genes revealed a total of 17 gene networks impacted in cows with metritis. The highest scored gene networks included 1) developmental disorder, neurological disease, cardiovascular disease; 2) cell-to-cell signaling and interaction, hematological system development and function, immune cell trafficking; 3) cell signaling, molecular transport, nucleic acid metabolism; 4) cell cycle, cellular assembly and organization, DNA replication, recombination, and repair; 5) cancer, cellular development, organismal injury and abnormalities; and 6) cellular function and maintenance, cellular growth and proliferation, amino acid metabolism. The involvement of specific differentially regulated genes in the cell-to-cell signaling and interaction, hematological system development and function, immune cell trafficking are shown in Figure 2-5; cell signaling, molecular transport, nucleic acid metabolism network are shown in Figure 2-6; and developmental disorder, neurological disease, cardiovascular disease are shown in Figure 2-7.

Further analysis to predict upstream regulators of affected gene networks suggested that IL-12 and IL-21 are upstream regulators of molecules involved in stimulation of lymphocyte and cytolysis gene networks, respectively (Figure 2-8). Similarly, NFκB and *E. coli* LPS were predicted as upstream regulators of differentially expressed genes in metritis cows (Figure 2-9).

Discussion

This is, to our knowledge, the first study evaluating the long term effects of postpartum metritis on granulosa cell transcriptome at the time of breeding. Even though the number of cows was limited, we observed a reduction in milk production in cows with metritis. This finding corroborates previous studies that report that uterine disease, metritis or retained placenta have a negative impact on milk production, and lead to an increase in culling rates (Dubuc et al., 2011). Metritis reduces pregnancy rates, increases pregnancy loss and decreases calving rates (Ribeiro et al., 2016). Although in our study we did not observe a significant reduction in pregnancy per AI at day 32, this may be explained by the limited number of cows with the experiment.

Reproductive failure is the main cause of culling cows with uterine disease (Dubuc et al., 2011). The mechanisms by which an acute episode of uterine disease within 21 days of parturition influences reproductive success after the clearance of disease is unknown. Cows with uterine disease accumulate LPS in follicular fluid, display slower growth of the dominant follicle and altered steroidogenesis (Sheldon et al., 2002; Herath et al., 2007), potentially burdening the oocyte and ultimately disrupting fertility. Previous studies have focused on the impacts of uterine disease to the ovary during active disease, and did not look at possible repercussions after disease clearance. Due to the voluntary waiting period, cows will only be submitted to AI 50 to 70 days after parturition, when the medium and large follicles present during active disease have either ovulated or undergone atresia. The small follicles present during disease, which will potentially ovulate at the time of AI, are susceptible to uterine disease. Ovarian changes observed during

active infection include a reduction in dominant follicle diameter, plasma estradiol and plasma progesterone (Sheldon et al., 2002; Williams et al., 2007). However, these perturbations are no longer present at the time of breeding; we also did not observe differences in dominant follicle size and follicular fluid estradiol concentration of cows that had metritis. As previously shown, cows with uterine disease often have extended luteal phase (Williams et al., 2007), and in our study cows with metritis took longer to return to cyclicity, as shown by plasma progesterone concentration.

Here, we evaluated granulosa cells from dominant follicles at 63 DIM, which means these follicles were in the early stages of development during active disease. Studies *in vitro* demonstrate that exposure of ovarian cortical tissue to LPS results in premature activation of primordial follicles and increased accumulation of inflammatory mediators in culture (Bromfield and Sheldon, 2013). Interestingly, we observed 177 genes in granulosa cells differentially expressed between cows that had metritis and cows that did not, 40 days after the resolution of disease. Among the genes differentially expressed in our dataset, 144 were upregulated and 33 genes were down regulated. The most upregulated gene in metritis cows was Intelectin 1 (*ITLN1*), a carbohydrate binding protein which might play an important role during immune response, as it has been shown to recognize carbohydrate chains in bacterial cell walls (Tsuji et al., 2001), and is upregulated in parasitic infections of sheep (French et al., 2008).

Expression of Genes Involved in Steroidogenesis and Immune Response

Specific genes involved in steroidogenesis and immune function were evaluated despite statistical analysis, due to their importance in granulosa cell function and response to infection. Previous reports have shown that granulosa cells decrease estradiol secretion when exposed to LPS and that this is due to a reduction in *CYP19A1* (aromatase) expression (Herath et al., 2007). Here, cows that had metritis presented a numerical reduction in expression of enzymes involved

in steroidogenesis such as *CYP11A1, CYP19A1, HSD3B1* and *STAR;* and a significant increase in expression of *HSD17B2,* that is involved in the interconvertion of testosterone and androstenedione, and estradiol and estrone (Wu et al., 1993). *In vitro,* androstenedione production by theca cells challenged with LPS was previously evaluated, as granulosa cells depend on theca-derived androstenedione for estradiol production, but no effect of LPS was observed (Herath et al., 2007).

Among the selected inflammatory genes evaluated, most presented a numerical increase in expression in metritis cows. Chemokine ligand 2 (*CXCL2*) is a powerful neutrophil chemoattractant secreted in response to endotoxin (Wolpe et al., 1989), and was significantly upregulated in metritis cows. Expression of the cytokine *IL18* was also significantly upregulated in metritis cows. IL-18 is involved in the initiation of cell mediated immunity and also play a role in natural killer (NK) cell response by increasing their production of interferon (Netea et al., 2015). This findings suggest there is an ongoing inflammatory process present in the granulosa cells of cows that had metritis when compared to non-metritis cows at the time of breeding.

Enhancement of Immune Response Pathways

The analysis of differentially regulated genes resulted in 39 significantly affected canonical pathways, including 18 pathways associated with immune response. Interesting pathways such as natural killer cell signaling, and Th1 and Th2 activation are among the differentially affected canonical pathways. Th1 and Th2 cells are involved in the immune response to bacteria and parasites, respectively, as well as in the transition from innate immune responses to cell mediated responses (Romagnani, 1999). Also, networks associated with immune cell trafficking were among the networks impacted by the genes in our dataset. Upstream regulators of genes differentially expressed in metritis cows, including IL-12 and IL-21, were predicted to enhance gene networks involved in “stimulation of lymphocytes” and

"cytolysis", respectively. The enhancement of pathways associated with immune response is surprising when we consider that no active disease has been present in the cow for the past 40 days. In agreement with the enhancement of immune pathways, molecules such as NFκB and *E. coli* LPS were predicted as active upstream regulators of differentially expressed genes in metritis cows. Identification of these two active upstream regulators of genes in our dataset reiterate the presence of a high number of genes associated with inflammation. Taken together, granulosa cell gene expression in metritis cows suggest the persistence of inflammation within the ovarian follicle, which might disrupt oocyte development. Oocyte maturation and growth is dependent on granulosa cells, while granulosa cell development relies on oocyte signaling (Dong et al., 1996; Gilchrist et al., 2008).

Among the gene networks affected in metritis cows there were networks involved in cell-to-cell communication, cell signaling, and molecular transport, that indicates a disruption within this communication system. The connection between these two cell types within the follicle is often achieved by signaling through inflammatory mediators (Matzuk, 2002; Richards et al., 2008). The prolonged increase in the concentration of inflammatory mediators inside the follicle caused by the metritis episode may perturb oocyte growth and quality, and ultimately offspring fate. Although we did not observe changes in follicle size or follicular fluid estradiol concentration at the time of follicle aspiration, the changes in granulosa cell gene expression were compelling. Our data suggest that postpartum metritis leaves an enduring mark on the granulosa cells transcriptome 40 days after the clearance of uterine disease. The comparison between the transcriptome of metritis and non-metritis cows contributes to a better understanding of possible mechanisms involved in the decreased fertility observed in dairy cows long after the resolution of uterine disease.

Table 2-1. Incidence of various postpartum diseases among metritis and no metritis cows

	No metritis	Metritis	*P*-value
Parity	2.21 ± 0.15	2.24 ± 0.28	0.94
Dystocia	3.6 (1/28)	17.6 (3/17)	0.11
Ketosis	21.4 (6/28)	70.6 (12/17)	< 0.01
Laminitis	10.7 (3/28)	0 (0/17)	NA
Other disease	25 (7/28)	47.1 (8/17)	0.13
Pregnancy per AI (D32)	39.7%	28.9%	0.43

Table 2-2. Body weight and milk yield between metritis and no metritis cows

	No metritis	Metritis	SEM	*P*-value
Body weight (kg)	660	639	6.56	0.04
Milk yield (kg/d)	36.3	31.7	0.80	< 0.01
Milk fat (%)	3.5	3.6	0.04	0.10
Milk protein (%)	2.8	2.8	0.02	0.34
Milk lactose (%)	4.4	4.4	0.02	0.28
Milk fat yield (kg/d)	1.3	1.2	0.03	< 0.01
Milk protein (kg/d)	1.0	0.9	0.02	< 0.01
Milk lactose (kg/d)	1.6	1.4	0.04	< 0.01

Table 2-3. Highest expressed genes in all samples independent of disease incidence

Gene		Number of reads (Base mean)
INHBA	Inhibin beta A	316,389.9
SERPINE2	Serpin family E member 2	270,521.4
GSTA3	Glutathione S-transferase alpha 3	213,754.6
LRP8	LDL receptor related protein 8	134,089.7
CYP19A1	Cytochrome P450, family 19, subfamily A, polypeptide 1	116,835.5

Table 2-4. The ten most differentially regulated genes in metritis cows

	Gene	No metritis	Metritis	Fold Change (Log_2)	*P*-value
ITLN1	Intelectin 1	0.3	193.0	9.5	0.002
NCF2	Neutrophil cytosolic factor 2	0.1	22.7	7.9	0.006
CLRN3	Clarin 3	0.4	12.5	5.0	0.038
FSIP2	Fibrous sheath interacting protein 2	0.3	8.4	4.9	0.0001
ANKRD17	Ankyrin repeat domain 17	0.1	2.7	4.8	0.035
ACSM1	Acyl-CoA synthetase medium chain family member 1	4.7	0.1	-5.1	0.044
NR4A2	Nuclear receptor subfamily 4 group A member 2	5.8	0.2	-4.7	0.028
GHITM	Growth hormone inducible transmembrane protein	3.0	0.1	-4.5	0.018
CBARP	CACN subunit beta associated regulatory protein	2.4	0.1	-4.4	0.040
NR1I3	Nuclear receptor subfamily 1 group I member 3	2.3	0.1	-4.3	0.038

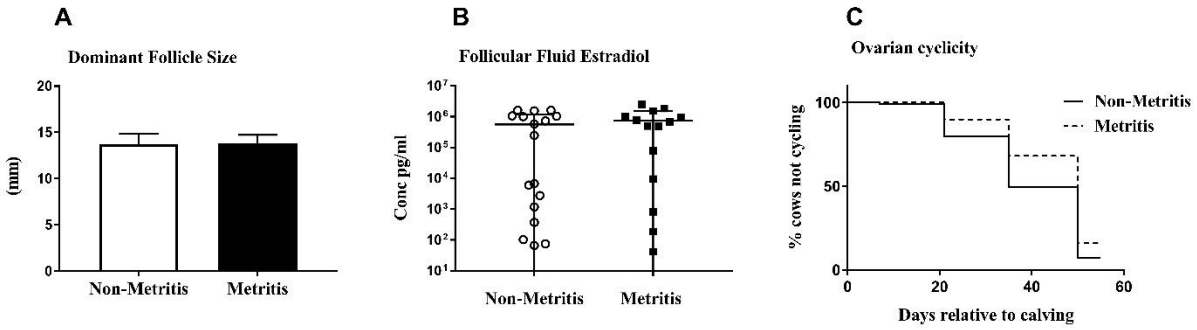

Figure 2-1. (A) Dominant follicle size (mm) at aspiration between non-metritis and metritis cows. (B) Concentration of estradiol (pg/mL) in follicular fluid of non-metritis and metritis cows. Graph presented as measurements for individual cows. (C) Ovarian cyclicity of non- metritis and metritis cows evaluated by progesterone plasma concentration every 14 days.

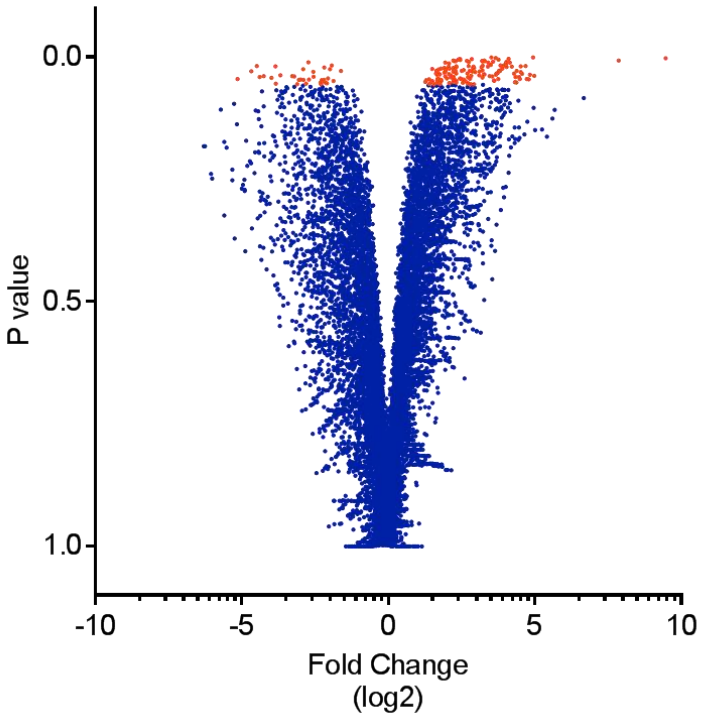

.

Figure 2-2. Volcano plot representing the distribution of all genes detected in metritis cows by RNAseq. Data are displayed as fold change (log_2) from non-metritis cows. Significant differentially expressed genes are displayed in orange ($P < 0.05$).

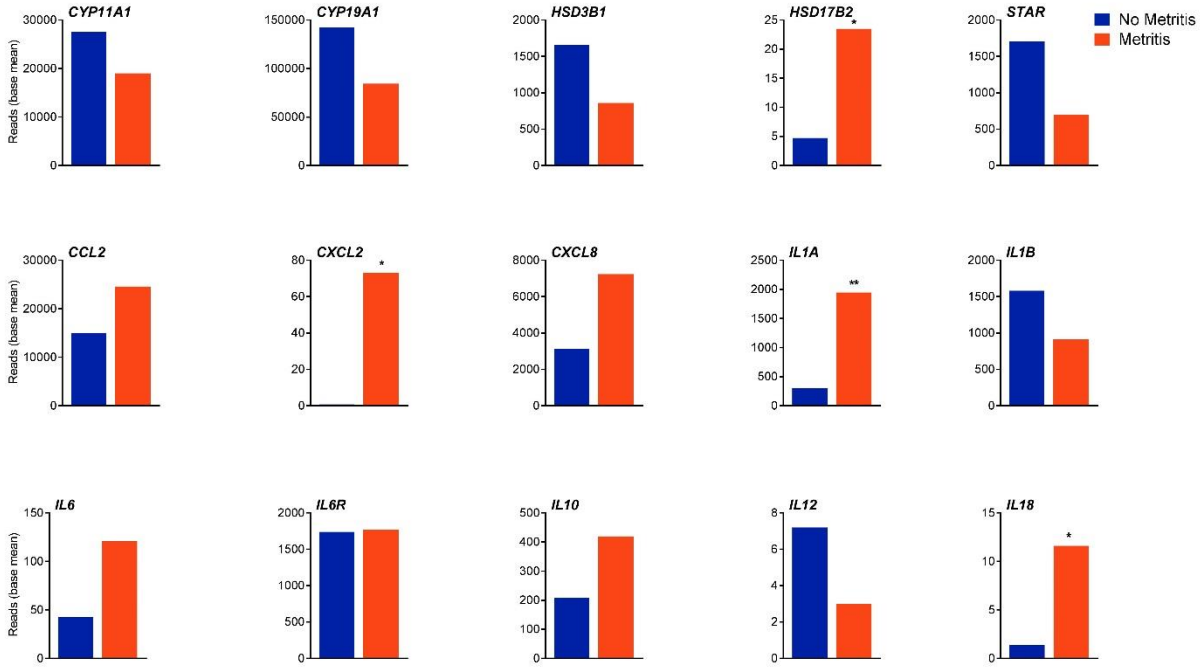

Figure 2-3.Selective evaluation of genes involved in steroidogenesis and immunity. Asterisk (*) indicates a significant difference for the specific gene (*$P \leq 0.05$ and ** $P \leq 0.08$). Data is presented as the mean number of reads (base mean) for non-metritis and metritis animals.

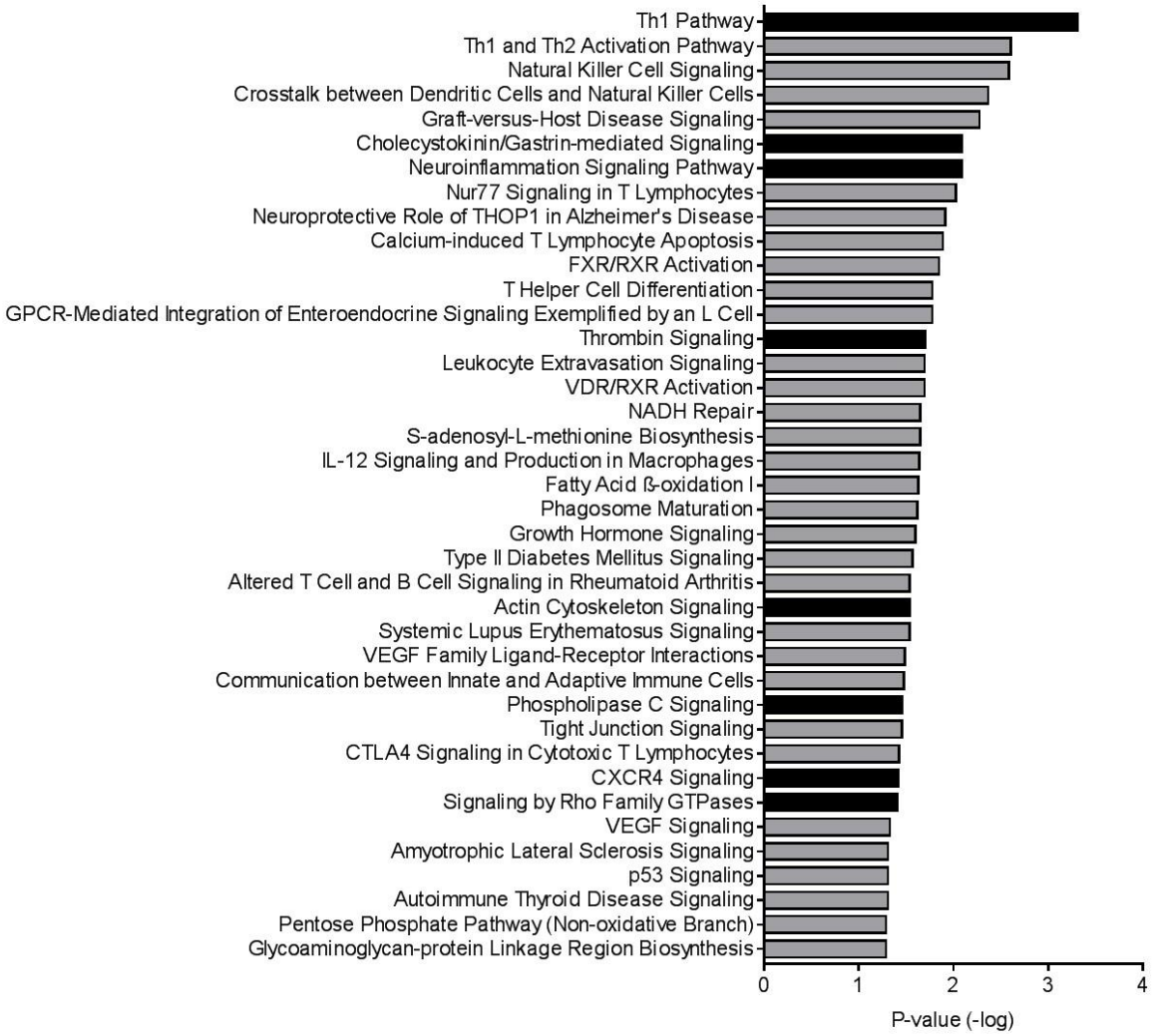

Figure 2-4. Significantly affected canonical pathways enriched by genes differentially expressed in granulosa cells of cows with metritis. Pathways with significant positive z-scores are in black.

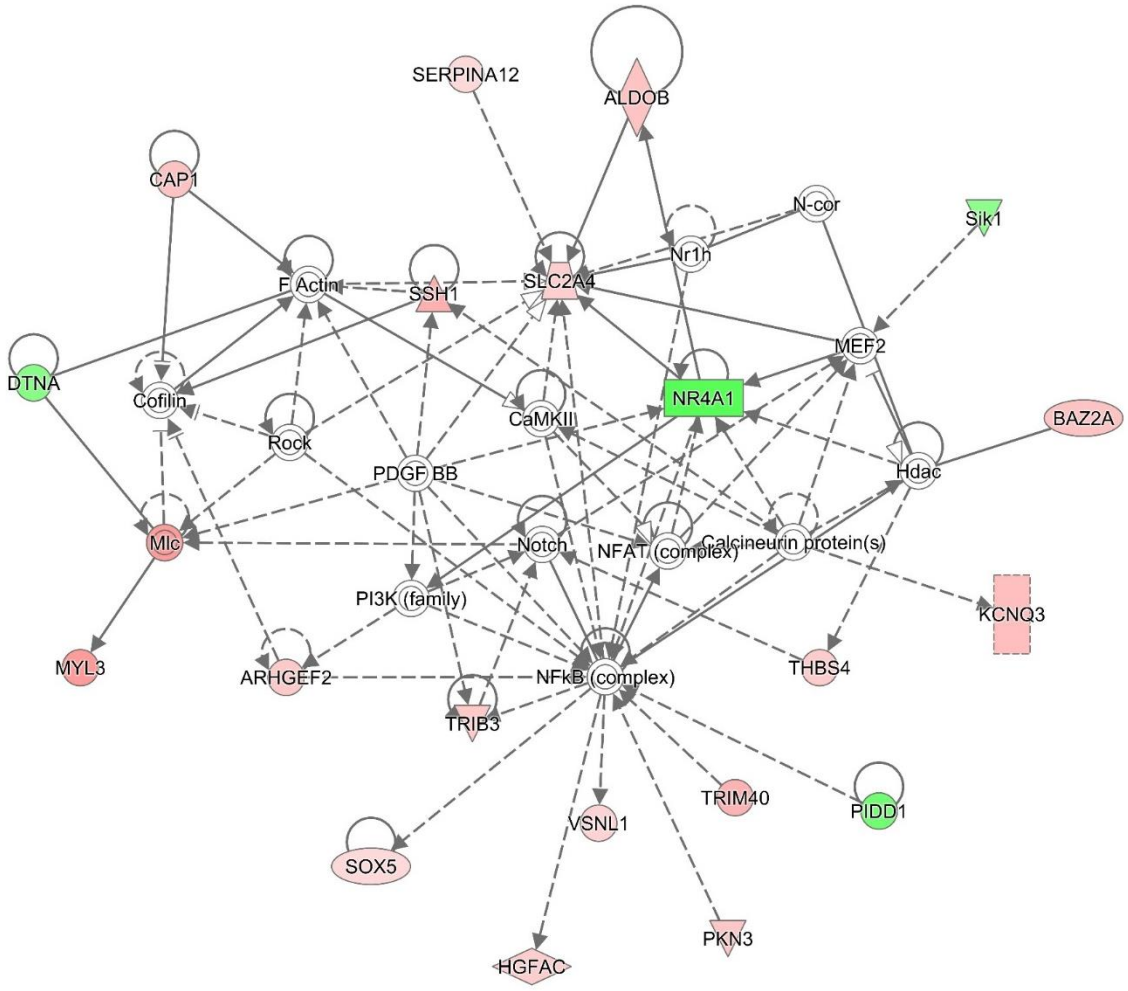

Figure 2-5. Differentially regulated genes in the cell-to-cell signaling and interaction, hematological system development and function, immune cell trafficking gene network. Genes shown in red (up) or green (down) and differentially expressed in metritis cows.

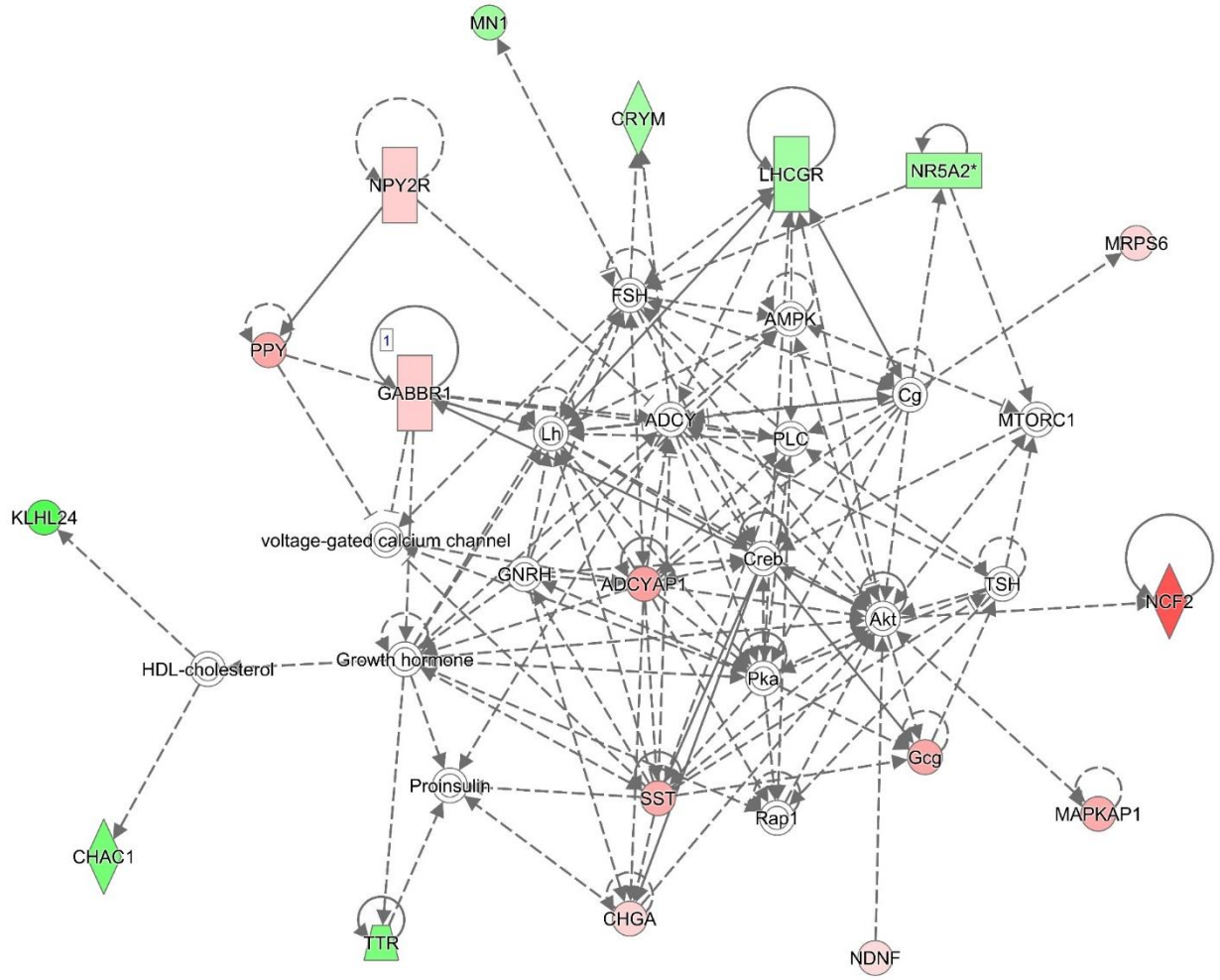

Figure 2-6. Differentially regulated genes in cell signaling, molecular transport, nucleic acid metabolism gene network. Genes shown in red (up) or green (down) and differentially expressed in metritis cows.

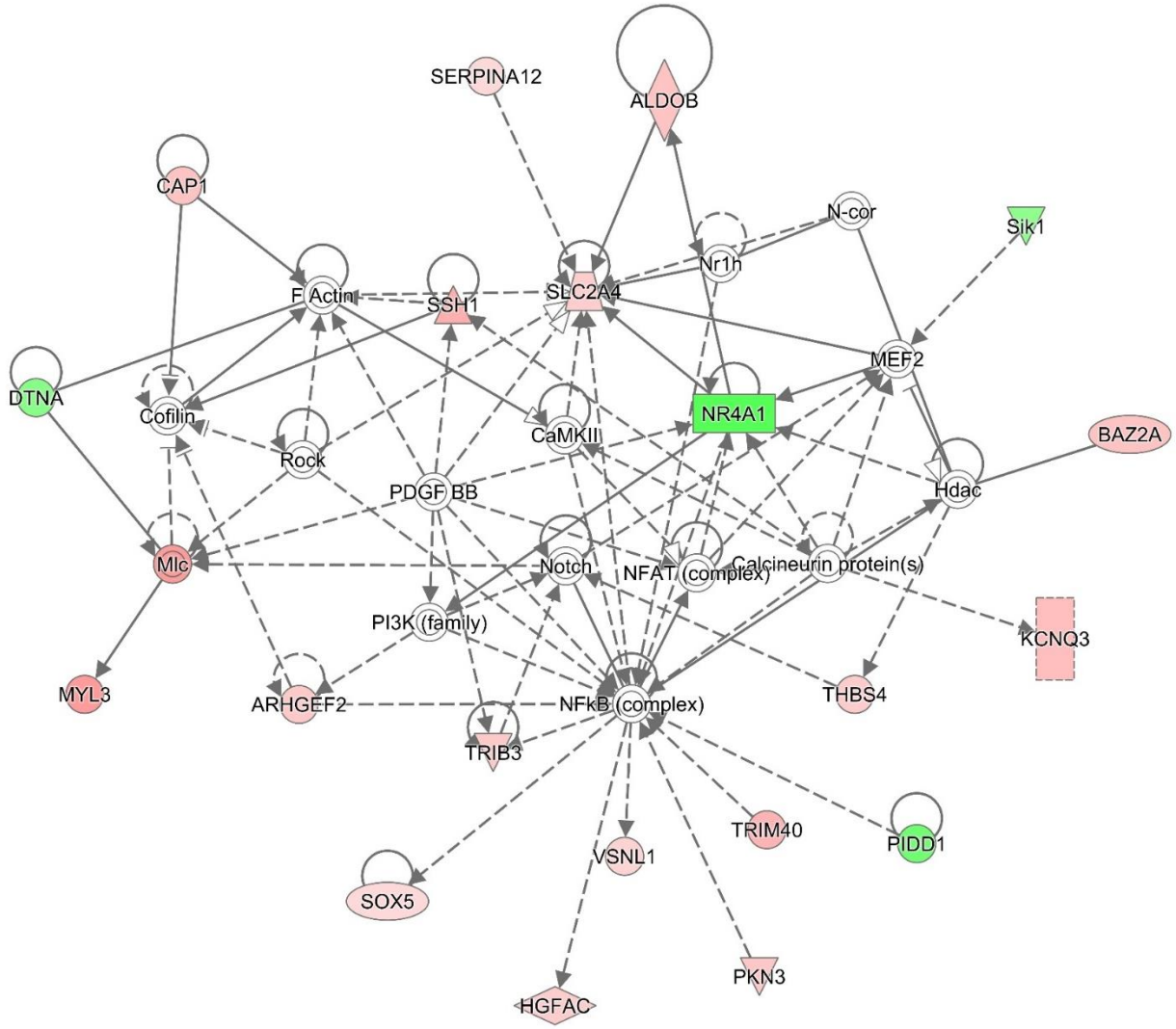

Figure 2-7. Differentially regulated genes in developmental disorder, neurological disease, and cardiovascular disease gene network. Genes shown in red (up) or green (down) and differentially expressed in metritis cows.

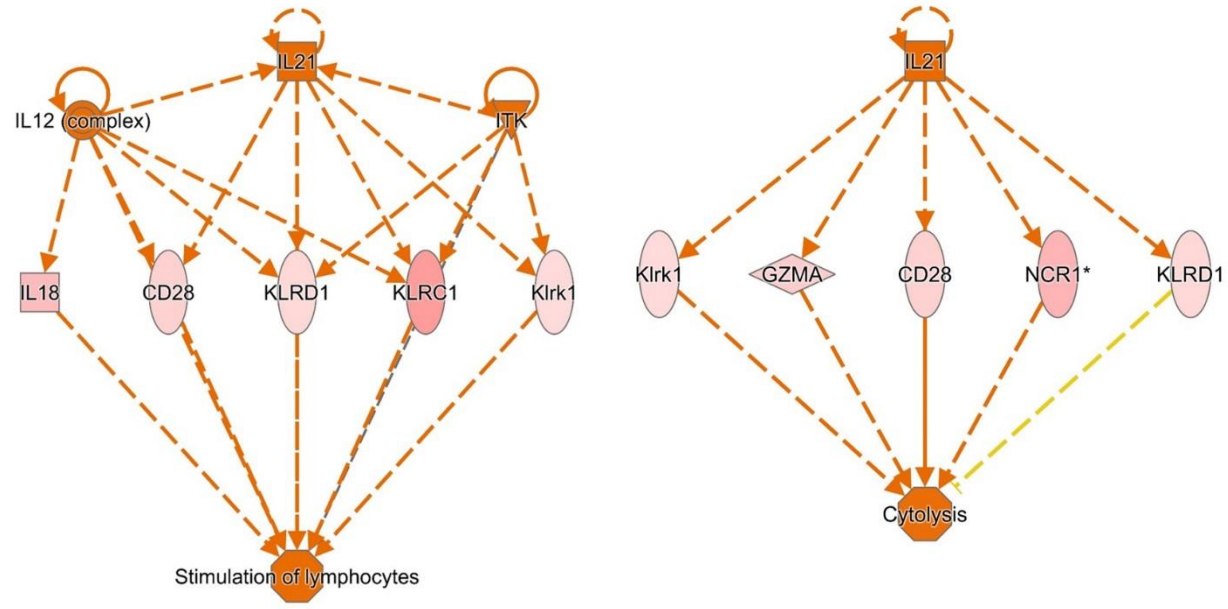

Figure 2-8. Predicted (orange) upstream regulators of differentially expressed genes (red) involved in the gene network of (A) stimulation of lymphocytes or (B) cytolysis.

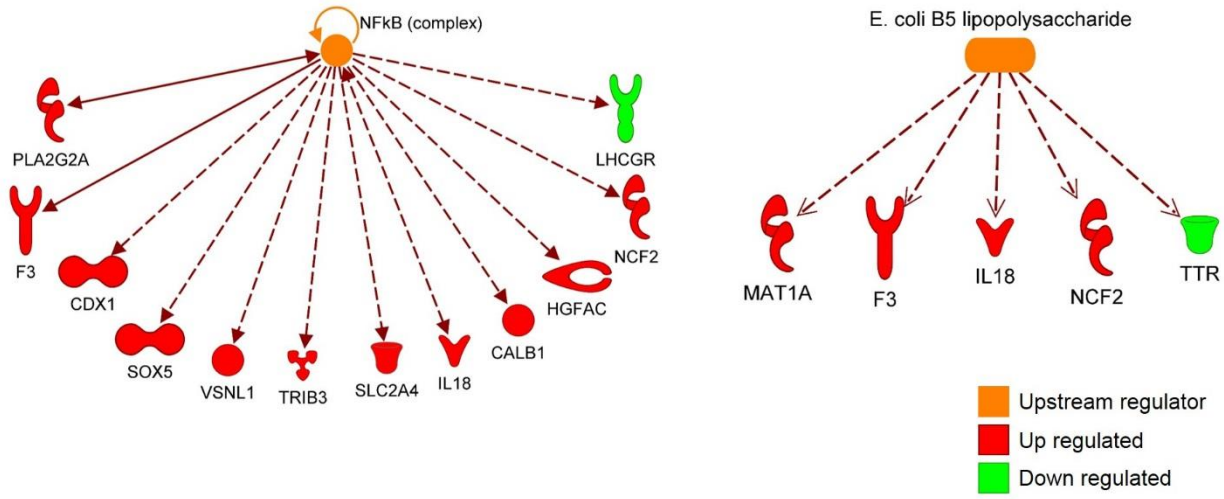

Figure 2-9. Molecules predicted (orange) to be upstream regulators of differentially expressed genes in metritis cows. Genes shown in red (up) or green (down) and differentially expressed in metritis cows.

CHAPTER 3
LIPOPOLYSACCHARIDE AND TUMOR NECROSIS FACTOR-ALPHA ALTER GENE EXPRESSION OF OOCYTES AND CUMULUS CELLS DURING BOVINE IN VITRO MATURATION

Introduction

Successful production of an offspring relies on proper development and maturation of the oocyte. Although the sperm cell and the oocyte contribute equally to the genetic material of the newly formed embryo, the necessary molecular and organelle machinery for growth and regulation of early embryonic development are supplied by the oocyte (Coticchio et al., 2014). Oocyte growth involves the increase of cell mass, proliferation of organelles, accumulation of maternal transcripts and translational products that are required after fertilization, prior to activation of the embryonic genome (Li et al., 2010). Additionally, oocyte maturation requires changes to oocyte chromatin, repositioning of organelles, and facilitating meiotic resumption in response to the LH surge (Coticchio et al., 2014).

The follicular environment is critical to the developmental competence of the growing oocyte. Oocyte growth and maturation depends on close communication between the oocyte and the surrounding cumulus granulosa cells. Transzonal projections (TZPs) play an important role in facilitating oocyte and cumulus cell communication by direct cell to cell contact prior to retraction at the time of the LH surge (Albertini et al., 2001; McGinnis et al., 2013). The interaction between the oocyte and surrounding cumulus cells is bidirectional; the cumulus cells supply the oocyte with essential molecules for proper metabolism and regulation of meiotic maturation, while the oocyte secretes factors that regulate cumulus cell growth, differentiation, apoptosis and expansion (Matzuk, 2002; Gilchrist et al., 2008).

A large part of the communication between oocytes and cumulus cells is conveyed by molecules known for their role as immune mediators. Elements from the TGF-β superfamily,

BMP-15 and GDF-9, are secreted by the oocyte to act on the granulosa cells to control proliferation, development and expansion (Matzuk, 2002).

Likewise, TLRs are involved in the immune response to pathogens, and when activated by bacterial LPS increases expression of cytokines such as IL-1β, IL-6, IL-8 and TNFα. Granulosa cells of hens, pigs, cows, mice and humans express TLRs and respond to bacterial LPS to increase expression of inflammatory cytokines (Álvarez et al., 2006; Subedi et al., 2007; Price et al., 2013; Ibrahim et al., 2016). Cows with uterine infection accumulate LPS in follicular fluid, potentially altering the environment for oocyte development (Herath et al., 2007). *In vitro* maturation of bovine COCs in the presence of LPS results in the accumulation of IL-6 in culture supernatant and decreases oocyte meiotic progression (Bromfield and Sheldon, 2011). While the infusion of TNFα into the ovarian bursa in rats, inhibits ovulation, decreasing the number of oocytes released by the ovary (Yamamoto et al., 2015). Additionally, cumulus cell TLRs are activated by endogenous ligands including hyaluronic acid (HA) during ovulation, cumulus expansion and fertilization (Liu et al., 2008). The proinflammatory cytokine IL-6 acts as an autocrine regulator of COC expansion in the mouse, facilitated by HA/TLR4 activation (Liu et al., 2009), reiterating the importance of inflammatory mediators in oocyte development.

The dual role of molecules involved in the immune response and reproductive physiology can possibly become an issue during infection and inflammation when normal cytokine expression is altered in response to infection. In addition to increasing expression of proinflammatory mediators, bovine granulosa cells reduce expression of *CYP19A1,* subsequently reducing estradiol secretion in response to bacterial LPS (Price et al., 2013). The addition of LPS during IVM does not affect the proportion of oocytes that cleave after IVF but decreases blastocyst development. When LPS is added after fertilization, cleavage rates is reduced but

there is no effect on blastocyst development (Soto et al., 2003a). *In vitro* maturation (IVM) of bovine oocytes in the presence of TNFα did not altered the proportion of cleaved oocytes following IVF, but decreased the number of oocytes that developed to the blastocyst stage (Soto et al., 2003b). These data suggest that the detrimental effects of LPS and inflammatory mediators, such as TNFα, during IVM might impact the oocytes ability to supply the embryo with the necessary tools for proper development. The mechanisms by which LPS and TNFα decrease the oocytes ability to develop to the blastocyst stage are not fully understood; however LPS also perturbs oocyte cytoplasmic maturation by altering the distribution of active mitochondria in the oocyte cytoplasm (Magata and Shimizu, 2017).

Although the effects of LPS and inflammatory mediators on bovine COCs have been studied, no assessment has been made to understand how the oocyte and the cumulus cells gene expression is affected by exposure to LPS or inflammatory mediators. Here, we hypothesize that exposure of COCs to LPS or TNFα during IVM will alter oocyte competence and gene expression of cumulus cell and oocytes.

Materials and Methods

Ovaries were collected at a local abattoir and transported to the laboratory in 0.9% saline solution containing 1% penicillin/streptomycin (10000 IU) (Caisson Labs, Smithfield, UT) at 23°C. Ovaries were processed within 4 h of collection and were the source of all COCs. Cumulus oocyte complexes were collected by bisecting 3 to 8 mm follicles using a sterile scalpel blade and vigorously washing the ovary in oocyte collection medium (BoviPRO, MOFA Global, Verona, WI). Fluid containing COCs and cells was then passed through a 100 μm filter (Falcon Cell Strainers, Corning Falcon, Tewksbury, MA) to collect COCs. The isolated COCs were then retrieved using a wiretrol pipette (Drummond Scientific Company, Broomall, PA) under a dissecting stereo microscope. The COCs were washed three times in fresh oocyte collection

medium. An average of 10 to 15 COCs, having at least one layer of cumulus cells and an oocyte containing a homogeneous cytoplasm, were collected from each ovary and pooled together. Groups of 10 to 15 COCs were matured in organ culture dishes (Corning, Tewksbury, MA) for 22 to 24 h in 1 mL of oocyte maturation medium (all medium is presented in Appendix B) in the presence of either ultrapure *E. coli* 0111:B4 LPS (InvivoGen, San Diego, CA), recombinant bovine TNFα (R&D Systems, Minneapolis, MN), or medium alone. Oocyte maturation was performed in humidified air containing 5% CO_2 at 38.5°C. Treatments were defined as LPS (1, 10, 100, 1000 or 10,000 ng/mL), TNFα (1, 10 or 100 ng/mL) or control medium alone.

Following maturation, COCs were washed three times in fresh Dulbecco's phosphate-buffered saline (DPBS) containing 0.1% polyvinylpyrrolidone (DPBS-PVP; Kodak, Rochester, NY). Expansion of COCs was graded from 1 to 3 (1 not expanded, 2 partially expanded, 3 fully expanded). Cumulus cells were removed from oocytes using 1000 U/mL of hyaluronidase in HEPES-TALP. The zona pellucida of denuded oocytes were removed with 0.1% protease from *Streptococcus griseus* (Sigma-Aldrich, St. Louis, MO) in DPBS, and zona-free oocytes were washed three times in fresh DPBS-PVP. Zona free oocytes were collected and stored in 350 uL RLT buffer (Qiagen, Valencia, CA) at -80°C. Cumulus cells were obtained by centrifugation of the hyaluronidase medium following removal of denuded oocytes. Cumulus cells were re-suspended in 350 uL RLT buffer and stored at -80°C.

Each treatment was performed in 4 to 6 replicates per treatment. A replicate was defined as a single IVM procedure containing one dish per treatment. A total of 542 COCs were subjected to IVM in the presence of LPS, 378 in the presence of TNFα and 194 in control medium.

Multiplex Fluidigm Analysis of Oocyte and Cumulus Cell Gene Expression

Oocyte and cumulus cell RNA extraction was performed using the RNeasy Micro kit with DNase treatment (Qiagen) according to the manufacturer's instructions.

The Fluidigm qPCR microfluidic device Biomark HD system (Fluidigm Co., San Francisco, CA) was used for gene expression assays at the University Of Miami Miller School Of Medicine, Center for AIDS Research (CFAR). Primers were designed by Fluidigm Delta Gene assays (Fluidigm). Primer validation was performed using cDNA obtained from bovine oocytes, endometrium, peripheral white blood cells, granulosa cells and ovarian cortex. All primers were validated using the Fluidigm primer quality control criteria: $R^2 \geq 0.97$, efficiency 0.8 to 1.3 and slope (-3.92) – (-2.76).

Primers (Appendix A – Table 1) were validated for 4 housekeeping genes, 6 oocyte specific genes, 29 genes involved in cell growth and proliferation, 10 genes involved in the regulation of cell cycle, 19 genes related to immune response, 9 genes involved in control of gene expression and DNA modifications, 7 genes associated to apoptosis and cell death, and 12 other genes of interest (Table 2-1).

Target specific pre-amplification after reverse transcription (RT-STA) was performed on all samples using the Preamp and Reverse Transcription Master Mix (Fluidigm) for 20 cycles. The procedure for real time RT-PCR using the BioMark HD system (Fluidigm) (Dominguez et al., 2013) was as follows; primer sets and samples were loaded on an Integrated Fluidic Circuit (IFC) plate and placed into a controller that prepares the nano-volume reactions. Real time RT-PCR was carried out on the BioMark HD system. A total of 40 PCR cycles were performed using EvaGreen (Bio-Rad, Hercules CA) chemistry on the 96.96 dynamic array IFC developed by the manufacturer. Cycle threshold (Ct) values were calculated by the Fluidigm real-time PCR analysis software. The cutoff for detectable genes was set at $Ct < 29$. The geometric mean of the

four housekeeping genes was calculated and fold change relative to house keeper was calculated for the 92 genes of interest using the $2^{-\Delta Ct}$ method.

In Vitro Production of Embryos

The production of bovine embryos was performed with oocytes produced *in vitro* using the protocol described above. Treatment of COCs with 100 ng/mL of ultrapure LPS, 100 ng/mL of recombinant bovine TNFα or control medium alone occurred during IVM only. The IVF and embryo culture procedures were previously reported by Ortega et al (Ortega et al., 2016, 2017). Briefly, following IVM COCs were washed 3 times in HEPES-TALP medium (Tyrode's albumen lactate pyruvate) and placed in a 35-mm dish (Corning) containing 1.7 mL of fertilization medium (IVF-TALP). Fertilization of COCs was performed with semen pooled from 3 bulls representing a mixture of various *B. taurus* and *B. indicus* breeds. Sperm were purified from frozen-thawed straws of extended semen using an isolate two gradient system, PureSperm 40% and PureSperm 80% (Nidacon, Sweden), diluted in IVF-TALP to achieve a final concentration of 1×10^6/mL. To promote fertilization, 80 µL of penicillamine-hypotaurine-epinephrine solution was added to each fertilization reaction. Fertilization proceeded for 12 to 14 h at 38.5°C in a humidified atmosphere of 5% CO_2. Presumptive zygotes were collected and exposed to hyaluronidase (1000 U/mL in HEPES-TALP) to remove the cumulus cells, washed three times in HEPES-TALP and placed in groups of 25 to 30 zygotes per 50 µL drop of SOF-BE2 (all medium is presented in Appendix B) overlaid with mineral oil in a humidified gas atmosphere of 5% CO_2, 5% O_2 and balanced nitrogen at 38.5°C. The proportion of embryos that cleaved was assessed 3 d post-fertilization and the proportion of embryos that developed to the blastocysts stage was determined 7.5 d (182 ± 2 h) post fertilization.

A replicate was defined as a single IVF procedure involving 50 to 100 COCs. A total of six replicates were performed per treatment. Only replicates with a cleavage rate ≥ 50% in control embryos were used for further analysis.

Analysis of Blastocyst Gene Expression by Real-Time RT-PCR

Embryos were washed three times in DPBS-PVP, followed by incubation in 0.1% protease from *Streptococcus griseus* (Sigma-Aldrich) in DPBS for 3 min or until the zona pellucida dissolved. Zona free embryos were washed three times in fresh DPBS-PVP, snap frozen in liquid nitrogen and stored at -80°C until RNA isolation.

For extraction of total RNA, the RNeasy Micro kit (Qiagen) was used following the manufacturer's instructions, including a DNase treatment as part of the protocol. Reverse transcription was performed using the Verso cDNA synthesis kit (ThermoFisher Scientific) following manufacturer's instructions. Subsequent cDNA was stored at -20°C until further analysis.

Primers were previously published (Sagirkaya et al., 2006) or designed using the NCBI database (Appendix A – Table 2), and initial specificity was verified by NCBI BLAST (https://blast.ncbi.nlm.nih.gov/Blast.cgi) to ensure no cross-reactivity with other loci. Primer length between 70 to 150 bp and GC contents of each primer (50 to 60%) were selected to avoid primer dimer formation. Amplification efficiency was evaluated for each primer by performing serial dilutions of cDNA and confirming linear amplification of a single product confirmed by melt curve analysis. All primers had to meet MIQE guidelines for further use (Pearson correlation coefficient $r > 0.98$ and efficiency of 90% to 110%). A no template negative control was used in place of cDNA to determine non-specific amplification.

Real-time RT-PCR was performed in 20 µL reactions using iTaq Universal SYBR green chemistry (Bio-Rad) and 250 nM of each forward and reverse primer. A Bio-Rad CFX Connect

light cycler (Bio-Rad) was employed to perform real-time RT-PCR using a three-step protocol. The annealing temperature was adjusted (*RPL19, SLC2A 1, BCL2, BAX, HSP* at 60°C and *SDHA* at 62.4°C) according to the primer being used. The PCR protocol began with an initial denaturation step at 95°C for 30 sec followed by 40 cycles at 95°C for 5 sec, specific annealing temperature for 10 sec and 60°C for 30 sec. The geometric mean of two housekeeping genes (*SDHA* and *RPL19*) was calculated and relative expression for genes of interest were calculated using the $2^{-\Delta Ct}$ method relative to the housekeeping genes.

Statistical Analysis

The SAS v 9.4 software package (SAS Institute Inc., Cary, NC) was used for statistical analysis. Data obtained from PCR were analyzed using the MIXED procedure of SAS and the model included the fixed effect of treatment. Treatment effects were determined by analysis of ΔCt data, but results are shown as relative expression to housekeeping genes.

The generalized linear mixed models procedures (Proc GLIMMIX) was used to evaluate the effects of treatment on the percent of oocytes that cleaved and the percentage of putative zygotes to become blastocysts. Each embryo was considered as an individual observation and development considered as a binary variable (0 =did not occur; 1 = occurred). Treatment was considered as a fixed effect and replicate was used as a random effect. Unless otherwise stated, data are presented as the LSM $\pm$ SEM. A P-value ≤ 0.05 was considered statistically significant.

Results and Discussion

Previous studies have reported that COCs of mice and cattle respond to the presence of bacterial components and increase expression of inflammatory mediators during maturation (Shimada et al., 2006; Bromfield and Sheldon, 2011). The present study reveal a significant impact on oocyte (Figure 3-1 and 3-2) or cumulus cell (Figure 3-3 and 3-4) gene expression when COCs were exposed to either LPS (Figure 3-1 and 3-3) or TNFα (Figure 3-2 and 3-4)

during IVM. Interestingly, the number of altered genes was greatest in oocytes compared to cumulus cells.

Effect of LPS Treatment During IVM on COC Expansion and Oocyte Gene Expression

There was an observed treatment effect of LPS exposure on expression of 24 genes in oocytes from the 92 genes evaluated (Table 3-2). When the effect of various concentrations of LPS were considered on gene expression, 31 genes were differentially regulated in oocytes exposed to at least one concentration of LPS (Figure 3-1). Exposure of COCs to LPS altered expression of oocyte genes involved in oocyte maturation and embryonic development such as *BMP15* and *SOX2* (Masui et al., 2007; Gilchrist et al., 2008). Oocyte expression of *BMP15* was increased ($P = 0.01$) after LPS treatment, compared to controls. A member of the TGF-β superfamily, BMP-15 is a paracrine factor secreted by the oocyte that regulates cumulus granulosa cell function, including proliferation. Along with GDF-9 (Dong et al., 1996; Spicer et al., 2006), another oocyte secreted factor member of the TGF-β superfamily, BMP-15 regulates oocyte maturation, cumulus cell metabolism, growth, death and expansion (Matzuk, 2002; Gilchrist et al., 2008; Coticchio et al., 2014). While we did not observe an effect of LPS on COC expansion (Figure 3-5), it may be that increased *BMP15* expression in oocytes contributes to increased expansion observed by others in the absence of gonadotrophins (Bromfield and Sheldon, 2011). The increase in expression of *SOX2* ($P \leq 0.001$) in response to LPS exposure may be due to a premature activation of genes required for proper embryo development. The function of SOX2 remains to be fully clarified, but it is known to be involved in pluripotency of mouse embryonic stem cells (ESCs) (Masui et al., 2007). Expression of *SOX2* seems to be essential for embryo development, as knockdown of the gene results in rodent embryos that arrest at the morula stage of development (Pan and Schultz, 2011). Similarly, in cattle, zygotes injected with *SOX2* siRNA have a decline in development to the blastocyst stage (Goissis and

Cibelli, 2014). The changes observed here in oocyte expression of genes involved in oocyte maturation and embryo development after treatment with LPS can potentially alter embryonic development. The observed increase in expression of these important genes does not ensure a higher quality embryo. Indeed, these changes to expression may be causing the oocyte to activate expression of genes required for embryonic development prematurely, compromising development.

The expression of genes associated with apoptosis and cell death were also affected by exposure of COCs to LPS. Expression of *MADD* and *NEDD4* were both increased ($P = 0.031$ and $P = 0.005$, respectively) in oocytes following LPS treatment. MAP kinase-activating death domain protein (MADD) is involved in the propagation of TNFα pro-apoptotic signals (Schievella et al., 1997). Neural precursor cell expressed developmentally down-regulated protein 4 (NEDD4) is a ubiquitin ligase that regulates membrane channels and receptors by controlling their density and availability on the cell surface (Cao et al., 2010). *NEDD4* null mice present delayed embryonic development, as well as neonatal lethality due to the role of *NEDD4* in controlling insulin growth factor 1 (IGF-1) and insulin signaling (Cao et al., 2010). The expression of *XIAP* was also increased ($P = 0.009$). X-linked inhibitor of apoptosis protein (XIAP) is a protein that inhibits apoptosis and prevents cell death, even in response to TNFα signaling (Duckett et al., 1998). Culture of rodent COCs in the presence of LPS induced the secretion of TNFα (Shimada et al., 2006) and the inappropriate accumulation of this inflammatory mediators may alter the oocytes capacity to regulate the expression of pro- and anti-apoptotic genes.

Interestingly, genes involved in transcription and epigenetic regulation were differentially regulated in oocytes after exposure to LPS. The genes *DNMT1* ($P = 0.04$), *DNMT3A* ($P \leq 0.001$),

POLR2D (*P* = 0.008), *ILF3* (*P* = 0.008) and *H2AFX* (*P* = 0.03) were upregulated in oocytes after LPS exposure, while *H2AFZ* (*P* = 0.002) was downregulated. Epigenetic reprogramming is essential for embryonic development and heritable changes to the epigenome. Mechanisms involved in epigenetic regulation of gene expression include DNA methylation and posttranslational modifications of histone, such as acetylation, phosphorylation and methylation (Beaujean, 2015). Embryonic genome activation occurs at the 8-cell stage in the bovine when the embryo activates the newly formed genome, and no longer relies on maternal transcripts (Beaujean, 2015). The process of embryonic genome activation involves the erasure and settlement of epigenetic marks, as well as non-erasure and preservation of methylation in some areas within the genome (Chong and Whitelaw, 2004). This process may lead to epigenetic inherence and potentially change the fate of the embryo and subsequent offspring. The genes mentioned above can potentially disrupt this process and change how the epigenome is established in the developing embryo. DNMT1 and DNMT3A are methyltransferases that maintain methylation and *de novo* methylation, respectively. The process of DNA demethylation can occur actively, mediated by ten-eleven translocation methylcytosine dioxygenase (TET)1 and TET2, or passively by decreasing the expression of *DNMT1* and *DNMT3A* (Hackett et al., 2013).

Among the genes involved in transcription regulation that were differentially expressed following LPS treatment, *POLR2D* is a subunit of RNA polymerase II responsible for mRNA synthesis. Additionally, *ILF3* is a double-stranded RNA binding protein that regulates gene expression and stabilizes mRNAs. Both of these factors, POLR2D and ILF3 may be important to maintain the oocyte prior to embryo genome activation. Expression of *H2AFX* was increased after LPS exposure. H2AFX is an H2A histone family member involved in regulation of gene

expression and the cellular response to DNA damage and stress (Cloutier et al., 2015). Interestingly, oocyte *H2AFZ* was downregulated ($P = 0.035$) following LPS exposure. Another member of the H2A histone family, *H2AFZ* has been shown to have a critical role in embryo development, as *H2AFZ* null embryos fail to develop, thus supporting the theory that appropriate chromatin structure is crucial for proper embryonic development (Faast et al., 2001). The alterations to the epigenetic machinery may impact not only the quality of the developing embryo but modify enduring marks that will be carried through the following generations. It is unclear if offspring of cows suffering postpartum uterine infections display developmental defects or alterations to the epigenome.

Other oocyte genes altered in response to LPS treatment were associated with multiple cellular functions, including control of cell cycle, cell structure and immune response. While genes associated with immunity were altered in response to LPS, such as *ADAM10* ($P = 0.002$), expression of oocyte *IL6* was not affected by LPS treatment ($P = 0.87$). Increased secretion of IL-6 has been previously reported after treatment of COCs with LPS (Bromfield and Sheldon, 2011; Price et al., 2013), but it is likely this response is attributable to the cumulus cells of the COC.

Effect of LPS Treatment During IVM on Cumulus Cell Gene Expression

There was a treatment effect of LPS on the expression of 7 genes in cumulus cells (Table 3-2). When the effect of individual doses of LPS on cumulus cells was evaluated, 12 genes were differentially regulated compared to controls (Figure 3-3). Among the genes altered were *ACKR4* ($P = 0.008$) a chemokine receptor, *CCNB1* ($P = 0.027$) and *FGF4* ($P = 0.04$) that control cell cycle and cell growth, respectively (Eswarakumar et al., 2005; Nibbs and Graham, 2013; Fache and Hamdouch, 2014). Gene expression of the *POU5F1* ($P = 0.004$) was increased in cumulus cells, encoding the OCT-4 transcription factor that regulates pluripotency of the embryo (Niwa et

al., 2000; Masui et al., 2007). There is a delicate balance of OCT-4 that is present in the embryo, as too much or too little will disrupt cellular differentiation and self-renewal (Niwa et al., 2000).

Effect of TNFα Treatment During IVM on COC Expansion and Gene Expression

Exposure of COCs to TNFα only affected the expression of 1 gene in oocytes and 3 genes in cumulus cells (Table 3-2). The single gene affected in oocytes was *DTX3* ($P = 0.04$), a ubiquitin ligase involved in the Notch signaling pathway (Bray, 2006). The Notch pathway regulates cell proliferation, cell fate and death (Bray, 2006). Treatment of COCs with TNFα decreased expression of *GJA1* ($P = 0.04$), *PLD2* ($P = 0.008$) and *NOD2* ($P = 0.04$) (Table 3-2). *GJA1* is a connexin and a component of cellular gap junctions. Gap junctions are fundamental for communication between cumulus cells and also between the oocyte and cumulus cell during oocyte development and maturation. These gap junctions are formed at the end of the TZPs and allow the contact between the two cell types (Albertini et al., 2001). TNFα is a potent cytokine with contradictory roles: it is involved in the pro-inflammatory response and can further activate inflammation, but it can also exhibit a role in controlling the extent of the immune response and inflammation (Akdis et al., 2016). It may be that TNFα exerted a modulatory function during IVM, limiting the genes that were differentially expressed in our system, or even that the genes evaluated in our analysis were not targets for TNFα as they were for LPS.

The communication between the oocytes and the somatic cells surrounding it is essential for proper maturation of the COC. In part, the oocyte regulates cumulus cell growth and development (Matzuk, 2002; Su and Eppig, 2010), and signals to cumulus cells to facilitate its own nutrient supply for growth. Conversely, oocyte meiotic arrest and resumption are dependent on signals from the cumulus cells (Liu et al., 2014). The COCs response to the presence of LPS or TNFα is not restricted to only one of its cellular compartments, and appears to impact the

oocyte more than the cumulus cells. The impacts observed in gene expression have the potential to alter oocyte development and ultimately impact the development of the offspring.

Cumulus Expansion, Embryonic Development and Gene Expression

Addition of LPS to oocyte maturation medium did not impact expansion rate of COCs, independent of the dose (Figure 3-5A), similar to findings of others (Bromfield et al., 2011) that show no effect of LPS on COC expansion in the presence of gonadotrophins. However, expansion of the COC was significantly reduced ($P \leq 0.02$) after exposure to TNFα compared to control. The addition of either 1 ng/mL, 10 ng/mL or 100 ng/mL of TNFα reduced COC expansion rate by 24%, 25%, and 14% respectively (Figure 3-5B).

In order to further evaluate the effects of LPS or TNFα exposure on COCs, oocytes were subjected to *in vitro* fertilization and subsequent embryos cultured to the blastocyst stage of development. There was no significant effect of either LPS (Figure 3-6. A, B) or TNFα (Figure 3-6. C, D) treatment on the percentage of oocytes that cleaved following fertilization or the percentage of putative zygotes that became blastocyst stage embryos. Previous studies demonstrate a reduction in the number of putative zygotes that develop to blastocyst when oocytes were treated with LPS or TNFα during IVM (Soto et al., 2003a; b). In comparison to our study, we had a significantly smaller number of COCs per replicate (~50) which may have impacted our power to detect significant changes in embryo development.

Subsequent blastocysts were subjected to real-time RT-PCR analysis to evaluate gene expression of genes associated with embryo quality. The genes selected for evaluation of embryonic quality were *BCL2*, *BAX*, *HSPA1* and *SLC2A1*. Exposure of COCs to LPS or TNFα during IVM did not alter subsequent blastocyst gene expression of any genes evaluated (Figure 3-7 and 3-8). These data supports our observation of no effect of treatment on cleavage or blastocyst rates. The use of gene expression to evaluate the blastocysts was not performed in the

previous studies and could potentially predict embryonic quality (Corcoran et al., 2005). It is not surprising that oocytes that are able to reach the blastocyst stage of development after "surviving" the challenge of LPS or TNFα may not show changes in gene expression. These embryos were already able to bypass the detrimental treatment effects of LPS or TNFα and successfully become a blastocyst; however we did not evaluate alterations to the epigenome in these embryos, which may have an impact in later development or the future offspring.

Table 3-1. Selected target genes for analysis by Fluidigm.

Gene Symbol	RefSeq ID	Reason for selection
ACKR4	NM_174265.2	Chemokine receptor
ACTA2	NM_001034502.1	Cell structure and integrity
ACTB	NM_173979.3	Housekeeping
ACVR1B	XM_002687257.5	Activin receptor
ACVR2B	NM_174495.2	Activin receptor
ADAM10	NM_174496.2	TNFα activation
ADAM17	XM_002691486.5	TNFα activation
AJAP1	NM_001206815.1	Cell structure and integrity
APAF1	NM_001191507.1	Apoptosis – Cell death
APOPT1	NM_001076459.2	Apoptosis – Cell death
AREG	NM_001099092.1	Cell growth, proliferation and fate
ATM	XM_005215785.3	Cell cycle checkpoint
AY192564	AY192564.1	Cell growth, proliferation and fate
BAD	NM_001035459.1	Cell death
BAK1	NM_001077918.1	Cell death
BMP15	NM_001031752.1	Oocyte specific factor - oocyte maturation
C1QA	NM_001014945.2	Complement component
CACNA1G	NM_001193140.1	Calcium influx regulation
CASP7	XM_002698509.3	Cell death
CCNB1	NM_001045872.1	Essential for control of cell cycle
CCND2	NM_001076372.1	Ovarian granulosa and germ cell proliferation
CDC42EP4	NM_001046471.1	Cell structure - cytoskeleton
CDK1	NM_174016.2	MPF subunit
CREM	NM_001034710.3	Granulosa cell – control of cell cycle
CXCL12	NM_001113174.1	Chemokine induced by LPS and TNF
CXCL2	NM_174299.3	Cell proliferation suppression

Table 3-1. Continued

Gene Symbol	RefSeq ID	Reason for selection
CYP11A1	NM_176644.2	Steroidogenesis
DDX4	NM_001007819.1	Oocyte specific factor - germ cell development
DGAT2	NM_205793.2	Synthesis of triglycerides
DNMT1	NM_182651.2	Methyltransferase
DNMT3A	NM_001206502.1	Methyltransferase
DTX3	NM_001105393.1	Cell growth, proliferation and fate
ESRP1	XM_005215674.3	Oocyte specific factor - epithelial splicing regulation
ESRRB	XM_010809669.1	Estrogen receptor like protein
FGF10	NM_001206326.1	Cumulus expansion and embryo development
FGF4	NM_001040605.2	Embryonic development, cell growth
FGFR2	NM_001205310.1	FGF receptor
GAPDH	NM_001034034.2	Housekeeping
GATA6	XM_001253596.3	Regulation of cellular differentiation
GDF9	NM_174681.2	Oocyte specific factor - oocyte maturation
GJA1	NM_174068.2	Gap junctions
GREM1	NM_001082450.1	BMP antagonist
H2AFX	NM_001079780.2	Histone
H2AFZ	NM_174809.2	Histone
HAS2	NM_174079.2	Hyaluronan synthase
HDAC1	NM_001037444.2	Histone acetylation
HDAC8	NM_001076231.2	Histone acetylation
HPSE	NM_174082.2	Cell structure - extracellular matrix
HSD3B1	NM_174343.2	Steroidogenesis
IGF1	NM_001077828.1	Cell growth, proliferation and fate
IGF2	NM_174087.3	Cell growth, proliferation and fate
IL6	NM_173923.2	Proinflammatory cytokine
ILF3	NM_001206495.1	Cell growth, proliferation and fate
INHBA	NM_174363.2	Inhibin

Table 3-1. Continued

Gene Symbol	RefSeq ID	Reason for selection
ITPR2	NM_174369.2	IP3 receptor
MAB21L2	XM_002694319.3	Cell fate
MADD	NM_001193078.1	Cell death
MAPK13	NM_001014947.1	Activated by proinflammatory cytokines
MOS	XM_002692654.3	Oocyte specific factor - MAPK activation
NEDD4	XM_003582720.3	Control of cell cycle
NF2	XM_002694607.4	Cell structure - cytoskeleton
NLRP5	NM_001007814.2	Oocyte specific factor - embryo development
NOD2	NM_001002889.1	Inflammatory response to bacteria
NOTCH2	XM_002686114.4	Cell fate
NT5E	NM_174129.3	Inflammatory response
PIK3IP1	NM_001075552.1	Control of cell cycle
PLD2	NM_001075827.1	Cell structure - cytoskeleton
POLR2D	NM_001076458.2	RNA polymerase subunit
POU5F1	NM_174580.2	Stem cell pluripotency
PPBP	XM_002688351.3	Growth factor, chemoattractant and activator of neutrophils
PPP2R3A	XM_005201921.2	Control of cell division
PRKAR2B	NM_174649.2	Control of cell cycle
PTEN	XM_002698370.4	Regulates IP3
PTGER3	NM_181032.1	Prostaglandin receptor
PTGER4	NM_174589.2	Prostaglandin receptor
PTPPK	NM_001191537.1	Cell growth and differentiation
PTX3	NM_001076259.2	Innate resistance to pathogens
RAC1	NM_174163.2	Cell growth, cytoskeleton reorganization
RIPK3	NM_001101884.2	Component of TNFα receptor complex
S100A1	NM_001099042.2	Calcium influx regulation

Table 3-1. Continued

Gene Symbol	RefSeq ID	Reason for selection
SDHA	NM_174178.2	Housekeeping
SOX17	NM_001206251.1	Embryonic development
SOX2	NM_001105463.2	Embryonic development
STAT1	NM_001077900.1	Cytokine stimulated
STAT3	NM_001012671.2	Cytokine stimulated
TGFB1	NM_001166068.1	Cell growth, proliferation and differentiation
TJAP1	NM_001192419.1	Tight junction
TNF	NM_173966.3	Proinflammatory cytokine, cell death
TNFAIP6	NM_001007813.2	Cytokine stimulated
TNFSF8	NM_001025207.1	TNFα ligand
UBEA2A	NM_001105325.2	Ubiquitination – DNA damage
WEE1	NM_001101205.1	G2 checkpoint
XIAP	NM_001205592.1	Apoptosis inhibition through TNFα
YWHAZ	NM_174814.2	Housekeeping
ZAR1	NM_001076203.1	Zygote arrest

Table 3-2. Effect of LPS or TNFα exposure during IVM on oocyte gene expression.

Genes	Treatment					
	LPS	SEM	P value	TNFα	SEM	P value
ACKR4	0.0007	0.0001	0.931	0.0334	0.004	0.9328
APAF1	1.1607	0.0381	0.13	1.1607	0.0381	0.8624
C1QA	0.0013	0.0002	0.496	0.0019	0.0009	0.3877
CXCL12	0.0194	0.0020	0.3558	0.0219	0.0014	0.9422
ESRP1	2.4961	0.1672	0.0037*	2.0649	0.1066	0.7901
GJA1	0.1202	0.0101	0.3131	0.1274	0.0050	0.9379
HSD3B1	0.0084	0.0014	0.6664	0.0091	0.0007	0.4366
MAB21L2	0.0006	0.0003	0.0427*	0.0015	0.0005	0.3274
NOTCH2	0.0002	0.0001	0.3245	0.0002	0.0001	0.5252
PRKAR2B	0.0277	0.0194	0.0198*	0.0333	0.0115	0.0742
S100A1	0.0140	0.0020	0.5224	0.0170	0.0011	0.0784
TNF	0.0025	0.0006	0.4957	0.0025	0.0005	0.6251
ACTA2	0.0203	0.0027	0.1406	0.0167	0.0016	0.9939
APOPT1	0.3290	0.0212	0.3103	0.3033	0.0114	0.8395
CACNA1G	0.0018	0.0008	0.7926	0.0034	0.0043	0.2162
CXCL2	0.00004	0.00004	0.7387	0.00032	0.00014	0.0707
ESRRB	0.0010	0.0003	0.1232	0.0013	0.0002	0.6145
GREM1	0.0171	0.0023	0.5909	0.0139	0.0013	0.4434
IGF1	0.0023	0.0005	0.6496	0.0025	0.0003	0.8617
MADD	0.1156	0.0107	0.0319*	0.0923	0.0061	0.9448
NT5E	0.0330	0.0034	0.6429	0.0359	0.0017	0.6434
PTEN	0.6076	0.0337	<.0001*	0.5517	0.0326	0.2783
TNFAIP6	0.0013	0.0021	0.2488	0.0111	0.0078	0.9474
AREG	0.0010	0.0004	0.8393	0.0008	0.0002	0.94
CASP7	0.0017	0.0008	0.1777	0.0022	0.0004	0.5256
CYP11A1	0.0071	0.0106	0.0223*	0.0222	0.0136	0.2244
FGF10	0.0597	0.0084	0.4349	0.0631	0.0036	0.1783
H2AFX	0.1442	0.0124	0.0357*	0.1217	0.0041	0.8003
IGF2	0.0012	0.0003	0.8151	0.0016	0.0003	0.3687
MAPK13	0.0018	0.0003	0.9753	0.0017	0.0001	0.9957
PIK3IP1	0.0058	0.0016	0.9392	0.0064	0.0009	0.7364
PTGER3	0.0396	0.0052	0.959	0.0490	0.0058	0.4828
SOX17	0.0023	0.0006	0.8161	0.0023	0.0003	0.8579
TNFSF8	0.0102	0.0019	0.5494	0.0095	0.0010	0.821
ACVR1B	0.0561	0.0061	0.0349	0.0472	0.0033	0.4825
ATM	0.0006	0.0001	0.8868	0.0006	0.0000	0.7924
CCNB1	9.6978	0.5636	0.47	10.1756	0.3977	0.2734
DDX4	0.3304	0.0334	0.2069	0.2991	0.0165	0.8113
FGF4	0.0055	0.0013	0.4721	0.0060	0.0010	0.6461
H2AFZ	0.0236	0.0112	0.002*	0.0475	0.0118	0.1284
IL6	0.0020	0.0009	0.8777	0.0011	0.0005	0.4003
MOS	1.8365	0.0997	0.3445	1.8086	0.0887	0.3426
PLD2	0.0009	0.0006	0.0134*	0.0016	0.0006	0.3713
PTGER4	0.0012	0.0003	0.8657	0.0015	0.0003	0.7477
SOX2	0.0916	0.0097	0.0009*	0.0606	0.0059	0.7261
UBE2A	0.0029	0.0008	0.8866	0.0033	0.0005	0.7423
HAS2	0.3336	0.0231	0.0011*	0.2832	0.0164	0.4449

Table 3-2. Continued

Genes	Treatment					
	LPS	SEM	P value	TNFα	SEM	P value
FGFR2	0.0683	0.0074	0.6933	0.0672	0.0033	0.8163
DGAT2	0.1063	0.0160	0.7432	0.1068	0.0059	0.5964
CCND2	0.0020	0.0018	0.0676	0.0029	0.0011	0.3904
AY192564	0.0007	0.0004	0.209	0.0004	0.0001	0.7437
ACVR2B	0.0571	0.0053	0.0688	0.0493	0.0036	0.8814
WEE1	0.3853	0.0563	0.5864	0.4486	0.0503	0.4206
STAT1	0.4372	0.0284	0.1688	0.4038	0.0110	0.9763
PTPRK	0.0963	0.0092	0.4132	0.1084	0.0053	0.896
POLRD2	1.6775	0.0884	0.0081*	1.4198	0.0615	0.8111
NEDD4	1.6740	0.0858	0.0059*	1.4097	0.0626	0.8394
ILF3	0.6176	0.0381	0.0076*	0.5013	0.0354	0.9791
HDAC1	0.3182	0.0158	0.2322	0.3019	0.9301	0.8998
DNMT1	2.6157	0.1469	0.0405*	2.4392	0.0975	0.3144
CDC42EP4	0.0368	0.0040	0.0347*	0.0328	0.0027	0.3393
BAD	0.0440	0.0043	0.9165	0.0421	0.0014	0.702
ADAM10	0.6347	0.0288	0.0028*	0.5843	0.0192	0.1483
XIAP	0.4186	0.0249	0.0095*	0.3683	0.0193	0.7149
STAT3	6.9344	0.2891	0.2883	7.1652	0.2107	0.1272
PTX3	0.0006	0.0001	0.4087	0.0014	0.0005	0.1863
POU5F1	0.1242	0.0070	0.1915	0.1315	0.0052	0.9408
NF2	0.0843	0.0062	0.0011*	0.0674	0.0039	0.4735
INHBA	0.0177	0.0131	0.0416*	0.0265	0.0120	0.08
HDAC8	0.2325	0.0150	0.0589	0.2224	0.0098	0.4425
GATA6	0.0007	0.0005	0.131	0.0021	0.0011	0.6746
DNAMT3A	0.0406	0.0039	0.0007*	0.0307	0.0022	0.3849
CDK1	0.4638	0.0344	0.182	0.4489	0.0183	0.4117
BAK1	0.0256	0.0032	0.5485	0.0218	0.0012	0.4642
ADAM17	0.2880	0.0243	0.5861	0.2808	0.0113	0.324
TGFB1	0.0104	0.0024	0.8631	0.0161	0.0064	0.5142
RAC1	1.7192	0.0896	0.0732	1.5524	0.0505	0.9976
PPBP	0.0022	0.0019	0.8833	0.0097	0.0048	0.461
NLRP5	0.0814	0.0120	0.2959	0.0667	0.0029	0.8073
IRF6	0.0083	0.0014	0.1785	0.0067	0.0003	0.677
HPSE	0.0027	0.0059	0.0249*	0.0062	0.0046	0.1882
GDF9	0.9065	0.0769	0.3141	0.8806	0.0420	0.6936
DTX3	0.0157	0.0022	0.3269	0.0207	0.0034	0.0364*
CREM	0.1317	0.0105	0.0039*	0.1082	0.0074	0.3938
BMP15	8.6017	0.5417	0.0199*	8.2590	0.2618	0.084
AJAP1	0.0004	0.0002	0.8235	0.0004	0.0001	0.7844
ZAR1	4.9473	0.1697	0.1996	4.6386	0.1153	0.8133
TJAP1	0.0998	0.0058	0.2484	0.0924	0.0029	0.9306
RIPK3	0.0020	0.0007	0.7107	0.0019	0.0004	0.5337
PPP2R3A	0.0013	0.0006	0.4911	0.0022	0.0006	0.2434
NOD2	0.0001	0.0003	0.6025	0.0001	0.0001	0.8586
ITPR2	0.0540	0.0067	0.2599	0.0496	0.0053	0.7604

Data was normalized to the geometric mean of housekeeping genes, and treatment effect (vehicle/LPS or vehicle/TNF) is presented as least-squares means ± SEM.

Table 3-3. Effect of LPS or TNFα exposure during IVM on cumulus cell gene expression.

Genes	Treatment					
	LPS	SEM	P value	TNFα	SEM	P value
ACKR4	0.2554	0.0678	0.0082	0.1915	0.0274	0.0802
APAF1	0.0595	0.0321	0.4803	0.0508	0.0131	0.3024
C1QA	0.0408	0.0284	0.5821	0.0545	0.0234	0.8348
CXCL12	0.0032	0.0052	0.8085	0.0182	0.0076	0.4152
ESRP1	0.6080	0.1837	0.7477	0.3532	0.0580	0.1911
GJA1	0.0756	0.0502	0.1337	0.0653	0.0156	0.044
HSD3B1	0.2320	0.0941	0.1503	0.3293	0.0855	0.4417
MAB21L2	0.2937	0.0602	0.1651	0.2407	0.0377	0.8938
NOTCH2	0.0014	0.0014	0.192	0.0061	0.0048	0.5965
PRKAR2B	0.5980	0.2436	0.8036	0.4079	0.1112	0.6308
S100A1	0.0136	0.0104	0.3574	0.0170	0.0061	0.9266
TNF	0.0208	0.0112	0.2835	0.0273	0.0089	0.6464
ACTA2	0.0013	0.0039	0.0709	0.0036	0.0024	0.7868
APOPT1	0.0471	0.0176	0.5363	0.0644	0.0143	0.8771
CACNA1G	0.9556	0.3057	0.8617	0.7769	0.1329	0.6598
CXCL2	0.0470	0.0234	0.8402	0.0450	0.0123	0.7575
ESRRB	0.0003	0.0005	0.719	0.0000	0.0002	0.6212
GREM1	0.5193	0.1269	0.239	0.4204	0.0443	0.4358
IGF1	0.0518	0.0264	0.3012	0.0745	0.0310	0.3788
MADD	0.0039	0.0036	0.6078	0.0028	0.0014	0.5621
NT5E	0.0342	0.0412	0.3747	0.0404	0.0118	0.7679
PTEN	1.2049	0.5870	0.2371	1.8903	0.5531	0.8824
TNFAIP6	0.1405	0.1290	0.819	0.2045	0.1589	0.1697
AREG	0.0008	0.0051	0.1906	0.0004	0.0031	0.5347
CASP7	0.0331	0.0237	0.4825	0.0561	0.0190	0.1877
CYP11A1	0.3391	0.1427	0.2893	0.2517	0.0546	0.1271
FGF10	0.0584	0.0211	0.796	0.0895	0.0305	0.7154
H2AFX	0.1094	0.0305	0.1795	0.0829	0.0153	0.8861
IGF2	0.0286	0.0128	0.427	0.0336	0.0078	0.6394
MAPK13	0.0087	0.0065	0.8211	0.0079	0.0039	0.4407
PIK3IP1	0.1836	0.1092	0.0393	0.2241	0.0711	0.1857
PTGER3	1.9176	0.7802	0.3242	2.9119	0.7431	0.6979
SOX17	0.0279	0.0306	0.5423	0.0795	0.0370	0.305
TNFSF8	0.00002	0.00002	0.87140	0.0001	0.0001	0.8238
ACVR1B	0.0027	0.0036	0.715	0.0003	0.0002	0.4916
ATM	0.0122	0.0056	0.7135	0.0162	0.0039	0.9713
CCNB1	0.8013	0.3845	0.0277	0.4483	0.0786	0.6499
DDX4	0.2207	0.1147	0.2121	0.3238	0.0992	0.4157
FGF4	0.1753	0.0844	0.0414	0.2254	0.0619	0.2212
H2AFZ	0.4561	0.0879	0.8542	0.5111	0.0612	0.8102
IL6	0.0004	0.0019	0.0994	0.0009	0.0014	0.3219
MOS	0.1299	0.0608	0.1937	0.0818	0.0155	0.4569
PLD2	0.0136	0.0127	0.2608	0.0017	0.0030	0.0085
PTGER4	0.0802	0.0263	0.0472	0.0719	0.0121	0.0867
SOX2	0.0569	0.0242	0.9475	0.0610	0.0108	0.8964
UBE2A	0.0714	0.0467	0.2368	0.1157	0.0377	0.8412
HAS2	0.0201	0.0101	0.389	0.0101	0.0034	0.9256

Table 3-3. Continued

Genes	Treatment					
	LPS	SEM	P value	TNFα	SEM	P value
FGFR2	0.0070	0.0062	0.7215	0.0123	0.0096	0.6368
DGAT2	0.1361	0.0294	0.4805	0.1447	0.0195	0.6906
CCND2	0.0441	0.0200	0.9252	0.0209	0.0052	0.1422
AY192564	0.0041	0.0067	0.9211	0.0105	0.0085	0.9741
ACVR2B	0.0100	0.0044	0.9537	0.0068	0.0014	0.4428
WEE1	19.7180	8.9168	0.3962	29.3262	7.6778	0.7744
STAT1	0.0863	0.0506	0.3965	0.0989	0.0178	0.1928
PTPRK	0.0415	0.0196	0.1175	0.0473	0.0102	0.2507
POLRD2	0.1242	0.0752	0.6455	0.1498	0.0314	0.6779
NEDD4	0.1223	0.0742	0.719	0.1428	0.0288	0.6451
ILF3	0.5829	0.1251	0.1941	0.4155	0.0588	0.8003
HDAC1	0.0407	0.0197	0.497	0.0555	0.0114	0.3662
DNMT1	0.4276	0.1032	0.9251	0.4340	0.0657	0.8312
CDC42EP4	0.1562	0.0443	0.2883	0.1475	0.0223	0.2419
BAD	0.0247	0.0081	0.6903	0.0186	0.0046	0.2582
ADAM10	5.3458	2.3687	0.3128	7.7050	2.1515	0.6018
XIAP	0.3959	0.1004	0.4735	0.3203	0.0548	0.9855
STAT3	1.1509	0.4279	0.2618	0.7628	0.1290	0.6367
PTX3	0.0141	0.0045	0.5713	0.0194	0.0042	0.9849
POU5F1	0.1211	0.0307	0.004	0.1155	0.0248	0.0787
NF2	0.0063	0.0048	0.8676	0.0150	0.0050	0.4707
INHBA	0.1748	0.0938	0.6488	0.1468	0.0284	0.4961
HDAC8	0.0115	0.0084	0.0291	0.0355	0.0102	0.2413
GATA6	0.0260	0.0156	0.1793	0.0418	0.0133	0.5882
DNAMT3A	0.0097	0.0071	0.457	0.0030	0.0014	0.6322
CDK1	0.2752	0.0950	0.9126	0.1865	0.0319	0.3125
BAK1	0.0097	0.0072	0.8403	0.0203	0.0076	0.6613
ADAM17	0.0107	0.0132	0.7061	0.0068	0.0037	0.6781
TGFB1	0.0090	0.0071	0.8498	0.0549	0.0165	0.2017
RAC1	0.1432	0.0688	0.614	0.2128	0.0505	0.3431
PPBP	1.5729	0.5020	0.9311	1.2004	0.1765	0.2554
NLRP5	0.0012	0.0016	0.8004	0.0003	0.0003	0.7966
IRF6	0.0001	0.0002	0.994	0.00002	0.00001	0.8726
HPSE	0.0176	0.0250	0.4226	0.0723	0.0591	0.7634
GDF9	0.0819	0.0369	0.7254	0.0963	0.0226	0.7363
DTX3	0.8639	0.2336	0.494	0.6575	0.0682	0.9796
CREM	0.0023	0.0031	0.3517	0.0022	0.0021	0.4698
BMP15	0.8632	0.2949	0.3108	0.5399	0.0663	0.8607
AJAP1	0.0134	0.0130	0.8871	0.0188	0.0080	0.6511
ZAR1	0.4673	0.1371	0.3039	0.3155	0.0521	0.9858
TJAP1	0.1070	0.0439	0.7611	0.1169	0.0236	0.5766
RIPK3	0.0035	0.0040	0.2667	0.0028	0.0022	0.7953
PPP2R3A	0.0054	0.0075	0.838	0.0034	0.0035	0.9876
NOD2	0.0032	0.0086	0.0553	0.00001	0.0027	0.038
ITPR2	0.0055	0.0086	0.1	0.0076	0.0042	0.5157

Data was normalized to the geometric mean of housekeeping genes, and treatment effect (vehicle/LPS or vehicle/TNF) is presented as least-squares means ± SEM.

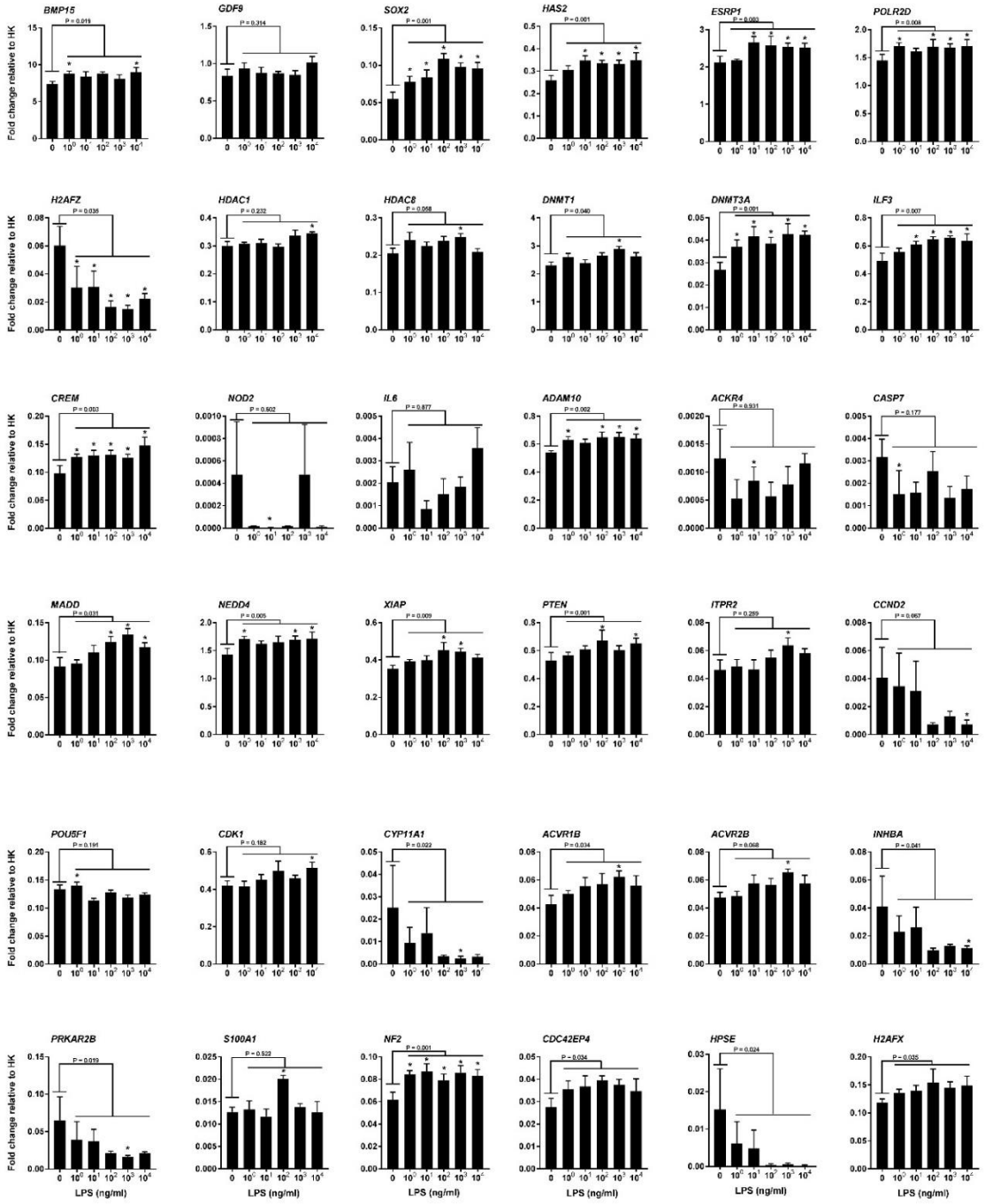

Figure 3-1. Effect of LPS during IVM on oocyte gene expression. Genes are grouped according to function from left to right, per row: oocyte maturation, embryo development, epigenetic machinery, inflammation, cell death and others. Data are presented as fold change relative to the housekeeping gene (HK); housekeeping genes were *SDHA*, *GAPDH*, *ACTB* and *YWHAZ*. Data were analyzed as least-squares means ± SEM. The *P* values for effect of treatment are indicated by the value above the bars. Asterisk (*) indicates a significant effect for the specific dose of LPS ($P \leq 0.05$) compared to controls.

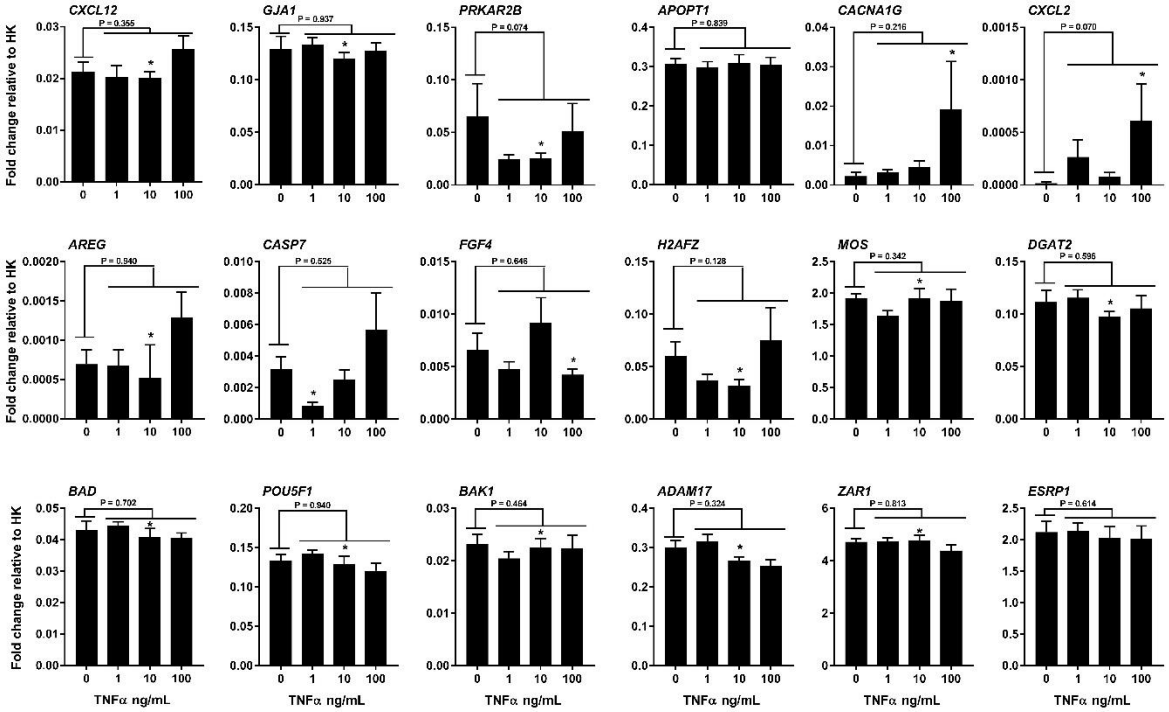

Figure 3-2. Effect of TNFα during IVM on oocyte gene expression. Data are presented as fold change relative to the housekeeping gene (HK); housekeeping genes were *SDHA*, *GAPDH*, *ACTB* and *YWHAZ*. Data were analyzed as least-squares means ± SEM. The *P* values for effect of treatment are indicated by the value above the bars. Asterisk (*) indicates a significant effect for the specific dose of TNFα ($P \leq 0.05$) compared to controls.

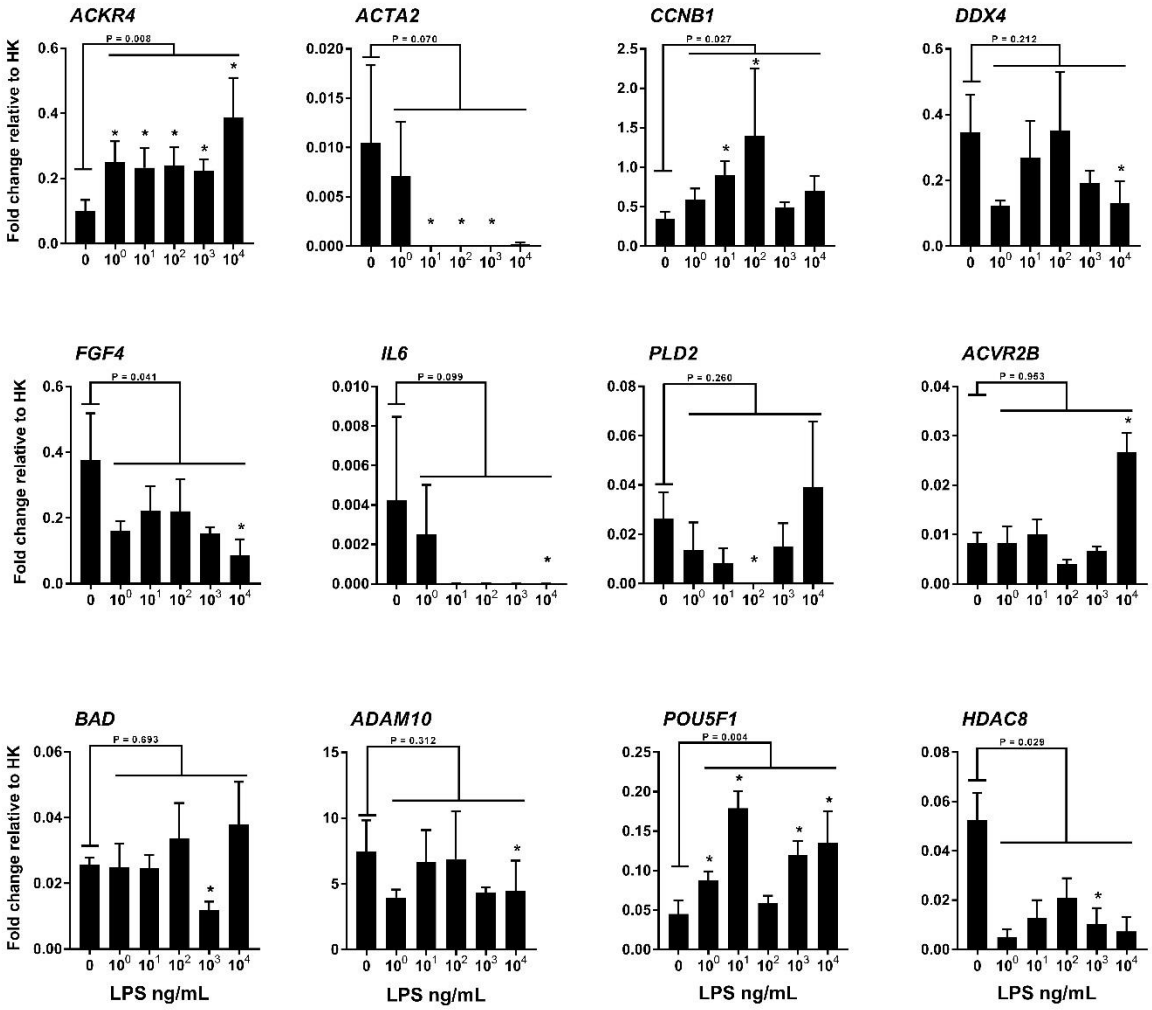

Figure 3-3. Effect of LPS during IVM on cumulus cell gene expression. Data are presented as fold change relative to the housekeeping gene (HK); housekeeping genes were *SDHA*, *GAPDH*, *ACTB* and *YWHAZ*. Data were analyzed as least-squares means ± SEM. The *P* values for effect of treatment are indicated by the value above the bars. Asterisk (*) indicates a significant effect for the specific dose of LPS ($P \leq 0.05$) compared to controls.

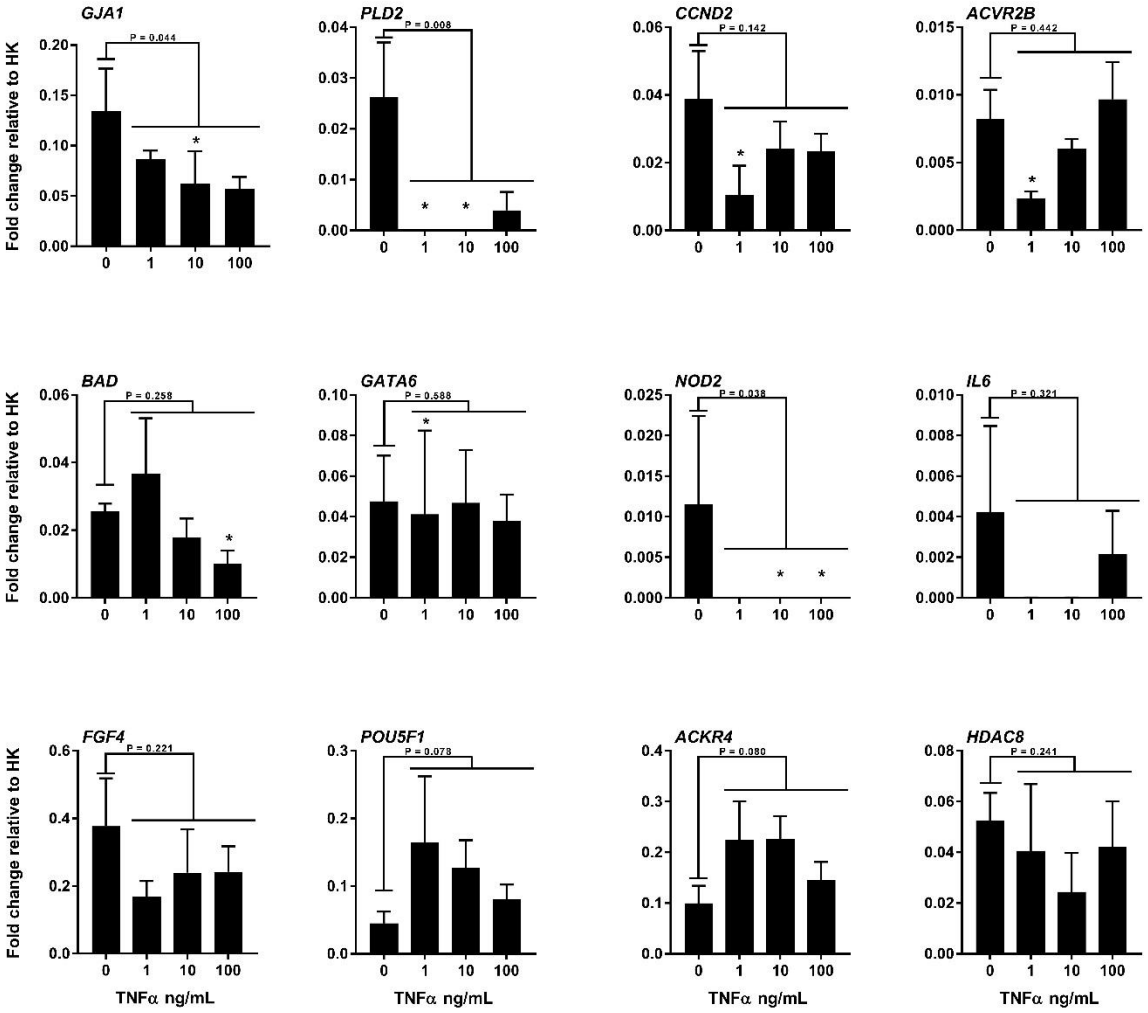

Figure 3-4. Effect of TNFα during IVM on cumulus cell gene expression. Data are presented as fold change relative to the housekeeping gene (HK); housekeeping genes were *SDHA*, *GAPDH*, *ACTB* and *YWHAZ*. Data were analyzed as least-squares means ± SEM. The *P* values for effect of treatment are indicated by the value above the bars. Asterisk (*) indicates a significant effect for the specific dose of TNFα ($P \leq 0.05$) compared to controls.

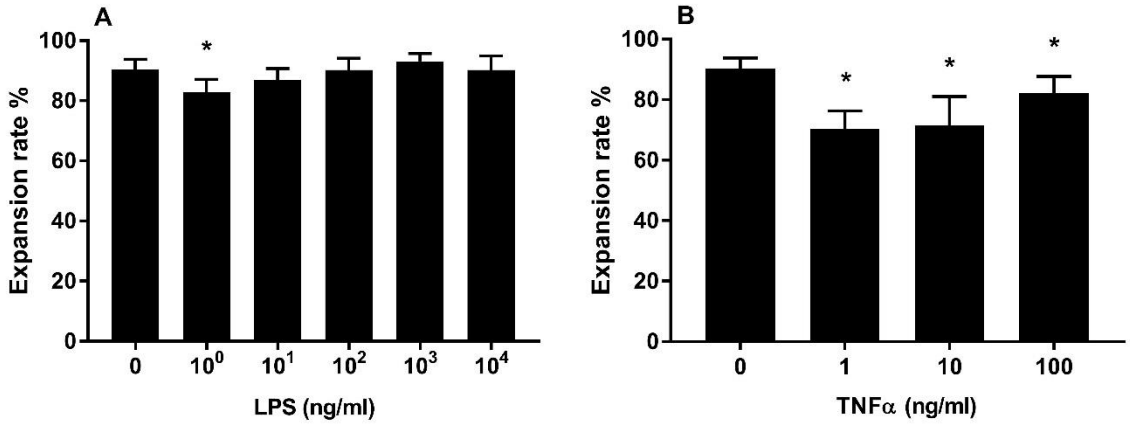

Figure 3-5. Effect of LPS (A) or TNFα (B) exposure during IVM on COC expansion. Data are presented as least-squares means ± SEM. Asterisk (*) indicates a significant effect compared to vehicle controls ($P \leq 0.05$).

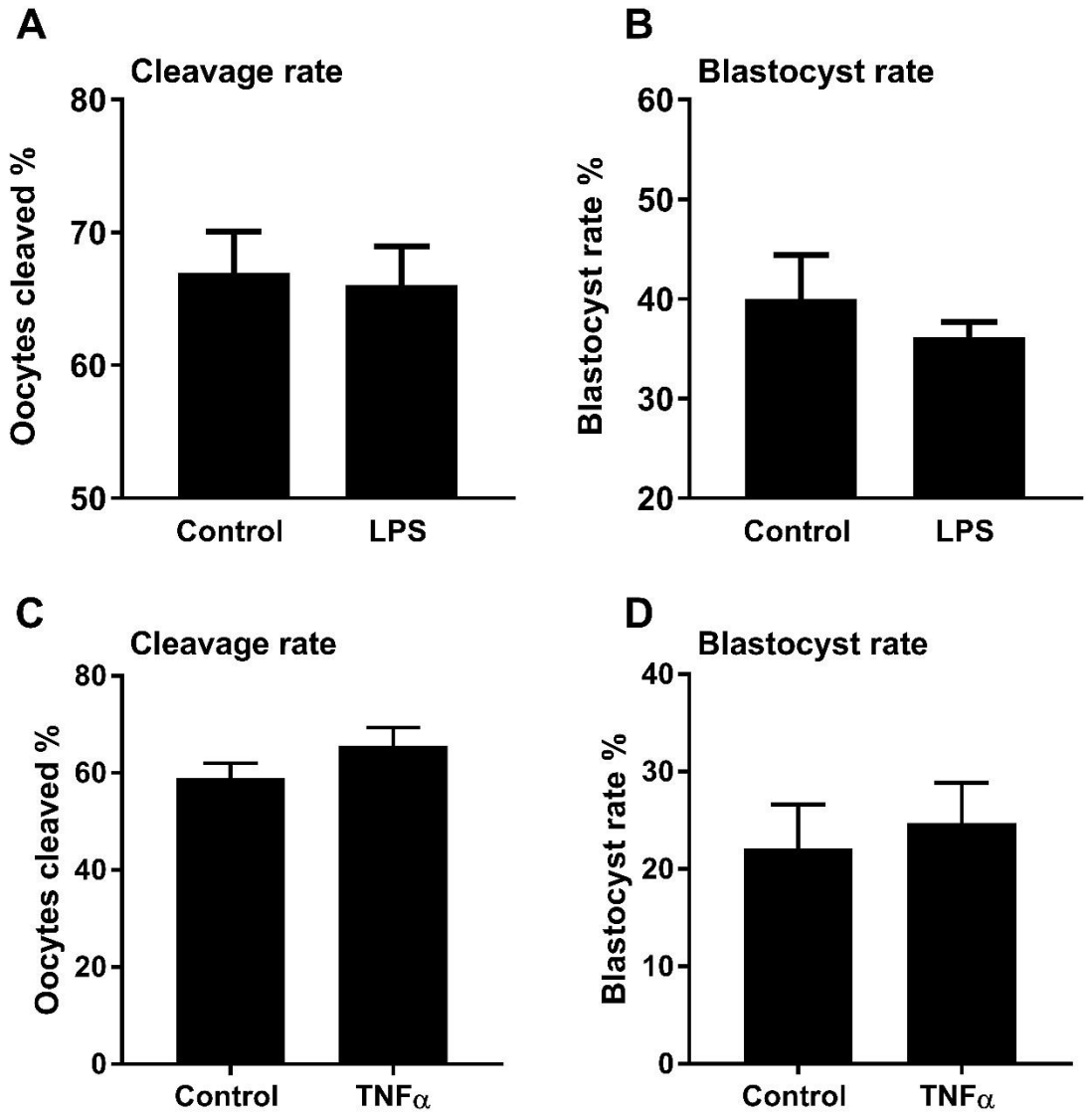

Figure 3-6. Effect of LPS (A, B) or TNFα (C, D) exposure during IVM on developmental competence of oocytes to achieve cleavage or the blastocyst stage of development. The percentage of oocytes cleaved (A, C) and percent of putative zygotes that became blastocysts (B, D) are shown. Data are presented as least-squares means ± SEM. (LPS n= 377, control n = 355; TNFα n= 331, control n =335).

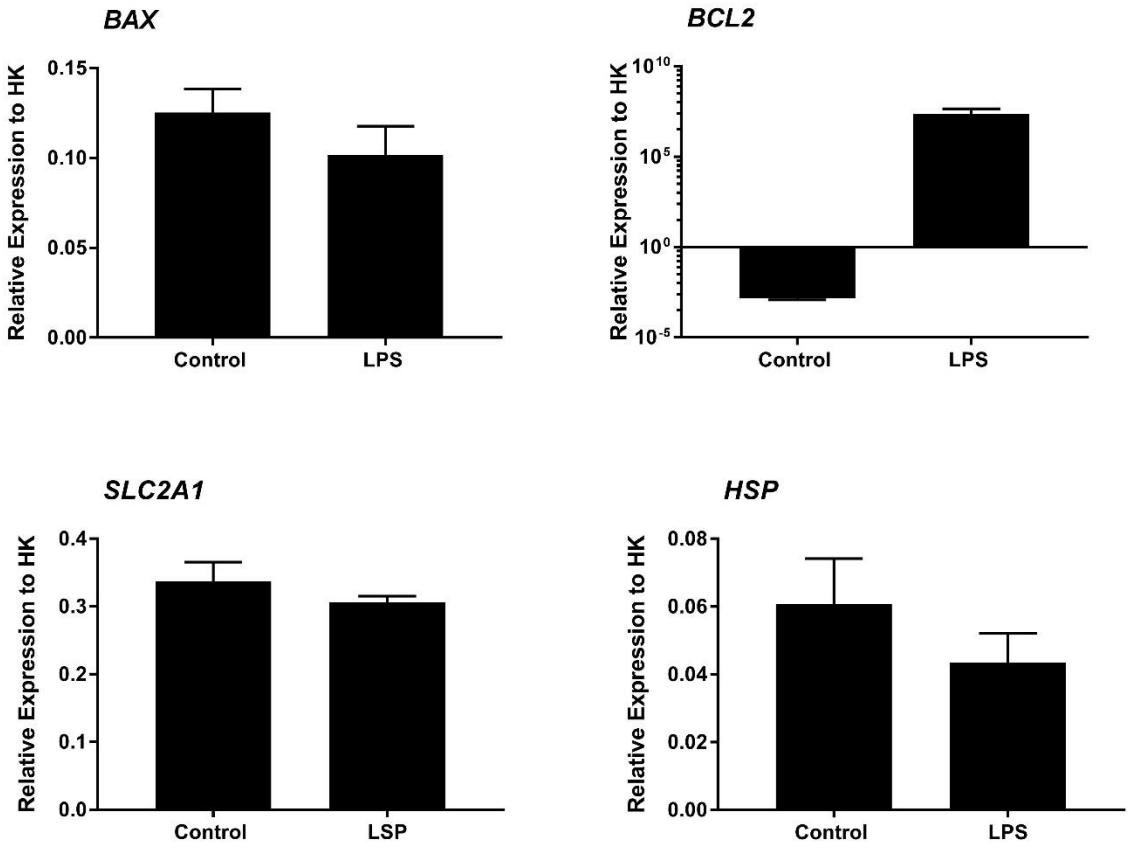

Figure 3-7. Effect of LPS (100ng/mL) exposure during IVM on blastocyst gene expression. Data are presented as relative expression to the housekeeping gene (HK); housekeeping genes were SDHA and RLP19. Data was analyzed as least-squares means ± SEM.

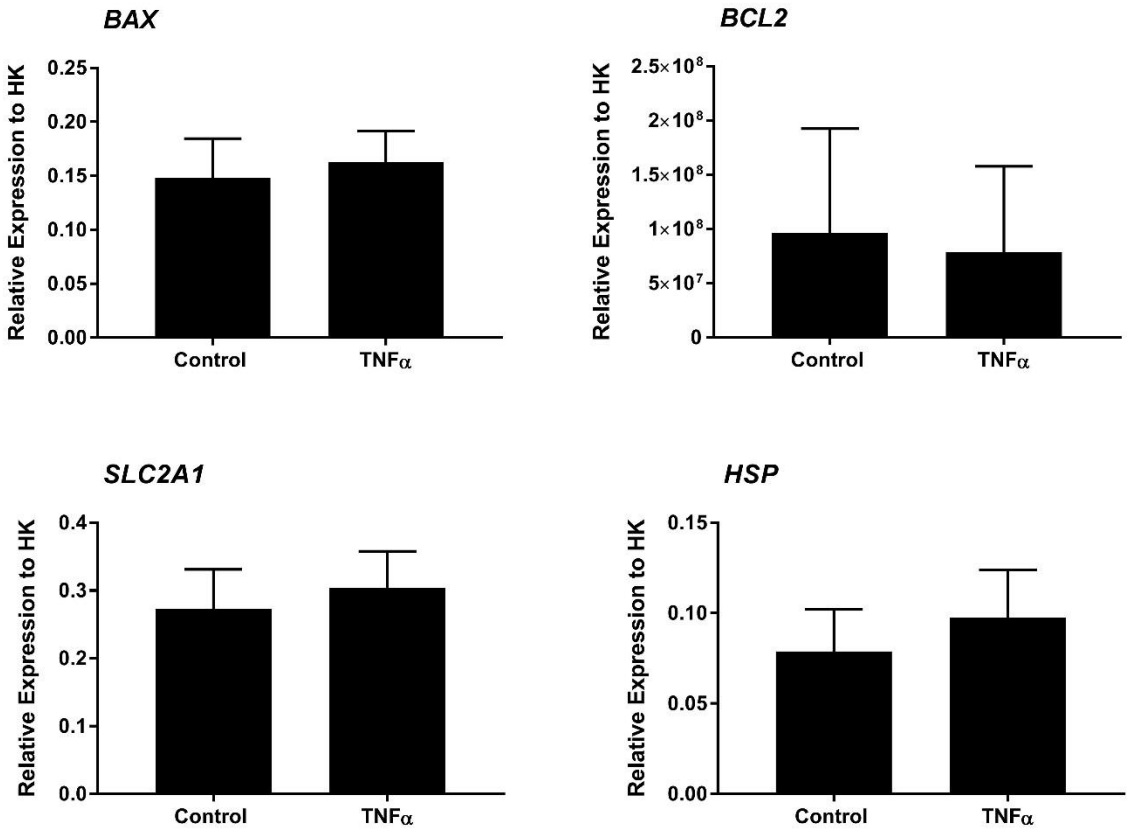

Figure 3-8. Effect of TNFα (100ng/mL) exposure during IVM on blastocyst gene expression. Data are presented as relative expression to the housekeeping gene (HK); housekeeping genes were SDHA and RLP19. Data was analyzed as least-squares means ± SEM.

CHAPTER 4
A MODEL OF CLINICAL ENDOMETRITIS IN HOLSTEIN HEIFERS USING PATHOGENIC *ESCHERICHIA COLI* AND *TRUEPERELLA PYOGENES*

Introduction

Clinical endometritis is characterized by inflammation resulting from bacterial infection of the endometrium that causes a purulent uterine discharge that is present 21 days or more postpartum. Endometritis has a lactation incidence of 15 to 20%, and is important because, even after resolution of the clinical signs, cows have delayed conception and are more likely to be culled for reproductive failure than cows without endometritis (LeBlanc et al., 2002, Gernand et al., 2012, Ribeiro et al., 2013). However, understanding how uterine disease affects fertility is complicated because endometritis is associated with other peripartum problems as well as metabolic challenges associated with the onset of lactation, which also impair fertility (LeBlanc, 2012, Ribeiro et al., 2013). Developing an experimental model of clinical endometritis in heifers would help disentangle the mechanisms of how uterine disease impacts reproductive physiology.

Cows with clinical endometritis do not have systemic signs of disease, and diagnosis is based on the presence of a purulent uterine discharge detectable in the vagina 21 days or more postpartum (LeBlanc et al., 2002, Sheldon et al., 2006). The vaginal contents can be examined using a gloved hand, a Metricheck tool or a speculum, and the severity of clinical endometritis can be graded by the amount of pus in the mucus. There is debate about whether purulent vaginal discharge may also reflect cervicitis or vaginitis because not all cows with purulent vaginal discharge have infiltration of polymorphonuclear neutrophils detectable by endometrial cytology (Dubuc et al., 2010). Nevertheless, bacteria can be isolated from the uterus of cows with endometritis, and the presence of pus in the uterus or a slightly enlarged uterus can also be visualized using transrectal ultrasonography (Sheldon et al., 2002).

Clinical endometritis is associated with Gram-negative endometrial pathogenic *Escherichia coli*, Gram-positive *Trueperella pyogenes*, and several anaerobes (Sheldon et al., 2002, Bicalho et al., 2012). Lipopolysaccharide (LPS) from Gram-negative bacteria and lipopeptides from Gram-positive bacteria activate the innate immune system in the endometrium, leading to inflammation and increased concentrations of circulating acute phase proteins (Sheldon et al., 2001, LeBlanc, 2012, Turner et al., 2014). Pus forms in the uterus when neutrophils phagocytize bacteria or endometrial cells damaged by cytolysins, such as the pore-forming toxin pyolysin secreted by *T. pyogenes* (Sheldon et al., 2010, Bicalho et al., 2012, Amos et al., 2014). A notable feature of the pathogenesis of endometritis is that the adhesion of *E. coli* to endometrial cells and the cytolysis caused by pyolysin is greatest in the stroma, which is exposed when the epithelium is lost during the peripartum period (Sheldon et al., 2010, Amos et al., 2014). Furthermore, peripartum problems that traumatize the endometrium, such as dystocia and retained fetal membranes, increase the risk of developing endometritis (Dubuc et al., 2010, Potter et al., 2010, Ribeiro et al., 2013).

Uterine disease is associated with prolonged luteal phases, slowed rate of growth of ovarian follicles postpartum, and impaired ovarian endocrine function (Opsomer et al., 2000, Sheldon et al., 2002). However, the mechanisms linking endometritis with reproduction are not fully established because fertility is also perturbed by many of the risk factors for endometritis, including peripartum problems and the inability to adapt to the shifts in metabolism to accommodate lactation (Chagas et al., 2007, LeBlanc, 2012). Animal models of clinical endometritis have been reported using mature cows infused with *T. pyogenes* (Rowson et al., 1953, Ayliffe and Noakes, 1982, Amos et al., 2014). However, an experimental model of endometritis in heifers would be attractive for exploring how uterine infection affects

reproduction. Using heifers as the basis for the model circumvents many of the confounding effects of parturition and lactation observed in lactating cows. The aim of the present experiment was to develop a defined *in vivo* infection model of clinical endometritis in Holstein heifers using pathogenic *E. coli* and *T. pyogenes.*

Materials and Methods

The University of Florida Institutional Animal Care and Use Committee approved all procedures with heifers under the protocol number 201508884. The experiment was conducted from June to October, 2017 at the University of Florida Dairy Unit.

Establishment of Uterine Infection in Heifers

Ten virgin Holstein heifers aged between 11 and 13 months were enrolled in the experiment. All animals were free of general health conditions and tested negative for *Brucella abortus*, *Neospora caninum*, and *Leptospirosa*. Animals were vaccinated against bovine viral diarrhea, infectious bovine rinotracheitis, parainfluenza, bovine respiratory syncytial virus, and multiple serovars of Leptospira (Bovi-Shield Gold FP 5 VL5 HB; Zoetis, Parsippany NJ) and de-wormed using moxidectin (Cydectin; Bayer HealthCare, LLC, Animal Health Division, Shawnee Mission, Kansas). Heifers were fed a diet as TMR that was offered once a day in addition to pasture access and provided *ad libitum* access to water.

The experiment followed a randomized complete block design with heifer as the experimental unit. Heifers were blocked by age and weight, and randomly assigned to one of two infusion treatments: intra-uterine infusion of sterile vehicle medium alone (n = 5) or intra-uterine infusion of live bacteria (n = 5; details below).

Estrous cycles were synchronized using a modified 5-d Co-synch protocol (Lima et al., 2013). Briefly, heifers received 100 mg i.m. of GnRH (gonadorelin diacetate tetrahydrate; Ovacyst, Bayer) followed by 25 mg i.m. of $PGF_{2\alpha}$ (dinoprost tromethamine; Prostamate, Bayer)

administered 5 and 6 days later (Figure 4-1). Eight days following initial GnRH, heifers received a final dose of 100 mg of GnRH i.m. The final GnRH of the synchronization protocol was considered day 0 of a new estrous cycle. Starting on the day following the final GnRH, heifers received 200 mg i.m. of progesterone in corn oil (50 mg/mL; Sigma-Aldrich, St Louis MO) daily for 7 days. Exogenous progesterone was administered to mimic diestrus and ensure elevated circulating progesterone at the time of bacterial infusion.

Uterine infusion of treatments were performed 72 h following final GnRH administration and designated as experimental day 0 (Figure 4-1). Endometrial scarification was implemented before intra-uterine infusion to disrupt the endometrial epithelium. Heifers were restrained and received a caudal epidural injection of 60 mg of lidocaine hydrochloride 2% (Aspen Veterinary Resources, Greely CO). The perineum and vulva were cleaned and disinfected with povidone iodine followed by 70% ethanol, and a sterile metal scarification tool enclosed by a metal catheter covered in a sanitary sheath (IMV Technologies, Normandy, France) was introduced through the vagina and cervix. The scarification tool was manipulated through the cervix and into the uterus by transrectal palpation. Once inside the uterus, the sanitary sheath was retracted, and the scarification tool was placed in direct contact with the endometrium. The scarification tool was then rotated once to disrupt the endometrial lining before removal from the reproductive tract. Vehicle heifers and bacterial infused heifers were all scarified prior to infusion. Following endometrial scarification, a metal infusion catheter enclosed in a sanitary sheath was introduce into the body of the uterus transcervically. The sanitary sheath was retracted, and treatments were infused using 10 mL syringes. Bacterial infusion consisted of 10 mL of 4.64×10^7 CFU/mL of *E. coli* MS499, 10 mL of 3.38×10^7 CFU/mL *T. pyogenes* MS249 followed by 10 mL of sterile Luria-Bertani (LB) broth to flush the catheter (Goldstone et al., 2014a, Goldstone et al.,

2014b). Vehicle infusion consisted of 30 mL of LB broth. Heifers were returned to pasture and monitored for clinical signs for 24 h.

A total of 4 heifers received bacterial infusion and 5 heifers received vehicle infusion. One heifer initially assigned to the bacterial infusion group did not receive any treatment because of the inability to pass a catheter through the cervix. This heifer was assigned to the control group and received no intra-uterine infusion.

Animals did not receive any additional treatments or medication during the experimental period.

Bacterial Culture and Preparation of Inoculants

Escherichia coli MS499 and *T. pyogenes* MS249 were collected and isolated from cows with metritis and characterized previously (Goldstone et al., 2014a; b).

Escherichia coli was cultured from frozen glycerol stocks on LB agar. The day before infusion, a single colony was picked from the plate and inoculated into LB broth containing 1% tryptone, 0.5% yeast extract and 1% sodium chloride. The culture was incubated overnight at 37°C with shaking at 200 rpm. Growth was monitored by measuring optical density at 600 nm (OD_{600} = 5.0). A final preparation of 4.64×10^7 CFU/mL *E. coli* was diluted in sterile LB broth and loaded into 10 mL syringes for infusion.

Trueperella pyogenes MS249 was grown from frozen glycerol stocks on Trypticase Soy Blood agar and grown at 37°C for 48 h. The day before infusion, a single colony was selected and inoculated into Bacto Brain Heart Infusion broth (BHI; Fisher Scientific, Pittsburg, PA) supplemented with 5% fetal bovine serum (FBS; Fisher Scientific) and cultured overnight at 37°C with shaking at 200 rpm. Growth was monitored by measuring optical density at 600 nm (OD_{600} = 0.2). A final preparation of 3.38×10^7 CFU/mL *T. pyogenes* was diluted in sterile BHI and loaded into 10 mL syringes for infusion. Syringes were loaded with sterile LB broth for

flushing catheters and vehicle infusions. Inoculants were transported to the farm on ice for infusion.

Blood Sampling and Hematology

Blood was collected from the coccygeal vessels into evacuated tubes (Vacutainer, Becton Dickson, Franklin Lakes NJ) containing sodium heparin for plasma separation or potassium EDTA for hematology. Blood was sampled every other day from experimental d -2 to 18. Blood was placed on ice until further processing. Tubes containing heparin were centrifuged and plasma was collected, aliquoted, and stored at -20°C. Whole blood was transported to the laboratory on ice within 2 h of collection and used for hematology analysis performed using an automated hematology analyzer (ProCyte Dx Hematology Analyzer, IDEXX Laboratories, Westbrook ME). Hematology analysis included total and differential leukocyte counts (neutrophils, lymphocytes, and eosinophils), red blood cells and hemoglobin.

Plasma haptoglobin (Life Diagnostics, Inc., West Chester, PA) and progesterone (DRG International, Inc., Springfield, NJ) were measured using commercially available ELISA according to the manufacturer's instructions. The progesterone ELISA is human specific and was validated for bovine plasma using spike-in/recovery performance based on actual and expected recovery of progesterone supplied as standard with the kit. Intra-assay CV was calculated at 6.5%, while recovery of spike-in progesterone was 89% to 101.8% of expected progesterone.

Examination and Grading of Vaginal Mucus, Transrectal Ultrasonography, and Rectal Temperature

Vaginal mucus was collected and examined using a clean Metricheck tool (Metricheck, Simcro, New Zealand). Vaginal mucus was scored as grade 0, no mucus or clear or translucent mucus; grade 1, mucus containing flecks of white or off-white pus; grade 2, mucus containing ≤ 50% white or off-white mucopurulent material; and grade 3, mucus containing > 50% purulent

material (Sheldon et al., 2009). Evaluation of vaginal mucus was performed daily from d -1 to 7 relative to treatment (Figures 4-2A-C).

Transrectal ultrasonography with a linear 5.0 MHz probe (Aloka SSD-500, Hitachi Healthcare Americas, Twinsburg, OH) was performed to visualize fluid and pus in the uterus. Ultrasonography was performed every other day from -1 to 10 relative to treatment. Rectal temperature (AG-102 thermometer, AG-Medix, Mukwonago WI) was measured daily between 7 and 9 AM from d -11 to 10 relative to treatment. A rectal temperature of > 39.5°C was classified as fever.

Quantification of Total 16S rRNA Isolated From Vaginal Mucus

Vaginal mucus was stored in sterile bijou bottles at -20°C until processing. Total DNA was isolated from vaginal mucus using the DNeasy Power Soil Kit according to the manufacture's instruction with modification (Qiagen, Hilden, Germany). Briefly, samples were thawed on ice and vortexed and 250 mg of vaginal mucus was used for DNA extraction using a bead beater tissue homogenizer (Precellys 24, Bertin Technologies SAS, France). The mucus was added to guanidine thiocyanate and homogenized with garnet particles using 3 bead beater cycles (30 s at 6000 × *g*, 60 s pause, 30 s at 6000 × *g*) with a 5 min incubation on ice between each cycle. Following homogenization, supernatants were applied to the DNeasy Power Soil spin columns for DNA purification.

Total 16S rRNA was quantified using the Femto Bacterial DNA Quantification Kit according to the manufacture instructions (Zymo Research, Irvine CA). Thermocycling conditions included initial denaturation at 95°C for 10 min, 40 cycles of amplification consisting of denaturation at 95°C for 30 s, annealing at 50°C for 30 s and extension at 72°C for 1 min, followed by a final extension at 72°C for 7 min. A total of 2 μL of extracted total DNA sample

was applied to each PCR reaction. Quantification of 16S rRNA was analyzed based on a standard curve performed in parallel with mucus samples. Data for total 16S rRNA are described as nanograms of 16S rRNA per milligram of vaginal mucus. The quantification of 16S rRNA in mucus samples was validated using spike-in/recovery using the quantification kit 16S rRNA standard supplied with the kit.

Statistical Analysis

Descriptive statistics were used to evaluate the vaginal mucus grade and reported as the median for each treatment group. All other data were analyzed using SAS v. 9.4 (SAS Institute, Cary, NC). Haptoglobin, progesterone, hematology and 16S rRNA concentration were analyzed using the MIXED procedure of SAS and the models included the fixed effects of treatment (bacterial infusion), day (repeated measure), and their interaction. Heifer nested within treatment was considered as a random effect. First order autoregressive covariance structure AR (1) was used as the covariate structure. Values are reported as LSM ± SEM. Differences with $P \leq 0.05$ were considered statistically significant.

Results

Intra-Uterine Bacterial Infusion Increased Vaginal Mucus Grade

Vaginal discharge of pus was visually evident in heifers that were infused with live bacteria, but not in control heifers (Figure 4-2A). Vaginal mucus collected by Metricheck was graded and compared between treatments (Figure 4-2B-C). Heifers in both infusion groups had a median mucus grade of 0 prior to uterine infusion (Figure 4-3). Intra-uterine infusion of live bacteria resulted in a median mucus grade score of 2 on d 3 relative to treatment, whereas control heifers maintained a median mucus grade score of 0 (Figure 4-3). On d 4 to 6 relative to treatment, bacteria infused heifers had a median mucus grade score of 3, whereas control heifers presented a median mucus grade score ≤ 1. The presence of echogenic fluid in the uterus of bacterial

infused heifers was confirmed by transrectal ultrasound, and control animals had no evidence of increased fluid, or echogenic material present in the uterus (Figure 4-2D-E).

Intra-Uterine Bacterial Infusion Increased 16S rRNA Concentration in Vaginal Mucus

Total vaginal 16S rRNA was increased ($P < 0.01$) in bacteria infused heifers compared with control heifers on day 5 (Figure 4-4A). In addition, total vaginal 16S rRNA was greater ($P < 0.05$) on day 5 in heifers infused with bacteria compared to other sampled days (Figure 4-4A). There was no interaction between treatment and day relative to treatment ($P = 0.08$).

Effect of Uterine Bacterial Infusion on Hematology and Rectal Temperature

There was no effect of treatment on any hematological parameters measured (Table 4-1). There was an effect ($P < 0.05$) of day relative to treatment on the number of lymphocytes (K/μL), number of platelets, and number of eosinophils and proportion of eosinophils. In addition, an interaction ($P < 0.05$) between treatment and day relative to treatment was observed for the number of lymphocytes. There was an effect of treatment ($P < 0.05$) on rectal temperature with bacteria infused heifers showing elevated temperature on d 1 compared to control heifers (Table 4-1). Two bacteria infused heifers had rectal temperatures above 39.5°C on d 1 relative to treatment (40.0°C and 40.2°C). There were no overt signs of systemic disease observed in any heifers.

Effect of Bacterial Infusion on Circulating Concentrations of Haptoglobin and Progesterone in Plasma

Plasma concentration of haptoglobin did not differ ($P = 0.37$) between treatments; however, a significant effect ($P = 0.02$) of day was observed. A numerical 4.2-fold increase in haptoglobin concentration on d 13 relative to treatment was observed in bacteria infused heifers compared with control heifers (Figure 4-4B; $P > 0.05$).

Plasma concentrations of progesterone increased in both treatment groups as a result of exogenous progesterone supplementation (effect of day, $P < 0.001$), infusion with bacterial did not affect concentrations of progesterone in plasma (Figure 4-4C). The peak concentration was observed on experimental d 4 and, once exogenous progesterone supplementation was concluded on d 4, concentrations decreased in both treatments.

Discussion

The present experiment developed an *in vivo* model of clinical endometritis in Holstein heifers using pathogenic *E. coli* and *T. pyogenes*. Heifers that received intra-uterine infusion of pathogenic bacteria developed purulent vaginal mucus, accumulation of echogenic fluid in the uterus, and increased bacterial load in vaginal mucus. In parallel, bacteria infused heifers displayed no systemic signs of illness, such as altered hematology or general sickness. Control heifers did not display any of the clinical signs of clinical endometritis. Based on the criteria previously described for the disease, these results recapitulate the symptoms of clinical endometritis observed in the postpartum dairy cow (LeBlanc et al., 2002; Sheldon et al., 2006, 2009).

Previous experimental models of clinical endometritis have focused on the use of mature cows and intra-uterine infusion of *T. pyogenes* (Rowson and Lamming, 1953; Amos et al., 2014). These studies were capable of generating active infection of the uterus, evident by the presence of mucopurulent vaginal contents, using a single uterine pathogen. Although these models induce clinical symptoms of disease, it may be that the use of a second pathogen, *E. coli*, better reflects the molecular profile of endometritis to evaluate the consequences of disease on fertility. The dual pathogen model of Del Vecchio et al. (1992) utilized repeated infusions of both *E. coli* and *T. pyogenes* over the course of 3 days (Del vecchio et al., 1992); however, the strain and pathogenicity of bacteria used may also be important. Strains used by others include β-hemolytic

E. coli or *T. pyogenes* sourced from cows with severe endometritis (presumably from the uterus). Pathogenic strains of *E. coli* and *T. pyogenes* used in the current model were sourced from the uterus of cows with metritis and have subsequently been sequenced (Goldstone et al., 2014a, Goldstone et al., 2014b), allowing a detailed understanding of virulence factors and host-pathogen interactions involved in disease. The pore forming toxin produced by *T. pyogenes* is known to cause cellular damage to the endometrium during active infection, although little is known about its actions on ovarian function, especially after the clearance of disease. Conversely, LPS derived from Gram-negative bacteria such as *E. coli* is known to be present in follicular fluid after the resolution of uterine disease. Indeed, studies have demonstrated that the presence of LPS negatively effects oocyte development and alters the follicular environment of the growing oocyte *in vitro* (Bromfield and Sheldon, 2011). When generating a model of clinical endometritis to study the impacts of disease on reproduction, it may be important to incorporate multiple pathogens that could be responsible for any observed reproductive phenotype.

Species other than the cow have been used to develop models of uterine infection, including the sheep and mouse (Regassa et al., 2002; Sheldon and Roberts, 2010; Bromfield and Sheldon, 2013). However, when attempting to determine the mechanisms by which endometritis impacts fertility of the dairy cow, it is imperative to utilize the target species in question. Rodents are relatively inexpensive and convenient for such a model, but the reproductive physiology and immune function of the mouse is considerably different from those of the cow. Mice have been shown to be 1 million-fold less sensitive to LPS than humans (Seok et al., 2013). More appropriately, the human and bovine genomes share a high degree of amino acid sequence homology, limited species-specific orthologs and a similar chromosomal organization; suggesting the bovine as a better experimental model for human physiology than the commonly

used mouse (The Bovine Genome Sequencing and Analysis Consortium et al., 2009). In addition, bovine reproductive biology is closer to that of humans than mice; cows and humans are both monotocous with similar hormonal profiles over a 3 to 4 week ovarian cycle, compared to the polytocous mouse with a 4 day estrous cycle.

The use of the Holstein heifers in the present experiment was a deliberate choice in the generation of the experimental model presented. The long-term goal of this model is to study the mechanisms of endometritis mediated reproductive failure in the cow. As uterine disease occurs in the early postpartum period, a number of significant challenges can confound experimental investigation into the causes of endometritis-mediated infertility. Specifically, postpartum uterine damage, uterine involution, metabolic demands of lactation, negative nutrient balance, and additional postpartum illnesses which affect almost half of all postpartum cows (Ribeiro et al., 2016). Retained placenta and dystocia are significant risk factors for the development of endometritis, and are both associated with damage to the endometrium (Dubuc et al., 2010). To recapitulate postpartum endometrial damage, we performed a scarification procedure to disrupt the endometrial epithelial layer at the time of bacterial infusion. This process of scarification may be critical to the establishment of the disease model to facilitate bacterial access to the underlying stroma. Previous work has reported differential susceptibility of epithelial and stromal endometrial cells to pathogenic *E. coli*, with pathogenic *E. coli* binding with stronger affinity to stromal cells, and purified LPS inducing a stronger inflammatory reaction in the endometrial stroma (Sheldon et al., 2010). A similar phenomenon of differential cellular susceptibility has been described in the response of endometrial epithelial and stromal cells to *T. pyogenes* pyolysin, in which stromal cells are considerably more sensitive to the cytotoxic effects of pyolysin (Amos et al., 2014), suggesting the stoma is the target of pyolysin. These *in vitro*

experiments, in combination with the risk factors associated with endometritis, suggest that endometrial scarification may be an important procedure in the establishment of clinical endometritis observed in the present model.

The administration of exogenous progesterone was a calculated approach to modulate the immune function of heifers at the time of bacterial infusion. Rowson et al. (1953) reported that intra-uterine infusion of *T. pyogenes* (reported as *Corynebacterium pyogenes*) during the luteal phase of the estrous cycle resulted in "pyometritis"; however, no infection could be established when bacterial infusion was performed at estrus. These experiments were repeated using ovariectomized cows in conjunction with administration of exogenous progesterone or estradiol. Only with the administration of exogenous progesterone could pyometritis be achieved (Rowson et al., 1953). Since the 1950's, the immune modulating properties of progesterone and estrogen have been reported in immune cells and the endometrium (reviewed in detail by (Wira et al., 2015)) with various studies demonstrating the immune-suppressive function of progesterone within the endometrium of ruminants (Del vecchio et al., 1992; Hansen, 1998; Seals et al., 2002; Lewis, 2004). The ability of steroid hormones to modulate endometrial immune function have led to the practice of administering $PGF_{2\alpha}$ as a treatment for uterine infection to induce luteolysis in cows in diestrus, and elevate estrogen by stimulating a new follicular phase of the estrous cycle (Lewis, 1997); however this remains debated.

Vaginal mucopurelent content observed in heifers treated with intra-uterine infusion containing live bacteria could be associated with cervicitis or vaginitis as previously observed in spontaneously occurring cases in postpartum cows (Dubuc et al., 2010). Although the infusate was placed in the uterine horns, retrograde movement of the content could have inoculated the cervix and vagina. However, quantification of vaginal 16S rRNA the day after infusion on

experimental day 1 revealed comparable total bacterial load between treatments. This suggests that bacteria were infused into the uterus and retained there, otherwise 16S rRNA would have been greater in the bacteria infused heifers on d 1 compared with controls. Additionally, the presence of elevated 16S rRNA observed in the bacteria infused heifers 5 d following infusion suggests that mucopurelent vaginal discharge is derived from the infected uterus induced by infused bacteria, and not from environmental contamination. The accumulation of echogenic uterine fluid in bacteria-infused heifers supports these assumptions and suggests that any cervicitis or vaginitis would likely be the result of contamination or excessive manipulation, and would also be observed in vehicle infused controls.

Any experimental model of infection has limitations. Here, we propose using the described experimental model to define the mechanisms of endometritis mediated infertility. However, using heifers as the experimental unit limits our understanding of the reproductive potential of the individual animal, unlike using mature lactating cows that would normally have uterine disease. Additionally, the use of heifers revealed experimental limitations because of body size and ability to perform the manipulations in 12 to 13-mo old animals. Experimentation for the purposes of determining mechanisms of endometritis mediated infertility will require multiple, repeat manipulations which might be difficult in small frame heifers compared with mature cows.

Table 4-1. Effect of treatment on rectal temperature and hematology

Variable[2]	Days[3]	Treatment		SEM	*P*-value[1]		
		Control	Bacteria		TRT	Day	TRT × Day
Temp (°C)	-1	38.4	38.4	0.1	0.04	< 0.01	0.167
	1	38.8	39.5				
	3	38.3	38.8				
	7	38.5	38.5				
RBC (M/µL)	-1	6.84	6.36	0.389	0.07	0.07	0.05
	1	7.61	7.03				
	3	7.33	6.75				
	7	7.20	6.71				
HCT (%)	-1	31.73	29.60	2.038	0.34	0.17	0.18
	1	34.71	32.80				
	3	33.13	31.43				
	7	32.78	31.73				
HGB (g/dL)	-1	10.49	9.93	3.752	0.23	0.77	0.83
	1	11.66	10.98				
	3	11.17	10.55				
	7	11.07	10.43				
WBC (K/µL)	-1	11.74	11.72	1.288	0.48	0.09	0.58
	1	12.02	12.81				
	3	10.22	11.43				
	7	10.22	12.08				
NEU (%)	-1	29.11	22.33	4.071	0.45	0.54	0.10
	1	25.06	19.18				
	3	23.38	13.56				
	7	17.59	24.08				

Table 4-1. Continued

Variable[2]	Days[3]	Treatment		SEM	*P*-value[1]		
		Control	Bacteria		TRT	Day	Trt × day
NEU (K/µL)	-1	3.55	2.72	0.679	0.93	0.51	0.27
	1	3.01	2.58				
	3	2.40	1.42				
	7	1.70	3.19				
LYM (%)	-1	47.18	54.38	4.654	0.60	0.22	0.05
	1	51.48	58.35				
	3	52.76	51.23				
	7	62.48	52.70				
LYM (K/µL)	-1	5.35	6.25	0.833	0.27	0.02	0.03
	1	6.14	7.35				
	3	5.41	6.64				
	7	6.52	6.07				
MON (%)	-1	16.27	16.95	5.631	0.63	0.61	0.52
	1	16.72	14.93				
	3	17.14	26.60				
	7	14.97	17.18				
MON (K/µL)	-1	1.95	1.95	6.010	0.53	0.98	0.98
	1	2.06	2.18				
	3	1.73	1.84				
	7	1.50	2.11				
EOS (%)	-1	7.40	6.30	1.387	0.78	< 0.01	0.48
	1	6.70	5.50				
	3	6.70	9.18				
	7	4.81	6.03				

Table 4-1. Continued

Variable[2]	Days[3]	Treatment		SEM	*P*-value[1]		
		Control	Bacteria		TRT	Day	Trt × day
EOS (K/μL)	-1	0.87	0.80	0.205	0.76	0.01	0.56
	1	0.79	0.69				
	3	0.67	0.92				
	7	0.47	0.72				
PLT (K/μL)	-1	286.21	241.00	72.664	0.78	< 0.01	0.11
	1	390.04	261.00				
	3	337.71	221.00				
	7	169.37	117.75				

1 TRT = effect of treatment (control vs. bacteria); Day = effect of day relative to treatment; TRT × day = interaction between TRT and Day.
2 Data are presented as LSM with respective pooled SEM for the interaction between treatment and day.
Data quantified in whole blood included red blood cells count (RBC), hematocrit (HCT), hemoglobin concentration (HGB), white blood cells count (WBC), neutrophils (NEU), lymphocytes (LYM), monocytes (MON), eosinophils (EOS) and platelets (PLT) measured as the proportion of total cells (%) and number of cells per μL (K = 1,000; M = 1,000,000).
3 Sample days relative to infusion (d -1, 1, 3 and 7).

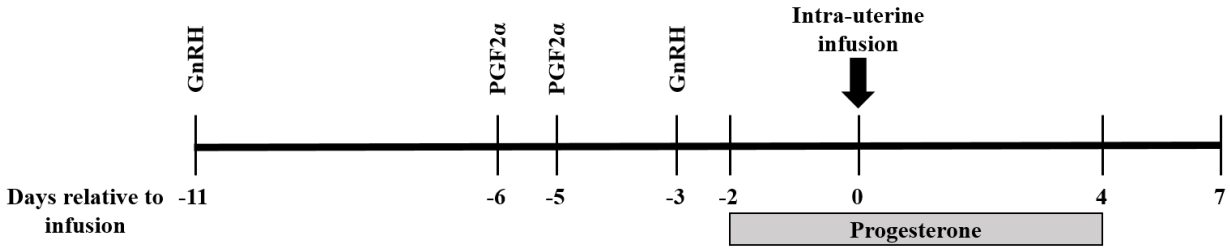

Figure 4-1. Timeline for establishment of experimental uterine infection. Gonadotropin releasing hormone (GnRH) and prostaglandin (PG) F2α were used to synchronize estrous cycles in 10 virgin Holstein heifers before intra-uterine infusion of treatments. On d 0, intra-uterine infusion of either vehicle or live bacteria was performed. Vehicle infusion consisted of 30 mL of sterile Luria-Bertani broth. Bacteria infusion consisted of 10 mL of *E. coli* MS 499 (4.64 × 107 CFU/mL), 10 ml of *T. pyogenes* MS249 (3.38 × 107 CFU/mL) and 10 mL of sterile Luria-Bertani broth. Progesterone was administered at 200 mg/d i.m.

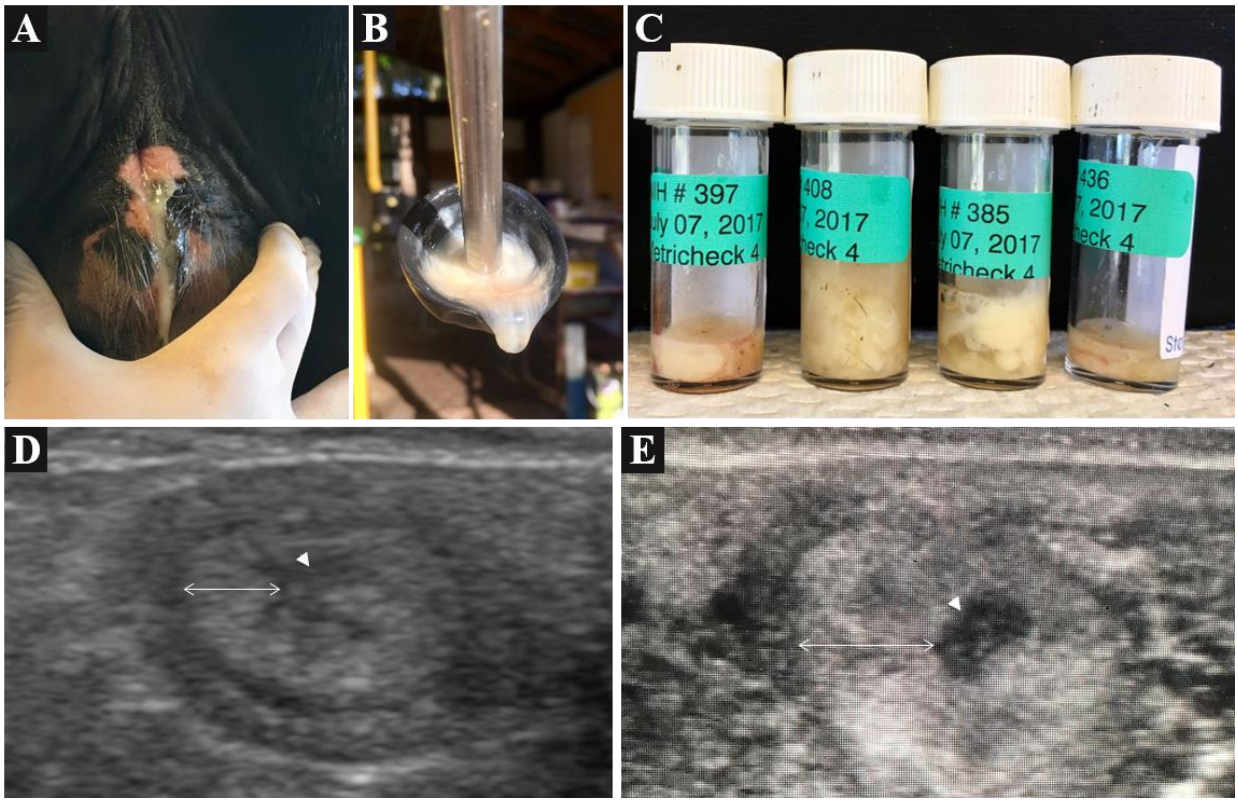

Figure 4-2. Clinical observations of induced uterine disease. (A) Vaginal mucus was visually confirmed in heifers receiving bacterial infusion. (B) Metricheck tool containing vaginal mucus of a bacteria infused heifers. (C) Examples of vaginal mucus samples collected from bacteria infused heifers using the Metricheck tool. (D and E) Representative ultrasound images of a transverse cross section of a uterine horn from a control (D) and bacteria infused (E) heifer. The arrow head denotes the uterine lumen; the double headed arrow denoted the uterine wall. Courtesy of author.

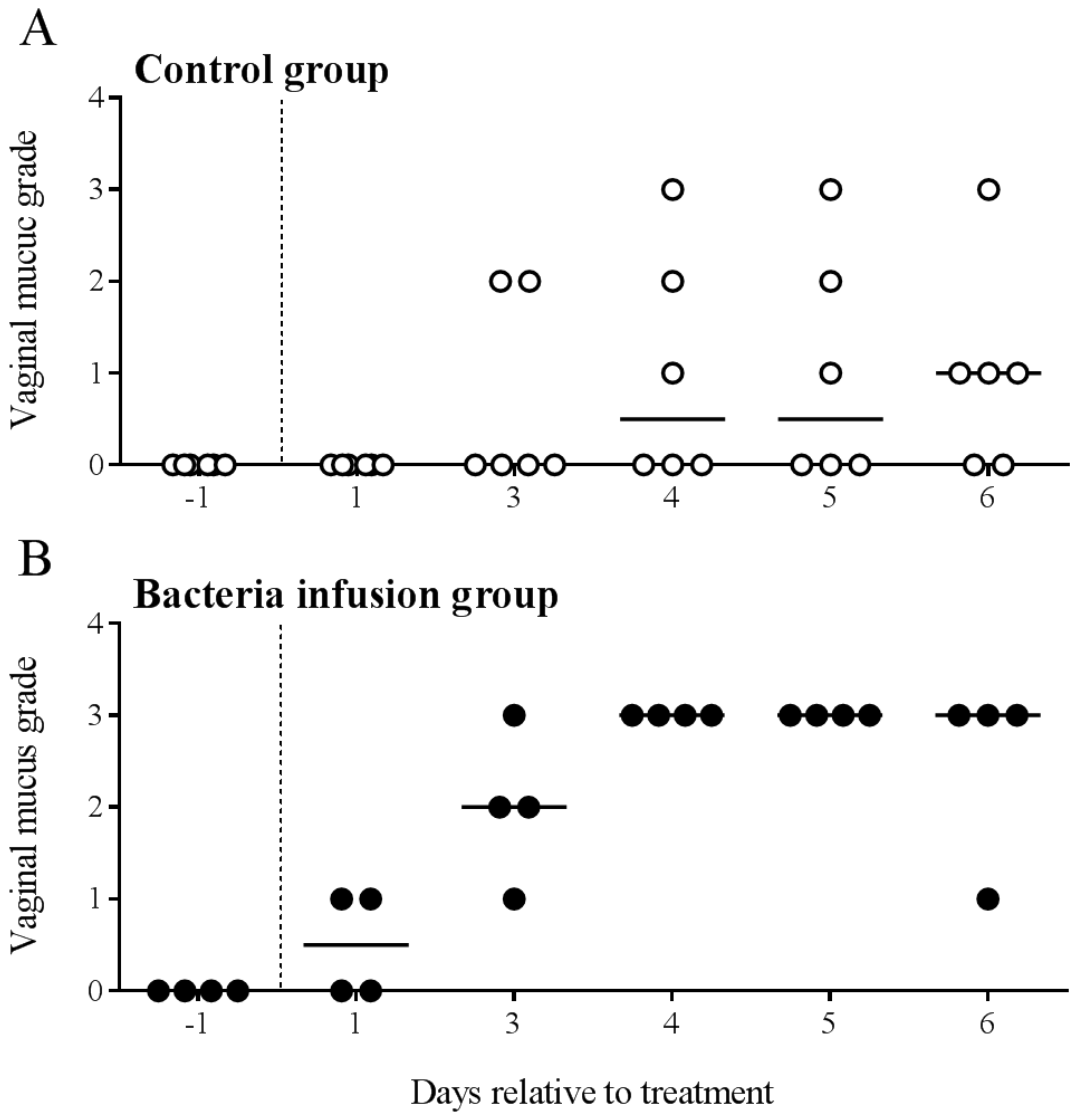

Figure 4-3. Vaginal mucus grade following intra-uterine infusion of bacteria. Vaginal mucus was collected using a Metricheck tool and graded according to Sheldon et al. (2009). Vaginal mucus was graded from 0 to 3 and each heifer is represented by a single circle. Control heifers are represented by open circles (A, ○), bacteria infused heifers are represented by filled circles (B, ●). The vertical dotted line denotes the day of treatment, solid horizontal lines indicate the median vaginal mucus score for the day of observation.

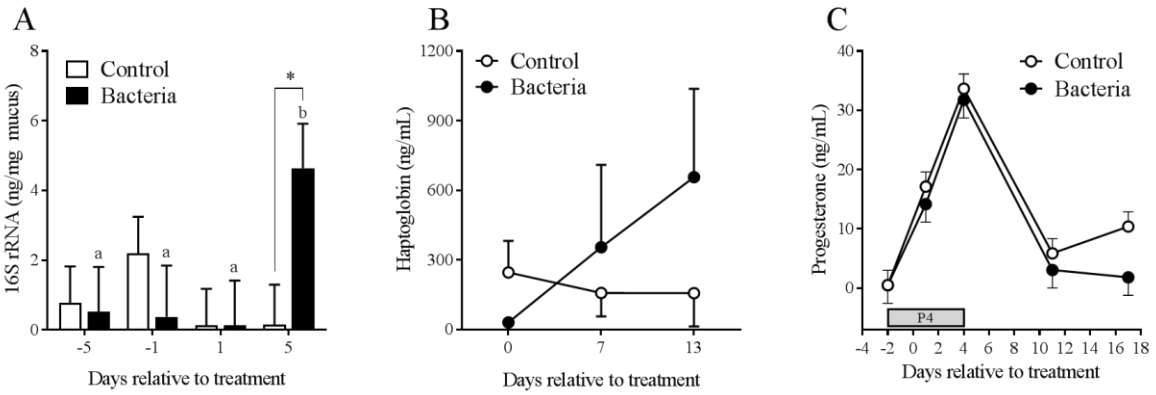

Figure 4-4. Effect of treatment on vaginal mucus 16S rRNA and circulating concentrations of haptoglobin and progesterone in plasma. (A) Total 16S rRNA quantification from vaginal mucus on d -5, -1, 1 and 5 relative to treatment in either control (open bars) or bacteria infused (solid bars) heifers. Total 16S rRNA was normalized to the weight of vaginal mucus processed for nucleic acid extraction (ng rRNA per mg mucus). Different superscript denote differences within the bacteria infused group; * denotes difference between treatment groups on a given day ($P < 0.05$). (B) Haptoglobin plasma concentration (pg/mL) was measured in control (○) and bacteria infused (●) heifers on d 0, 7 and 13 relative to treatment. (C) Progesterone plasma concentration (ng/mL) was measured in control (○) and bacteria infused (●) heifers on d -2, 1, 4, 11 and 15 relative to treatment. P4 denotes the period of exogenous administration of 200 mg/d of progesterone. All data are presented as LSM ± SEM.

CHAPTER 5
EFFECTS OF INDUCED CLINICAL ENDOMETRITIS ON OOCYTE TRANSCRIPTOME DURING ACTIVE DISEASE AND FOLLOWING DISEASE RESOLUTION

Introduction

Cows with retained fetal membranes and/or metritis during the first 10 DIM have reduced pregnancy at day 45, decreased calving rates and increased pregnancy loss (Ribeiro et al., 2016). Cows with clinical endometritis have decreased pregnancy at first AI and increased number of days open, resulting in an increased likelihood of being culled for reproductive failure (LeBlanc et al., 2002). While postpartum uterine diseases decrease fertility, the mechanisms by which this occurs are yet to be fully elucidated.

Uterine disease in cattle slows dominant follicle growth and estradiol secretion following parturition (Sheldon et al., 2002). Interestingly, the Gram-negative bacterial cell wall component, LPS, is concentrated in the follicular fluid of cows and is positively correlated with the severity of uterine inflammation (Herath et al., 2007). Granulosa cells respond to bacterial components like LPS via the Toll-like receptor (TLR) family of receptors, ultimately increasing expression of inflammatory mediators, and reducing expression of *CYP19A1* and estradiol secretion (Herath et al., 2007; Price et al., 2013). Cumulus granulosa cells exert similar responses to bacterial LPS, increasing expression of inflammatory mediators and ultimately increasing oocyte meiotic failure (Bromfield and Sheldon, 2011). These data suggest that the negative influence of LPS on the follicle may reduce the capacity of the oocyte to form a healthy embryo following fertilization. However, the majority of postpartum uterine disease occurs in the first 21 days after calving, while the first breeding attempt will only occur after the voluntary waiting period (50 to 70 days postpartum), meaning that the cows display no clinical signs of uterine disease at the time of breeding (Ribeiro et al., 2016). Could the negative impacts of uterine disease persist in granulosa

cells and oocytes after the resolution of disease, causing the decreased fertility in cows that once had postpartum uterine disease?

The postpartum period poses metabolic challenges to the dairy cow, and the development of uterine disease is intrinsically correlated with those challenges. Dairy cows are required to meet the metabolic demands of parturition and lactation, which results in negative energy balance shortly after parturition and increases the potential of developing uterine disease (Giuliodori et al., 2013; Ribeiro et al., 2013). The use of an experimental model of clinical endometritis in virgin Holstein heifers to study the impacts of uterine disease on fertility removes the various confounding effects of lactation and parturition that may impact subsequent fertility. In order to better understand the influence of clinical endometritis on the oocyte, we used the experimental model described in chapter 4 to induce clinical endometritis in virgin Holstein heifers and assess oocyte transcriptomics during active disease and following disease resolution.

Materials and Methods

The University of Florida Institutional Animal Care and Use Committee approved all procedures with heifers under the protocol number 201508884. The experiment was conducted from June to October, 2017 at the University of Florida Dairy Unit.

Induction and Clinical Evaluation of Endometritis in Virgin Holstein Heifers

In order to induce clinical endometritis in virgin Holstein heifers we used the model described in chapter 4. Heifers described here were the same as those described in chapter 4 and monitored for 91 days following infusion of treatments. See chapter 4 for details of disease induction.

Establishment of uterine disease was evaluated by visually assessing vaginal mucus discharge and evaluating clinical symptoms. Vaginal mucus was collected using a clean Metricheck tool (Simcro) between days 1 and 70 relative to treatment. Vaginal mucus was

scored as grade 0, no mucus or clear or translucent mucus; grade 1, mucus containing flecks of white or off-white pus; grade 2, mucus containing ≤ 50% white or off-white mucopurulent material; and grade 3, mucus containing > 50% purulent material according to Sheldon et al., (2009).

Blood Sampling and ELISA

Blood was collected from the coccygeal vessels into evacuated tubes (Vacutainer, Becton Dickson, Franklin Lakes NJ) containing sodium heparin for plasma separation. Blood was sampled every other day from experimental d -2 to 91. Blood was placed on ice until further processing. Tubes were centrifuged and plasma was collected, aliquoted, and stored at -20°C.

Plasma haptoglobin was measured using commercially available ELISA according to the manufacturer's instructions (Life Diagnostics, Inc., West Chester, PA). Validation of the haptoglobin assay was performed as described in chapter 4.

Follicle Aspiration and Ovum Pick-up

Ovum pick-up was performed on days 4 and 60 relative to treatment (Figure 5-1). Ovum pick-up was performed using transvaginal ultrasound guided follicle aspiration. Briefly, heifers received a caudal epidural injection of 60 mg of lidocaine hydochloride 2% (Aspen Veterinary Resources, Greely CO). The perineum and vulva were cleaned and disinfected with povidone followed by 70% ethanol. A vaginal lavage using 100 mL of 0.2% chlorohexidine in saline followed by two 100 mL lavages using sterile 0.9% saline were employed to wash the vagina. An oocyte pick-up handle including a 5 mHz convex ultrasound probe (Choice Medical) was covered in a sanitary cover sleeve (TNB, Sao Paulo, Brazil) and introduced into the vagina with sterile lubricant. Using rectal palpation the ovary was placed towards the ultrasound probe and visualized using an Aloka ultrasound (Aloka SSD-500, Hitachi Healthcare Americas, Twinsburg, OH). A 20 G aspiration needle (WTA) attached to a vacuum pump (WTA) was introduced into

the oocyte pick-up handle and using ultrasound guidance all follicles with exception of the dominant follicle, were aspirated into OPU collection medium (all medium is presented in Appendix B). The aspirate was filtered using an oocyte filter (WTA), washed with 30 to 50 mL OPU collection medium and placed into a gridded petri dish (ThermoFisher Scientific) for oocyte searching under a stereo microscope. Aspirated COCs were washed twice in fresh DPBS containing 0.1% PVP (Kodak). To remove cumulus cells, COCs were place in 1000 U/mL of hyaluronidase in HEPES-TALP for 4 minutes and oocytes were manually denuded using a Stripper pipette (Cooper Surgical, Denmark). Zona pellucida of denuded oocytes were subsequently removed using 0.1% protease from *Streptococcus griseus* (Sigma-Aldrich), and washed three times in fresh DPBS-PVP. Zona-free oocytes were snap frozen and stored at -80°C until further processing.

RNA Extraction and RNA Sequencing of Oocyte Transcriptome

Oocytes were thawed and re-suspended in 350 µl RLT buffer for extraction of total RNA using the RNeasy Micro kit (Qiagen) according to the manufacturer's instructions. Total RNA concentration was determined using a Qubit 2.0 Fluorometer (ThermoFisher, Grand Island, NY) and RNA quality was assessed using an Agilent 2100 Bioanalyzer (Agilent Technologies, Santa Clara CA). To produce RNAseq libraries, 200 pg of total RNA was used for library construction using SMARTer Universal Low input RNA kit (Takara Bio, Mountain View, CA) for sequencing combined with Illumina Nextera DNA Library Preparation Kit (Illumina, San Diego, CA) according to the manufacturer's instructions. Briefly, 1st strand cDNA was primed by a modified N6 primer (the SMART N6 CDS primer), then base-paired with additional nucleotides, creating an extended template. The reverse transcriptase then switches templates and continues transcribing to the end of the oligonucleotide, resulting in single-stranded cDNA, containing sequences that are complementary to the SMARTer oligonucleotide. The SMARTer anchor

sequence and the N6 sequence then served as universal priming sites for DNA amplification by PCR for 10 cycles. After this process the Illumina sequencing libraries were generated. Briefly, 125 pg of cDNA was fragmented by a tagementation reaction and then adapter sequences were added to the template cDNA by PCR amplification. Libraries were quantitated by Bioanalyzer and qPCR (Kapa Biosystems, Wilmington, MA).

Individual libraries were pooled at equal molar concentration and a total of 2 lanes were run on an Illumina HiSeq3000 (Illumina, San Diego, CA). RNA library construction and sequencing were performed at the University of Florida ICBR.

Read Mapping and Gene Expression Analysis

Reads acquired from the sequencing platform were cleaned with the Cutadapt program (Martin, 2011) to trim off sequencing adaptors, low quality bases, and potential errors introduced during sequencing or library preparation. Reads with a quality Phred-like score < 20 and read length < 40 bases were excluded from RNAseq analysis.

The transcripts of *Bos taurus* (80,896 sequences) retrieved from the NCBI RefSeq database were used as reference sequences for RNAseq analysis. The cleaned reads of each sample were mapped individually to the reference sequences using the bowtie2 mapper (v. 2.2.3) with a '3 mismatches a read' allowance (Langmead and Salzberg, 2013). The mapping results were processed with the samtools and scripts developed in house at the University of Florida ICBR to remove potential PCR duplicates and choose uniquely mapped reads for gene expression analysis. Gene expression between the control and treatment groups was assessed by counting the number of mapped reads for each transcript (Yao and Yu, 2011). Significant up and down regulated genes were selected using the *P*-value and fold-change. Adjusted *P*-values were cut-off at 0.1. All other data presented for differentially expressed genes are non-adjusted *P*-values < 0.05.

Ingenuity Pathway Analysis

Pathway analysis was performed using Ingenuity Pathway Analysis (IPA, Qiagen). Differentially expressed genes with a non-adjusted *P*-value < 0.05 were used for IPA analysis. Non-adjusted *P*-values were used due to the reduced number of significant genes following false discovery analysis. Represented canonical pathways with a –log *P*-value > 1.3 were determined with corresponding z-scores to describe predicted activation status. Represented gene networks were determined by assessing the number of differentially expressed genes in a given gene network. Upstream regulators of specific gene networks and upstream regulators of differentially expressed genes were predicted using IPA algorithms. Predicted upstream regulators of differentially expressed genes were assigned an activation z-score to predict the appropriate upregulation or down regulation of various downstream differentially regulated genes. A z-score ≥ 2 or ≤ -2 was assumed to be a significant prediction of activation or inhibition, respectively.

Statistical Analysis

Vaginal discharge score and haptoglobin concentration were analyzed using SAS v. 9.4 (SAS Institute, Cary, NC). Vaginal discharge scores were analyzed using the GLIMMIX procedure of SAS and the model included the fixed effects of treatment and day. Heifer nested within treatment was considered as a random effect. Haptoglobin concentration was analyzed using the MIXED procedure of SAS and the model included the fixed effects of treatment (bacterial infusion), day (repeated measure), and their interaction. Heifer nested within treatment was considered as a random effect. First order autoregressive covariance structure AR (1) was used as the covariate structure. Values are reported as LSM ± SEM. Differences with $P \leq 0.05$ were considered statistically significant.

Results

Clinical Endometritis Impacts Vaginal Mucus Grade

Heifers in both infusion groups had a median mucus grade of 0 prior to uterine infusion. Vaginal mucus grade did not differ between treatments during the course of the experiment (P = 0.54); however there was a tendency for an effect of day (P = 0.06) and a significant interaction between treatment and day (P = 0.001). Bacteria infused heifers had an increased vaginal mucus grade on days 3 to 9 compared to control cows ($P \leq 0.05$). (Figure 5-2).

Induction of Clinical Endometritis Effect on Plasma Haptoglobin Concentration

Plasma concentration of haptoglobin did not differ (P = 0.36) between treatments; however, an effect of day relative to treatment (P = 0.03) was observed. On day 13, bacteria infused heifers had increased plasma haptoglobin concentration compared to control heifers (P = 0.04) (Figure 5-3).

Overview of RNA Sequencing Results

Abundance of transcripts was evaluated in oocytes of control (n = 5) and bacteria (n = 3) infused heifers at day 4, and control (n = 6) and bacteria (n = 3) infused heifers at day 60. The total number of oocytes aspirated at day 4 was 28 for control heifers and 15 for bacteria infused heifers. The total number of oocytes aspirated at day 60 was 11 for control heifers and 9 for bacteria infused heifers. Two heifers were not aspirated due to limitations relative to body size and the requirement for repeated manipulations. A volcano plot represents the distribution of expression for all identified genes at day 4 (Figure 5-4) and at day 60 (Figure 5-5).

Following analysis, a total of 9 differentially expressed genes were observed in oocytes of bacteria infused heifers on day 4 compared to controls heifers, based on an adjusted P-value $\leq$ 0.1 (Table 5-1). A total of 42 differentially expressed genes were observed in oocytes of bacteria infused heifers on day 60 compared to controls heifers, based on an adjusted P-value ≤ 0.1

(Table 5-2). Removing false discovery and only assessing the non-adjusted *P*-value, a total of 474 genes were differentially expressed in oocytes at day 4 of heifers infused with bacteria compared to controls (Non adjusted $P < 0.05$). At day 60, 929 genes were differentially expressed in oocytes of heifers infused with bacteria compared to controls (Non adjusted $P < 0.05$).

Selectively assessing the expression of genes involved in immunity and oocyte/embryo quality was performed independently of statistical analysis on oocytes collected at day 4 (Figure 5-6 and 5-7) and day 60 (Figure 5-8 and 5-9). No significant difference was observed in any of the genes evaluated (Non-adjusted $P > 0.05$). Most genes associated with immunity at day 60 had a numerically higher expression in the bacterial infused group compared to controls, but this pattern of expression was not observed in oocytes collected at day 4. Expression of oocyte specific factors *GDF9*, *BMP15* and *NLRP5* was numerically increased (Non-adjusted $P > 0.05$) in the bacteria infused group at day 4 compared to controls, but this numerical increase was not as evident in oocytes collected at day 60.

Pathway Analysis of Differentially Expressed Genes in Oocytes at Day 4

All pathway analysis was performed using the 474 differentially expressed genes based on non-adjusted *P*-values ≤ 0.05. Canonical pathways enriched by genes differentially expressed in oocytes at day 4 from heifers infused with bacteria are shown in Figure 5-10. Of the 126 significantly affected canonical pathways, 4 pathways had significant positive z-scores suggesting an upregulation of the pathway and 54 pathways had significant negative z-scores suggesting a downregulation of the pathway. Among the top 10 canonical pathways altered at day 4 include, interferon signaling, TGF-β signaling, TNFR2 signaling, IL-6 signaling and the BMP signaling pathway are all downregulated.

Analysis of differentially expressed genes revealed a total of 21 gene networks impacted in oocytes collected from heifers infused with bacteria at day 4. The highest scored gene networks included 1) neurological disease, cellular movement, nervous system development and function; 2) cellular development, connective tissue development and function, tissue development 3) cardiovascular system development and function, cell-to-cell signaling and interaction, connective tissue development and function; 4) cellular development, cellular growth and proliferation, hematological system development and function; 5) cell signaling, antimicrobial response, inflammatory response. The involvement of specific differentially regulated genes in the cell signaling, antimicrobial response, inflammatory response are shown in Figure 5-11; cellular development, cellular growth and proliferation, hematological system development and function is shown in Figure 5-12.

Prediction of upstream regulators of differentially expressed genes in bacteria infused heifers included genes and molecules related to our hypothesis such as *SOX2,* LPS and NFκB (Figure 5-13, 5-14 and 5-15, respectively).

Pathway Analysis of Differentially Expressed Genes in Oocytes at Day 60

All pathway analysis was performed using the 929 differentially expressed genes based on non-adjusted *P*-values ≤ 0.05. Of the 50 significantly affected canonical pathways, 22 pathways had significant positive z-scores suggesting an upregulation of the pathway and no pathways had significant negative z-scores based on the pattern of expression of the differentially regulated genes. The identified canonical pathways enriched by genes differentially expressed in oocytes at day 60 from heifers infused with bacteria are shown in Figure 5-16. Among the top 10 canonical pathways altered at day 60 include, glycolysis, bile acid biosynthesis neutral pathway, gluconeogenesis, ILK signaling, interferon signaling and chondroitin sulfate degradation.

Analysis using differentially regulated genes (Non-adjusted $P < 0.05$) revealed a total of 25 gene networks impacted in oocytes collected at day 60 from heifers infused with bacteria. The highest scored gene networks included 1) amino acid metabolism, small molecule biochemistry, developmental disorder; 2) cellular assembly and organization, cellular compromise, cellular function and maintenance 3) embryonic development, cancer, organismal injury and abnormalities; 4) cell morphology, hematological system development and function, hematopoiesis; 5) carbohydrate metabolism, small molecule biochemistry, cell morphology. The involvement of specific differentially regulated genes in the amino acid metabolism, small molecule biochemistry, developmental disorder is shown in Figure 5-17; embryonic development, cancer, organismal injury and abnormalities is shown in Figure 5-18. Prediction of upstream regulators of differentially expressed genes in bacteria infused heifers include molecules and genes related to our hypothesis such as IL-6, IL-1β and LH (Figure 5-19).

Discussion

The induction of clinical endometritis was successfully achieved by the use of the model described in chapter 4. Heifers infused with bacteria had an increased vaginal mucus grade until day 9 after infusion compared to control heifers. When vaginal mucus grade was evaluated during the whole experimental period, there was no significant effect of treatment. Starting at day 4 after infusion, the heifers were submitted to extensive manipulation for evaluation of the estrous cycle and follicle aspiration. These manipulations in small heifers (10 to 13 months) may have caused the observed increase vaginal mucus grade observed in the control heifers. Plasma haptoglobin concentration did not differ between treatments which is in agreement with the characterization of clinical endometritis by Sheldon et al, (2009), which describes clinical endometritis as the presence of purulent discharge with no systemic signs of disease.

The goal of this study was to identify the impact of uterine infection and inflammation on the oocyte. This information may help elucidate why cows have reduced fertility after developing uterine disease. Oocytes were aspirated during active disease (day 4) and after the resolution of disease (day 60). A larger number of genes were differentially expressed in oocytes of bacterial infused heifers at day 60, more so than differentially expressed at day 4. None of the genes differentially expressed, based on adjusted *P*-values (< 0.1), were reported in oocytes on both day 4 and 60, emphasizing differential effects of active inflammation on oocyte transcription during disease (day 4) and following resolution (day 60). The selective evaluation of genes involved in immune response independent of statistical analysis demonstrated that on day 60, there was an overall numerical increase in the expression of immune mediators in oocytes of bacteria infused heifers compared to control heifers. In contrast, the same evaluation performed on oocytes collected on day 4 did not reveal the same pattern of expression. Immune mediators play important roles during normal oocyte development, mostly participating in signaling between the oocyte and granulosa cells (Richards, 2005; Shimada et al., 2006; Richards et al., 2008). Because of their dual function as signaling molecules for oocyte development, and inflammatory mediators, these molecules could potentially alter oocyte quality.

The assessment of genes important in oocyte and embryo development did not show significant differences between treatments. Interestingly, *GDF9, BMP15* and *NLRP5* were all numerically increased in oocytes collected from bacteria infused heifers at day 4. A previous study has shown the expression of GDF-9 within oocytes to be reduced in cows with chronic mastitis (Rahman et al., 2012), but we did not observe the same difference in gene expression in our study. The genes mentioned above encode oocyte specific factors that are essential for oocyte maturation, mitochondrial function, granulosa cell growth and expansion (Dong et al.,

1996; Gilchrist et al., 2008; Sudiman et al., 2014; Moussa et al., 2015). Alterations in their expression could influence embryo development and shape pregnancy outcome.

Pathway Analysis

Although a higher number of genes were differentially expressed in oocytes collected from bacteria infused heifers at day 60 compared to day 4, the number of affected canonical pathways at day 4 was more than double that identified at day 60. Among the 126 canonical pathways affected at day 4, it is important to notice that only 4 had positive z-scores indicating upregulation of the pathway and 54 had negative z-scores suggesting downregulation of the pathway. Many of the pathways with negative z-scores are involved in immune response, more specifically, pro-inflammatory responses and responses associated with bacterial components, including, LPS-stimulated MAPK signaling, IL-6 signaling, and NFκB signaling. Surprisingly these pathways are predicted to be downregulated in oocytes collected from bacteria infused heifers at day 4, when active disease is present. This presumed downregulation may be a protective mechanism of the oocyte to avoid potential damage caused by immune mediators, subsequently regulating their expression for specific stages of oocyte and follicle development. The follicles aspirated in these studies can all be consider antral follicles, according to their size, visualization by ultrasonography and ability to be aspirated. Previously, culture of ovarian cortex in the presence of LPS increased accumulation of inflammatory mediators, but when secondary follicles were cultured in the presence of LPS the production of IL-6 was only affected after 6 days of culture (Bromfield and Sheldon, 2013). Different follicle sizes may respond differently to the presence of bacterial components or inflammatory mediators, that could indicate their ability to tolerate the challenges imposed by disease.

Oocytes from bacteria infused heifers collected at day 60 had almost half the number of identified canonical pathways affected compared to oocytes collected at day 4. While a smaller

number of pathways associated with immune response were significantly affected in oocytes collected at day 60, compared to oocytes collected at day 4, all immune pathways were predicted to be upregulated. Interleukin signaling, acute phase response signaling and production of reactive oxygen species are some examples of activated canonical pathways identified in oocytes collected from bacteria infused heifers at day 60. It is unclear why oocytes collected on day 60 seem to be activating immune pathways after the resolution of disease while oocytes collected at day 4 are downregulating immune pathways. As previously mentioned, these immune mediators have roles outside of the inflammatory response, and signal between oocytes and granulosa cells. We can hypothesize that oocytes collected at day 60 are no longer under the acute influence of disease or inflammation, and do not need to decrease the expression of inflammatory mediators in order to regulate their accumulation.

This pattern of expression between oocytes collected at day 4 and day 60 can also be observed in the predicted upstream regulators of differentially expressed genes. Although associated to the immune response, NFκB and LPS are predicted inhibitors of down regulated genes identified in oocytes collected at day 4 of heifers infused with bacteria. The cytokines IL-6 and IL-1β were predicted as upstream promoters of upregulated genes in oocytes collected at day 60. These observations suggest that oocytes collected from bacterial infused heifers are under a stronger influence by these cytokines compared to control oocytes. The concept that the oocyte has a protective mechanism during active disease can be further argued by the gene networks impacted at day 4. The gene networks of oocytes collected at day 4 indicate a downregulation in cell signaling, antimicrobial response and inflammatory response, as well as cellular development, cellular growth and proliferation, and hematological system development and function. This supports the theory that the oocyte might be shutting down genes associated with

the immune response in addition to its normal cellular mechanisms such as growth and cell signaling, in order to avoid potential damage. Oocytes collected at day 60 had altered gene networks associated with amino acid metabolism, small molecule biochemistry and developmental disorder, embryonic development, cancer, organismal injury and abnormalities. This suggests that the possible protective mechanisms in place during acute disease are no longer present in oocytes collected at day 60. The enduring effects of disease at day 60 impact the oocyte in a different way from the effects of acute disease. Potentially, the reduced hazard at day 60 does not indicate to the oocyte to decrease its normal activities and metabolism as it does at day 4. This attempt from the oocyte to maintain its normal activity, may increase oocyte vulnerability to the remaining marks left by uterine disease in the ovary.

These results allow us to speculate that initially the oocyte has mechanisms in place to try to avoid the impacts of uterine disease. Studies *in vitro* have looked at the "acute" effects of disease in oocytes and COCs, and demonstrated that the oocyte increases meiotic failure when cultured in the presence of bacterial components, and show reduced blastocyst rates after IVF. These previous studies do not support the idea of an oocyte possessing a protective mechanism against infection or inflammation (Soto et al., 2003a; Bromfield and Sheldon, 2011). It is important to emphasize that oocyte maturation occurs *in vivo* during a period of months and is tightly coordinated by the follicle; while IVM occurs in a period of hours. Although extensive improvements has been made to IVM systems, it is still known to negatively impact oocyte development compared to *in vivo* maturation (Rizos et al., 2002; Sutton et al., 2003; Thélie et al., 2007). While it is important to understand the mechanisms by which uterine disease impacts the oocyte, the results observed in IVM studies may not mimic what is observed during the initial exposure of oocytes to the disease *in vivo.* Nonetheless, growing oocytes exposed to the acute

disease that continue to develop in the ovary may lose the ability to simply avoid the disease effects or may not find necessary to shut down development like during the strong insult. In both cases the oocyte may be more susceptible to the negative alterations of the follicular environment in response to uterine disease.

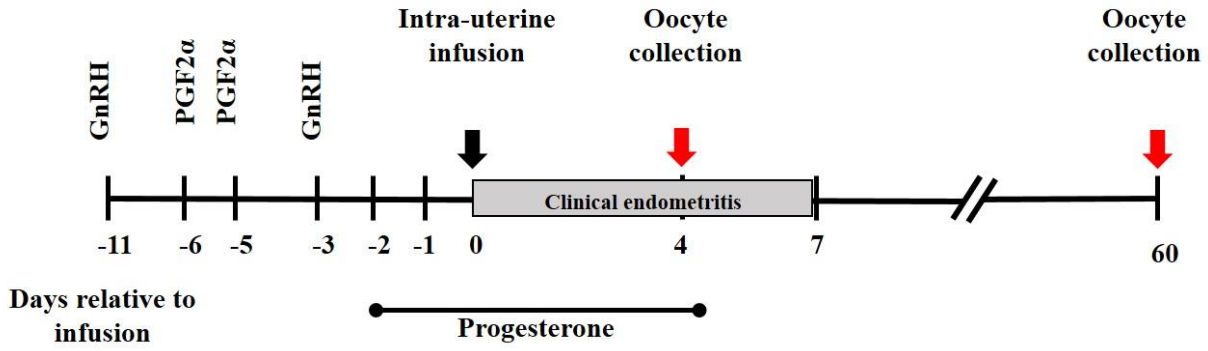

Figure 5-1. Timeline for establishment of experimental uterine infection and collection days for oocytes. Gonadotropin releasing hormone (GnRH) and prostaglandin (PG) F2α were used to synchronize estrous cycles in 10 virgin Holstein heifers before intra-uterine infusion of treatments. On d 0, intra-uterine infusion of either vehicle or live bacteria was performed. Progesterone was administered at 200 mg/d i.m. Oocyte collection was performed by ovum pick-up aspiration at days 4 and 60 after infusion of treatments.

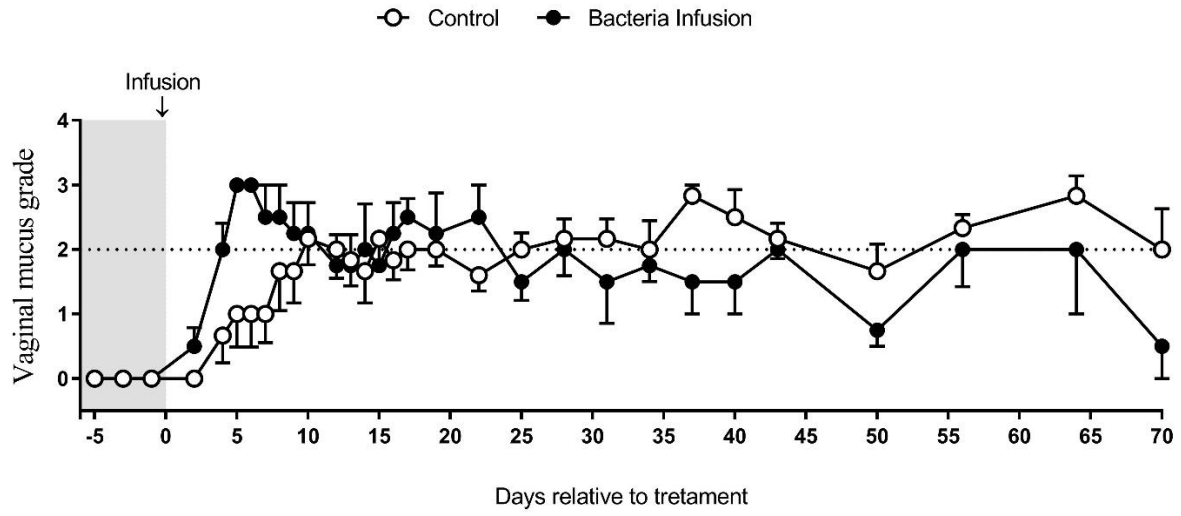

Figure 5-2. Vaginal mucus grade following intra-uterine infusion of treatment. Vaginal mucus was collected using a Metricheck tool and graded according to Sheldon et al. (2009). Vaginal mucus was graded from 0 to 3 and data is presented as mean score for each treatment. Control heifers are represented by open circles (A, ○), bacteria infused heifers are represented by filled circles (B, ●). There was no significant effect of treatment ($P = 0.54$) or effect of day ($P = 0.06$). There was a significant interaction between treatment and day ($P = 0.001$). Bacteria infused heifers had an increased vaginal mucus grade on days 3 to 9 compared to control cows ($P \leq 0.05$).

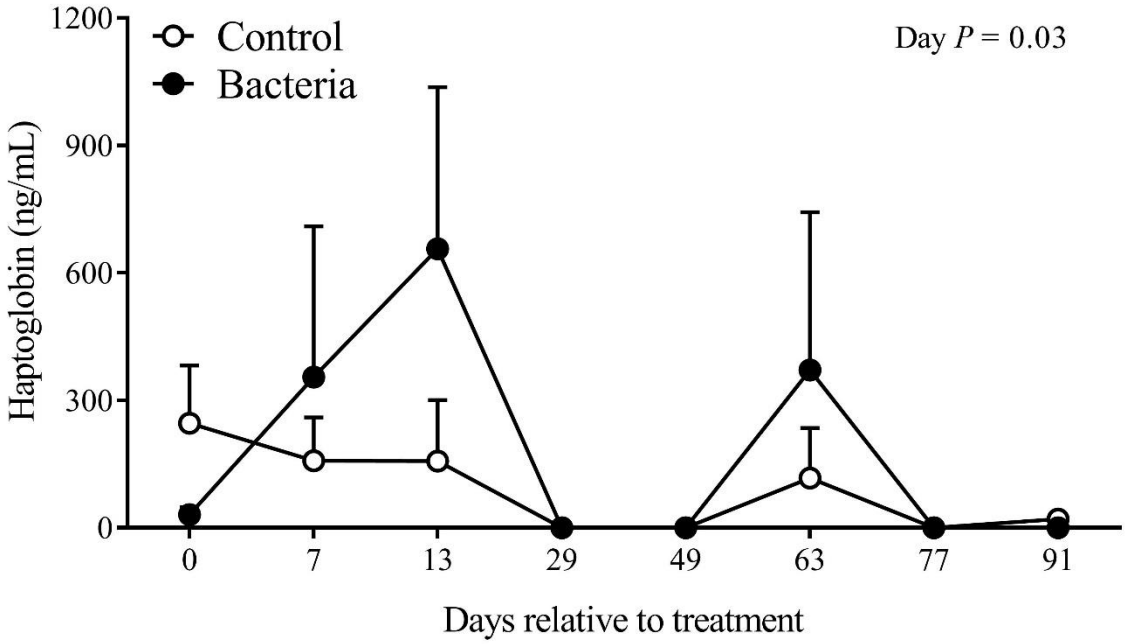

Figure 5-3. Effect of treatment on circulating concentrations of haptoglobin in plasma. Haptoglobin plasma concentration (ng/mL) was measured in control (○) and bacteria infused (●) heifers on d 0, 7, 13, 29, 49, 63, 77 and 91 relative to treatment. All data are presented as LSM ± SEM. There was no significant effect of treatment ($P = 0.36$) There was a significant effect of day ($P = 0.03$). On day 13, there was a significant effect of treatment ($P = 0.04$).

Table 5-1. Significant differentially expressed genes in oocytes collected 4 days after bacteria infusion, based on adjusted *P*-value ($P < 0.1$).

	Gene	Fold Change (Log_2)	Adjusted *P*-value	*P*-value
POLR2K	RNA polymerase II subunit K	10.1	9.39E-05	2.66E-09
NDP	Norrin cysteine knot growth factor	-6.98	5.54E-03	4.70E-07
GSN	Gelsolin	-6.44	1.17E-02	1.65E-06
S100A4	S100 calcium binding protein A4	-7.91	1.60E-02	2.72E-06
SPON2	Spondin 2	-8.55	2.12E-02	4.19E-06
LAPTM5	Lysosomal protein transmembrane 5	-4.87	3.63E-02	9.25E-06
KRT1	Keratin 1 type II	-5.88	6.41E-02	2.90E-05
TNFAIP3	TNF alpha induced protein 3	-7.20	6.71E-02	3.23E-05
AMIGO2	Adhesion molecule Ig like domain 2	-3.57	0.072657417	4.11E-05

Table 5-2. Significant differentially expressed genes in oocytes collected 60 days after bacteria infusion, based on adjusted P-value (P < 0.1)..

	Genes	Fold Change (Log_2)	*P*-value adjusted	*P*-value
LOC616942	Major histocompatibility complex, class I, A-like	5.002247	5.35E-07	2.98E-11
COL5A1	Collagen type V alpha 1	6.999139	1.28E-06	1.07E-10
CCT6A	Chaperonin containing TCP1 subunit 6A	2.744358	0.000974	1.15E-07
KLF10	Kruppel like factor 10	2.077653	0.000974	1.50E-07
INSL3	*I*nsulin like 3	2.850191	0.000974	1.63E-07
UPK1B	Uuroplakin 1B	3.260402	0.000986	1.92E-07
H2AFZ	H2A histone family, member Z	2.499388	0.004648	1.34E-06
LPL	Lipoprotein lipase	3.506794	0.004648	1.42E-06
LAPTM4B	Lysosomal protein transmembrane 4 beta	2.18545	0.005351	1.79E-06
GATA6	GATA binding protein 6	2.947589	0.005351	1.97E-06
ZNF484	Zinc finger protein 484	3.283334	0.005351	2.09E-06
PPP1R3B	Protein phosphatase 1 regulatory subunit 3B	3.922977	0.00557	2.33E-06
CUX1	Cut-like homeobox 1	3.452348	0.009016	4.07E-06
CD58	CD58 molecule	3.18432	0.009037	4.53E-06
PROS1	Protein S	2.494146	0.009085	4.90E-06
JAM2	Junctional adhesion molecule 2	2.970416	0.009085	5.31E-06
CYP19A1	Cytochrome P450, family 19, subfamily A, polypeptide 1	4.515587	0.015549	9.53E-06
MANF	Mesencephalic astrocyte derived neurotrophic factor	1.540591	0.017418	1.16E-05
ADAM22	ADAM metallopeptidase domain 22	-8.19946	0.019196	1.34E-05

Table 5-2. Continued

Genes		Fold Change (Log_2)	*P*-value adjusted	*P*-value
PSMA2	Proteasome subunit alpha 2	2.340089	0.02465	1.79E-05
IL27RA	Interleukin 27 receptor subunit alpha	2.188418	0.02465	1.85E-05
NAP1L5	Nucleosome assembly protein 1 like 5	4.1679	0.024751	2.00E-05
PRPS1	Phosphoribosyl pyrophosphate synthetase 1	2.098539	0.025982	2.32E-05
SMOC2	SPARC related modular calcium binding 2	1.836475	0.025982	2.39E-05
TMEM246	Transmembrane protein 246	2.518192	0.028939	2.82E-05
SERPINH1	Serpin family H member 1	2.182735	0.032372	3.38E-05
IPO8	Importin 8	2.467598	0.032372	3.43E-05
CTHRC1	Collagen triple helix repeat containing 1	7.925258	0.033011	3.59E-05
ETF1	Eukaryotic translation termination factor 1	2.678116	0.039247	4.59E-05
PLOD2	Procollagen-lysine,2-oxoglutarate 5-dioxygenase 2	2.372755	0.040729	4.88E-05
ISG20L2	Interferon stimulated exonuclease gene 20 like 2	2.288325	0.046779	5.73E-05
RAB34	*RAB34* member RAS oncogene family	1.802643	0.054296	6.81E-05
PKM	Pyruvate kinase M1/2	1.923183	0.05438	6.97E-05
AKAP2	A kinase anchor protein 2	2.160927	0.059837	7.83E-05
HPSE	Heparanase	2.312986	0.061346	8.20E-05
MBTPS2	Membrane bound transcription factor peptidase	3.23657	0.0682	9.31E-05
BCDIN3D	*BCDIN3* domain containing RNA methyltransferase	4.844768	0.069537	9.68E-05
MAOA	Monoamine oxidase A	3.502149	0.070477	0.000102

Table 5-2. Continued

	Genes	Fold Change (Log_2)	*P*-value adjusted	*P*-value
SRSF3	Serine and arginine rich splicing factor 3	1.451458	0.090595	0.000146
TAPBP	TAP binding protein	3.031681	0.097283	0.000162
TYW3	tRNA-yW synthesizing protein 3 homolog	3.408016	0.097283	0.000163
VSNL1	Visinin like 1	1.970246	0.097283	0.000165

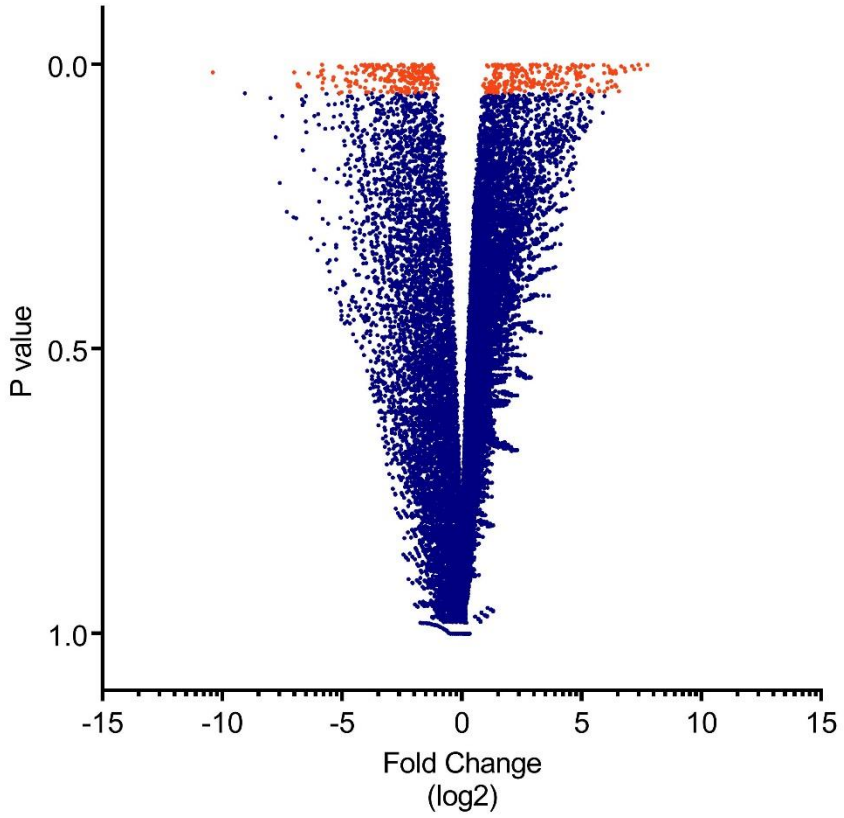

Figure 5-4. Volcano plot representing the distribution of all genes expressed in oocytes collected at day 4. Differentially expressed genes identified in oocytes from heifers infused with bacteria compared to control heifers are displayed in orange ($P < 0.05$).

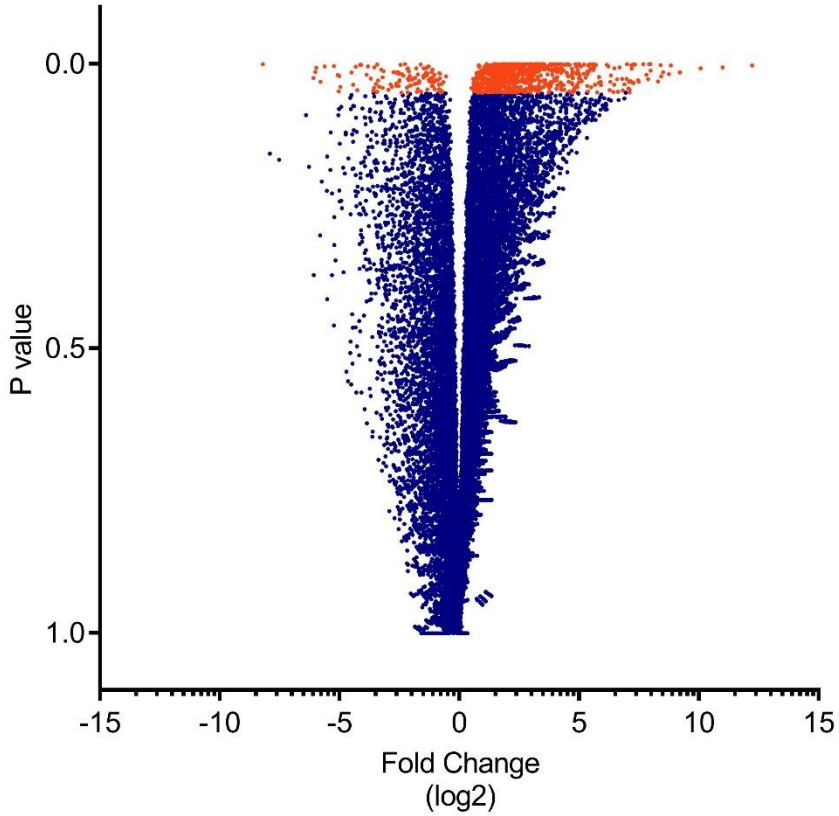

Figure 5-5. Volcano plot representing the distribution of all genes expressed in oocytes collected at day 60. Differentially expressed genes identified in oocytes from heifers infused with bacteria compared to control heifers are displayed in orange ($P < 0.05$).

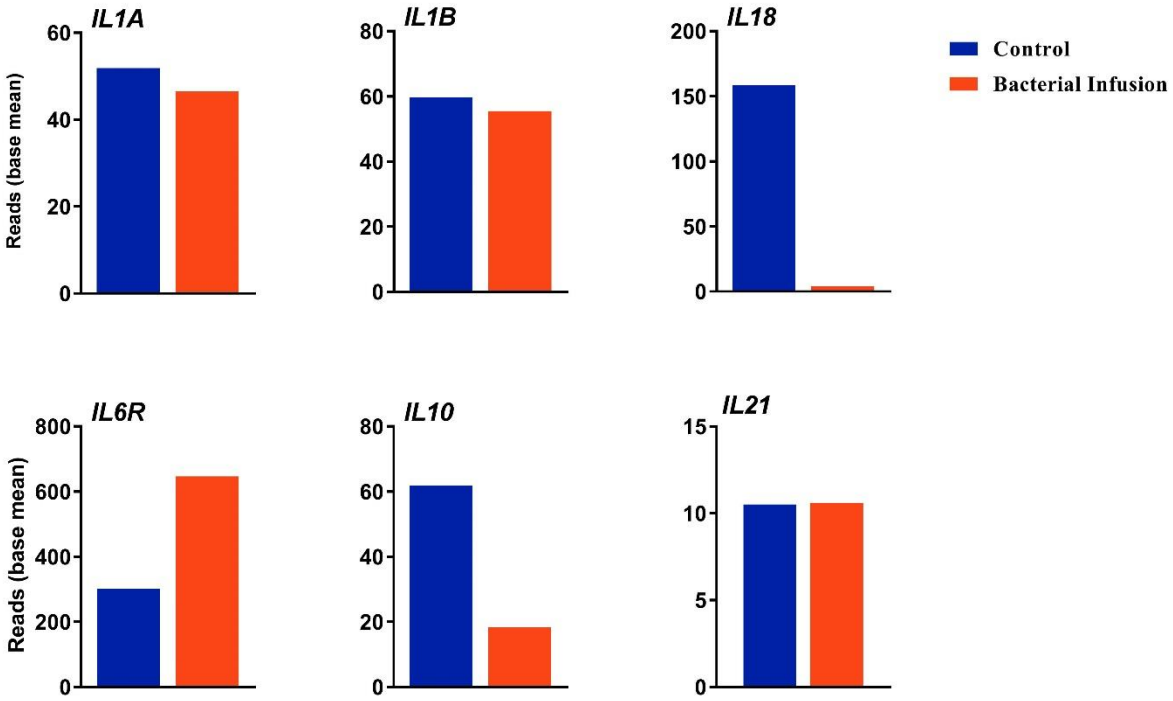

Figure 5-6. Evaluation of selected genes involved in immunity of oocytes collected at day 4. Asterisk (*) indicates a significant difference for the specific gene (*$P \leq 0.05$).

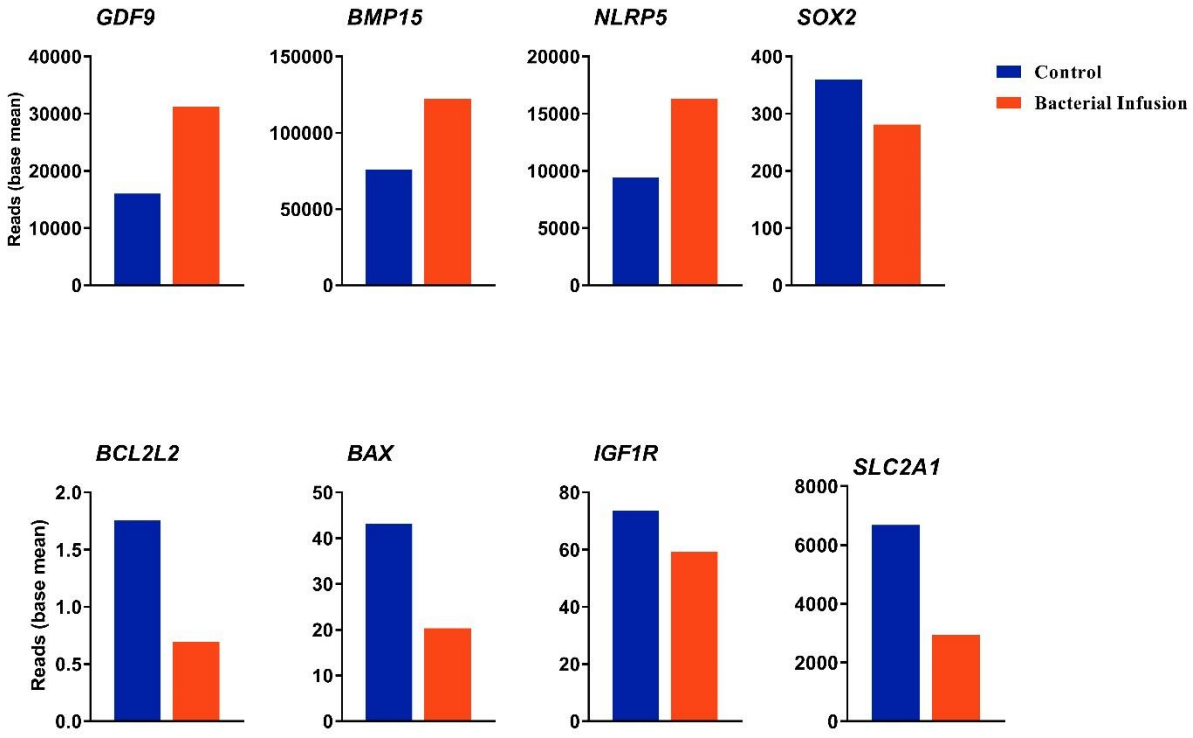

Figure 5-7. Evaluation of selected genes involved in oocyte and embryo quality of oocytes collected at day 4. Asterisk (*) indicates a significant difference for the specific gene (*$P \leq 0.05$).

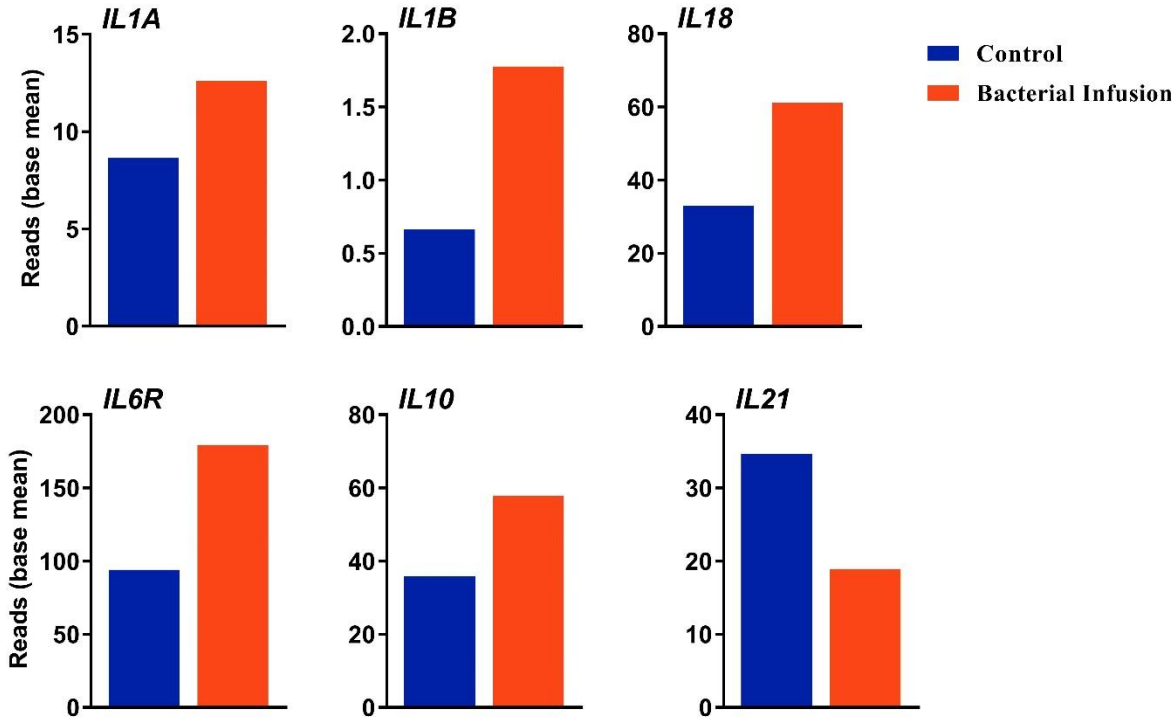

Figure 5-8. Evaluation of selected genes involved in immunity of oocytes collected at day 60. Asterisk (*) indicates a significant difference for the specific gene (*$P \leq 0.05$).

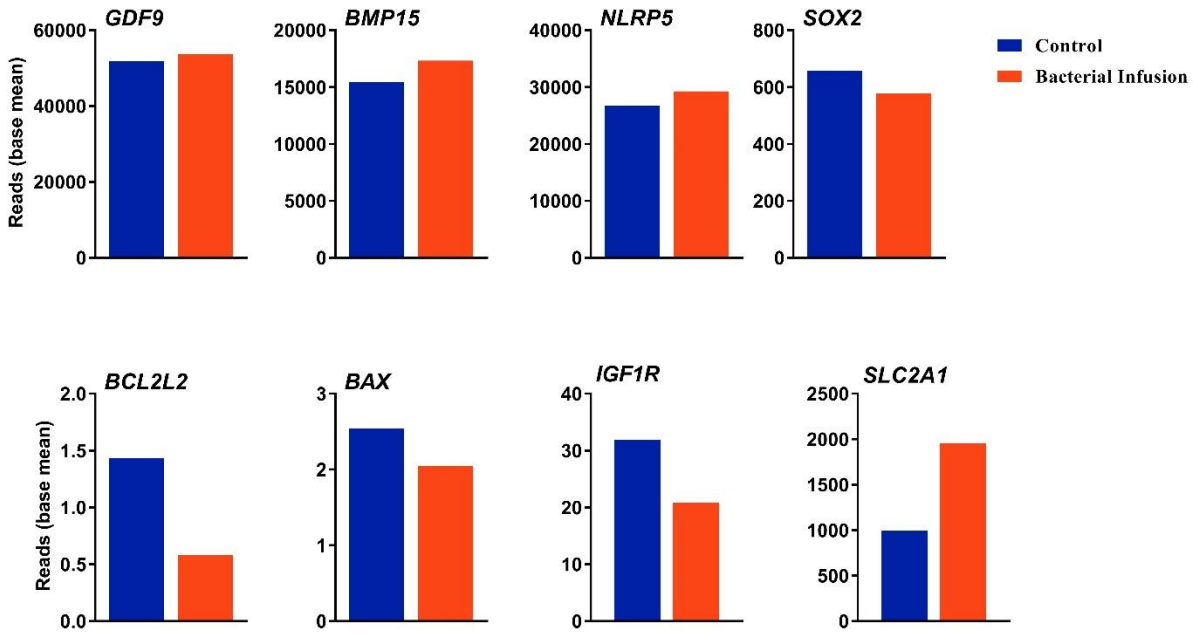

Figure 5-9. Evaluation of selected genes involved in oocyte and embryo quality of oocytes collected at day 60. Asterisk (*) indicates a significant difference for the specific gene (*$P \leq 0.05$).

A

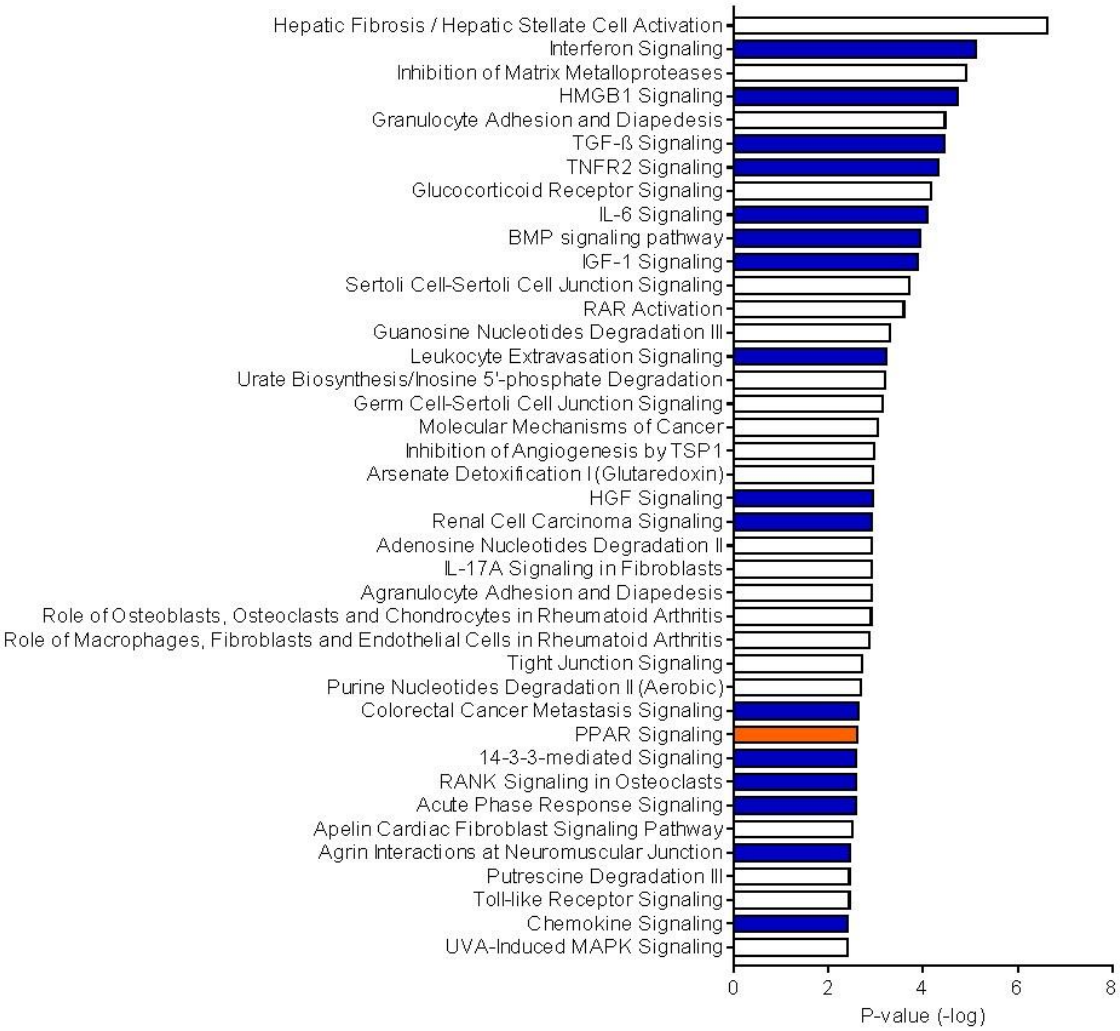
Hepatic Fibrosis / Hepatic Stellate Cell Activation
Interferon Signaling
Inhibition of Matrix Metalloproteases
HMGB1 Signaling
Granulocyte Adhesion and Diapedesis
TGF-ß Signaling
TNFR2 Signaling
Glucocorticoid Receptor Signaling
IL-6 Signaling
BMP signaling pathway
IGF-1 Signaling
Sertoli Cell-Sertoli Cell Junction Signaling
RAR Activation
Guanosine Nucleotides Degradation III
Leukocyte Extravasation Signaling
Urate Biosynthesis/Inosine 5'-phosphate Degradation
Germ Cell-Sertoli Cell Junction Signaling
Molecular Mechanisms of Cancer
Inhibition of Angiogenesis by TSP1
Arsenate Detoxification I (Glutaredoxin)
HGF Signaling
Renal Cell Carcinoma Signaling
Adenosine Nucleotides Degradation II
IL-17A Signaling in Fibroblasts
Agranulocyte Adhesion and Diapedesis
Role of Osteoblasts, Osteoclasts and Chondrocytes in Rheumatoid Arthritis
Role of Macrophages, Fibroblasts and Endothelial Cells in Rheumatoid Arthritis
Tight Junction Signaling
Purine Nucleotides Degradation II (Aerobic)
Colorectal Cancer Metastasis Signaling
PPAR Signaling
14-3-3-mediated Signaling
RANK Signaling in Osteoclasts
Acute Phase Response Signaling
Apelin Cardiac Fibroblast Signaling Pathway
Agrin Interactions at Neuromuscular Junction
Putrescine Degradation III
Toll-like Receptor Signaling
Chemokine Signaling
UVA-Induced MAPK Signaling
0
2
4
6
8
P-value (-log)

B

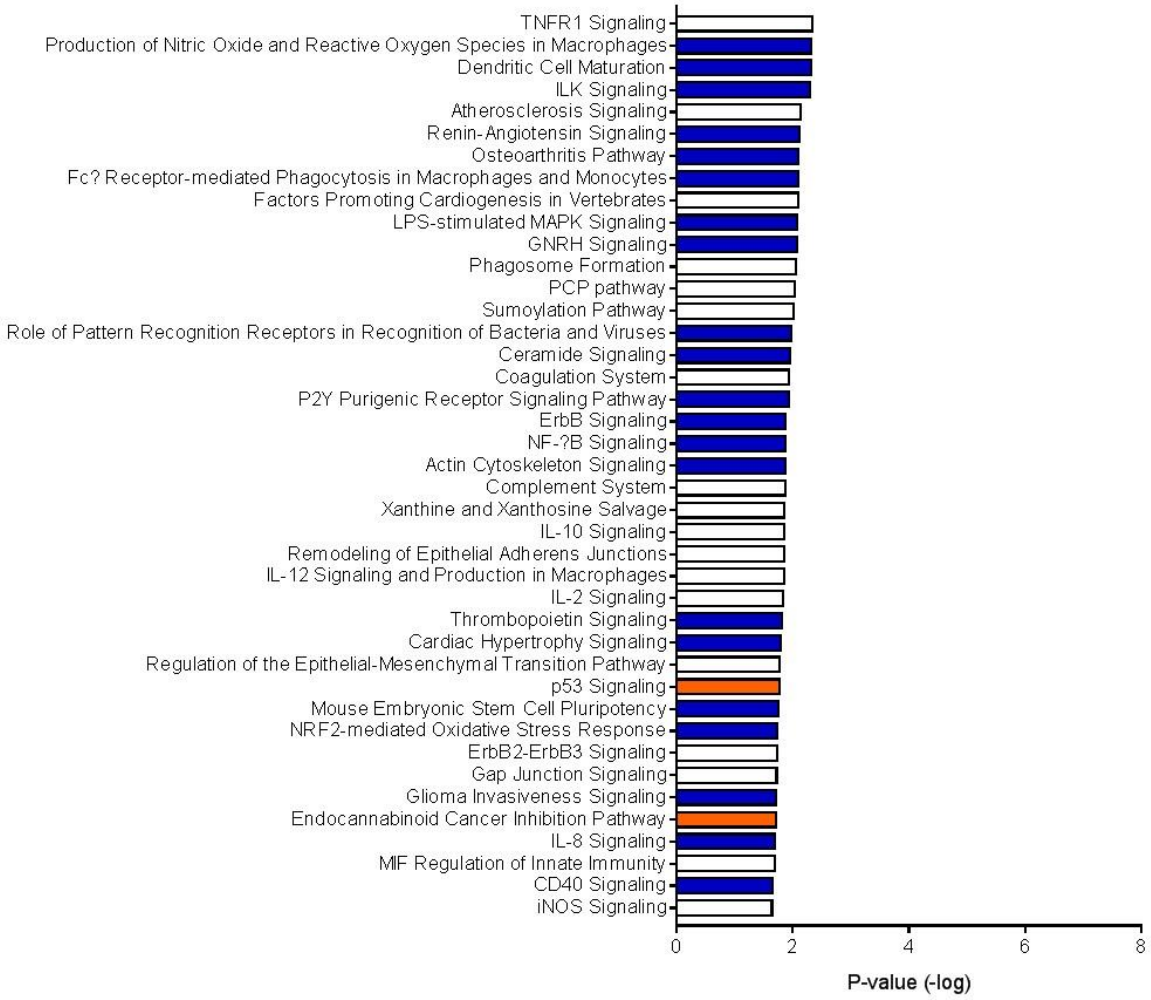
TNFR1 Signaling
Production of Nitric Oxide and Reactive Oxygen Species in Macrophages
Dendritic Cell Maturation
ILK Signaling
Atherosclerosis Signaling
Renin-Angiotensin Signaling
Osteoarthritis Pathway
Fc? Receptor-mediated Phagocytosis in Macrophages and Monocytes
Factors Promoting Cardiogenesis in Vertebrates
LPS-stimulated MAPK Signaling
GNRH Signaling
Phagosome Formation
PCP pathway
Sumoylation Pathway
Role of Pattern Recognition Receptors in Recognition of Bacteria and Viruses
Ceramide Signaling
Coagulation System
P2Y Purigenic Receptor Signaling Pathway
ErbB Signaling
NF-?B Signaling
Actin Cytoskeleton Signaling
Complement System
Xanthine and Xanthosine Salvage
IL-10 Signaling
Remodeling of Epithelial Adherens Junctions
IL-12 Signaling and Production in Macrophages
IL-2 Signaling
Thrombopoietin Signaling
Cardiac Hypertrophy Signaling
Regulation of the Epithelial-Mesenchymal Transition Pathway
p53 Signaling
Mouse Embryonic Stem Cell Pluripotency
NRF2-mediated Oxidative Stress Response
ErbB2-ErbB3 Signaling
Gap Junction Signaling
Glioma Invasiveness Signaling
Endocannabinoid Cancer Inhibition Pathway
IL-8 Signaling
MIF Regulation of Innate Immunity
CD40 Signaling
iNOS Signaling
0
2
4
6
8
P-value (-log)

C

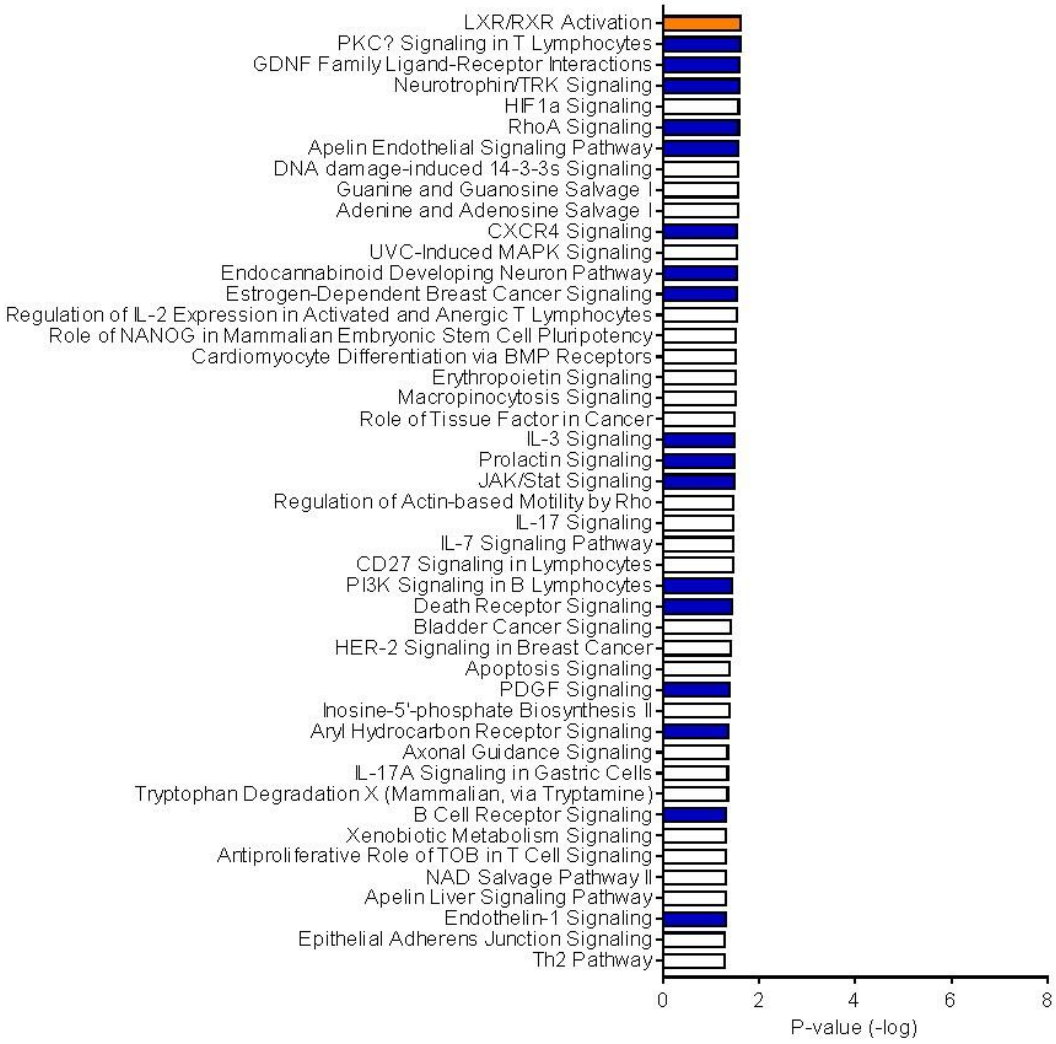

Figure 5-10. A, B, C - Affected canonical pathways predicted based on differentially expressed genes in oocytes from bacterial infused heifers at day 4. Pathways with significant positive z-scores are represented in orange and pathways with significant negative z-scores are represented in blue.

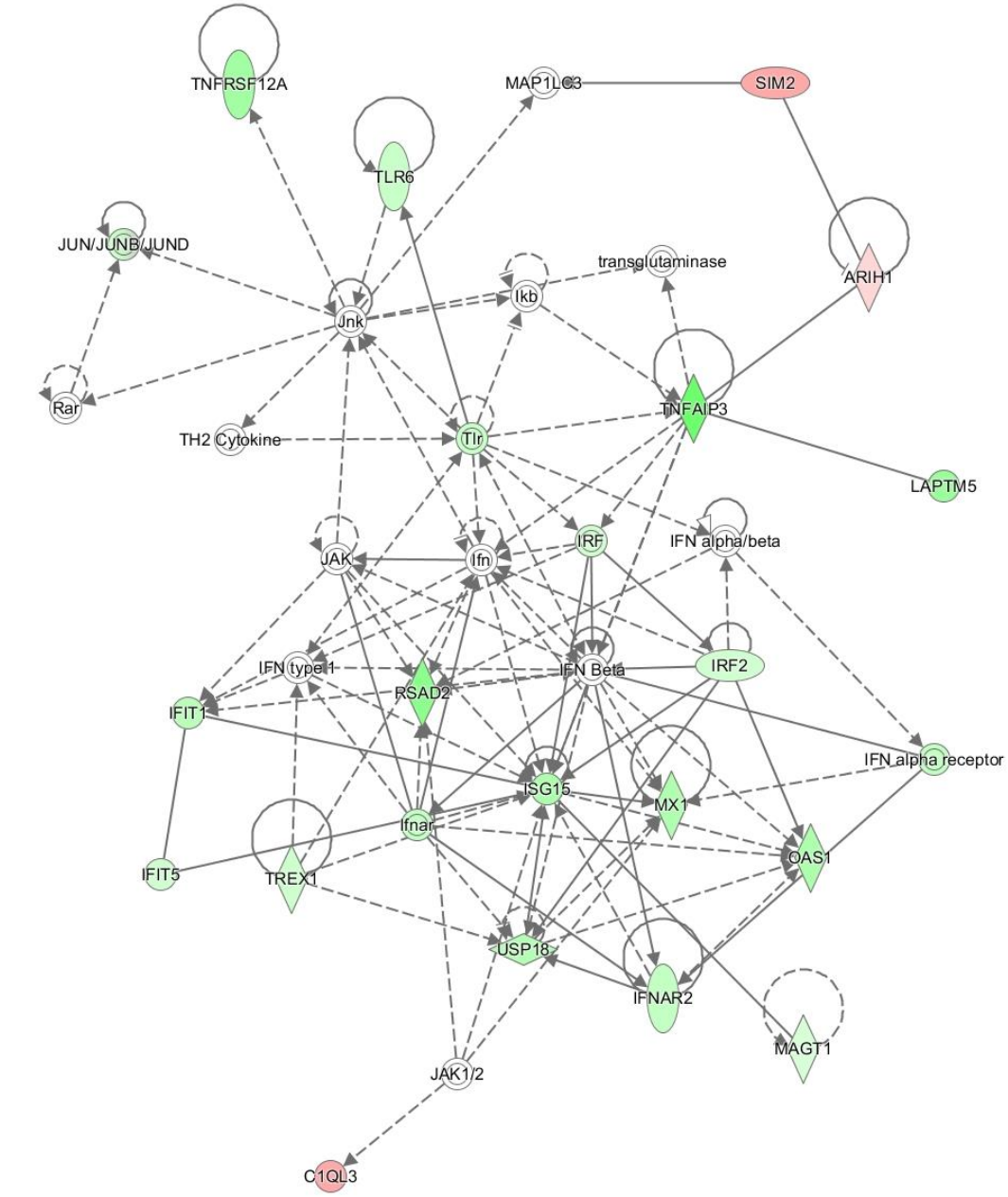

Figure 5-11. Gene network of specific differentially regulated genes in oocytes from bacterial infused heifers at day 4. Gene network in cell signaling, antimicrobial response and inflammatory response. Genes shown in red (up) or green (down) and differentially expressed in bacteria infused heifers.

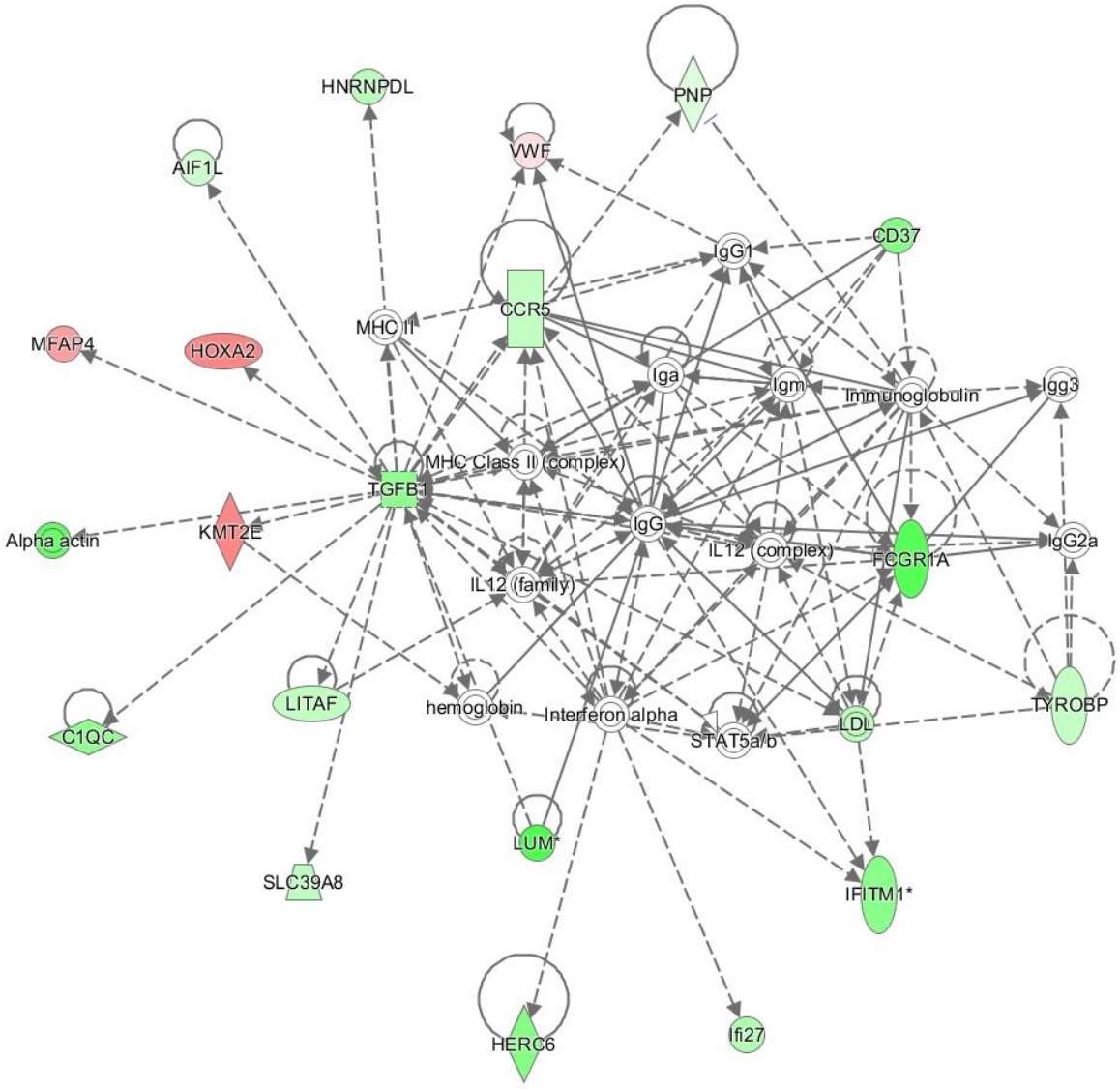

Figure 5-12. Gene network of specific differentially regulated genes in oocytes from bacterial infused heifers at day 4. Gene network in cellular development, cellular growth and proliferation and hematological system development and function. Genes shown in red (up) or green (down) and differentially expressed in bacteria infused heifers.

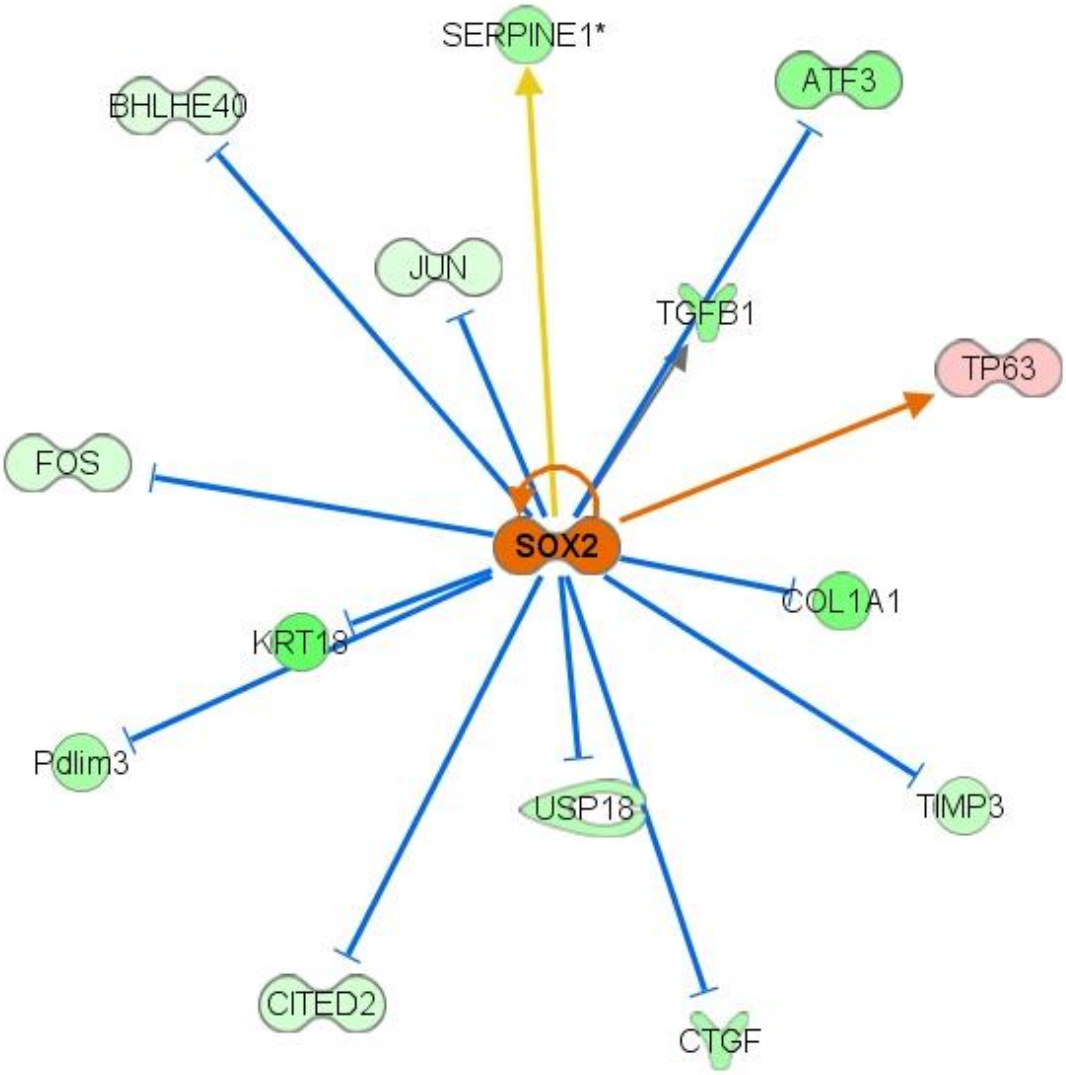

Figure 5-13. *SOX2* as a predicted upstream regulator of differentially expressed genes in oocytes of bacterial infused heifers at day 4. Genes shown in red (up) or green (down) and differentially expressed in bacteria infused heifers.

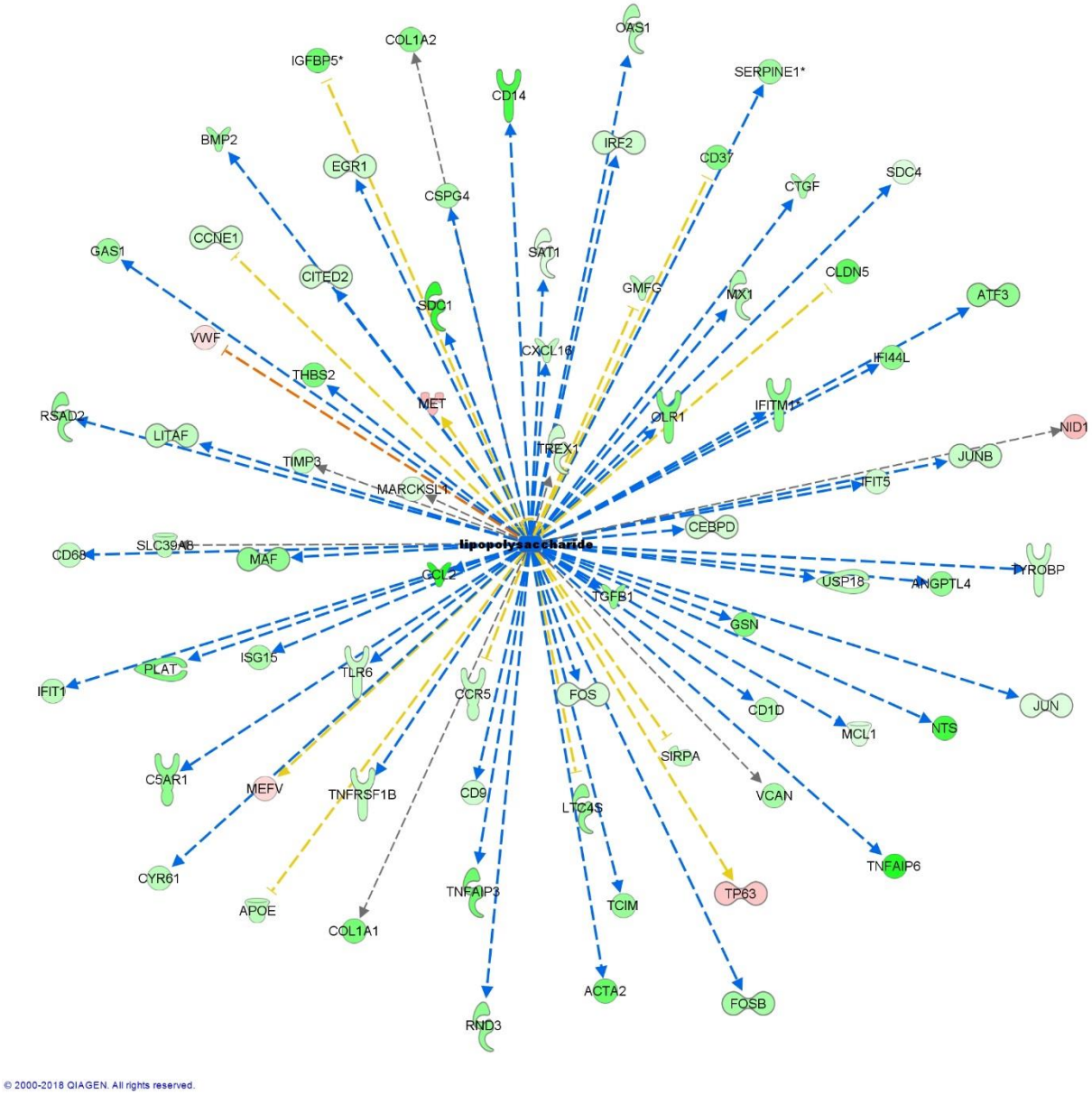

Figure 5-14. Lipopolysaccharide as a predicted upstream regulator of differentially expressed genes in oocytes of bacterial infused heifers at day 4. Genes shown in red (up) or green (down) and differentially expressed in bacteria infused heifers.

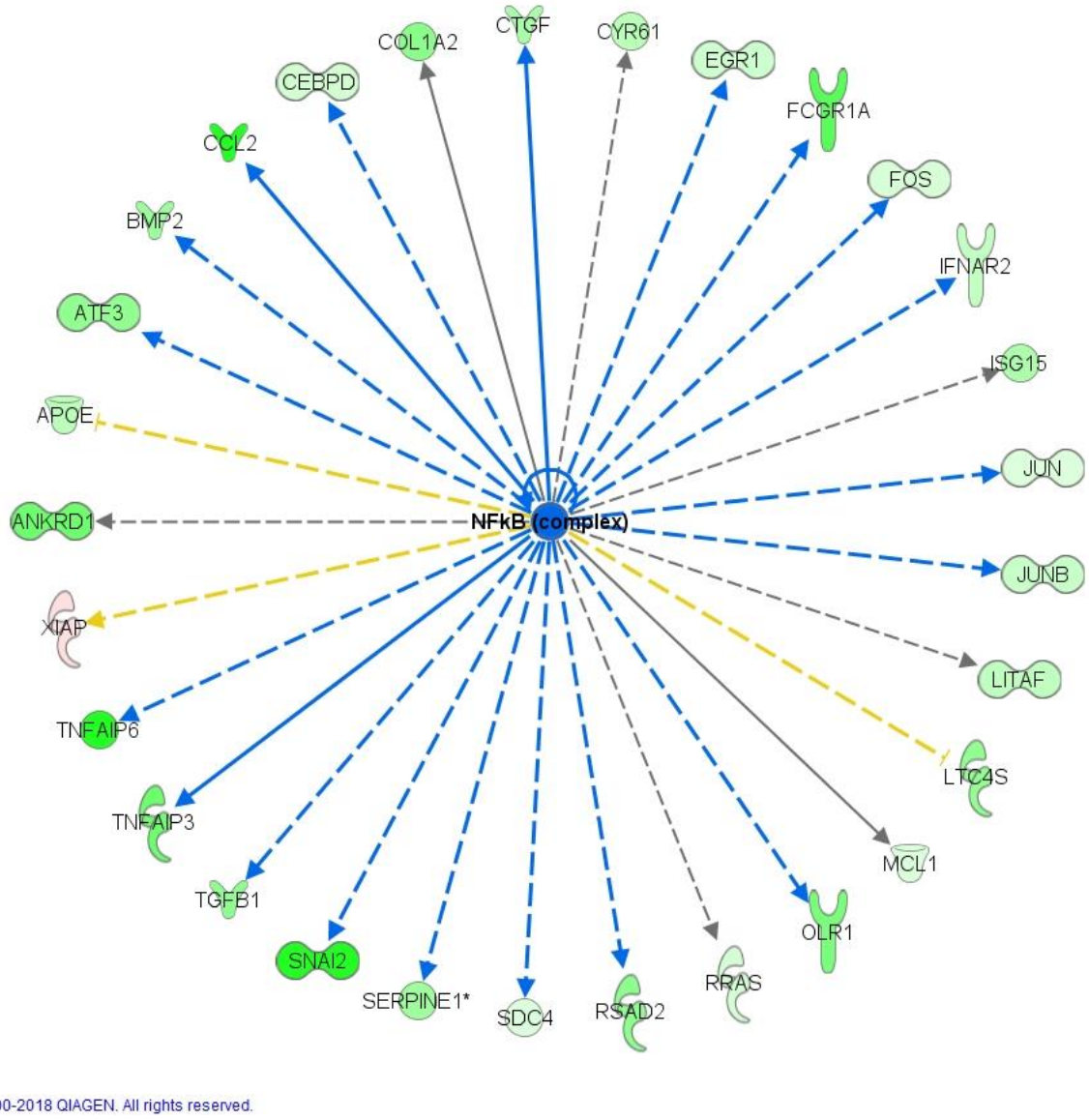

Figure 5-15. NFκB as a predicted upstream regulator of differentially expressed genes in oocytes of bacterial infused heifers at day 4. Genes shown in red (up) or green (down) and differentially expressed in bacteria infused heifers.

A

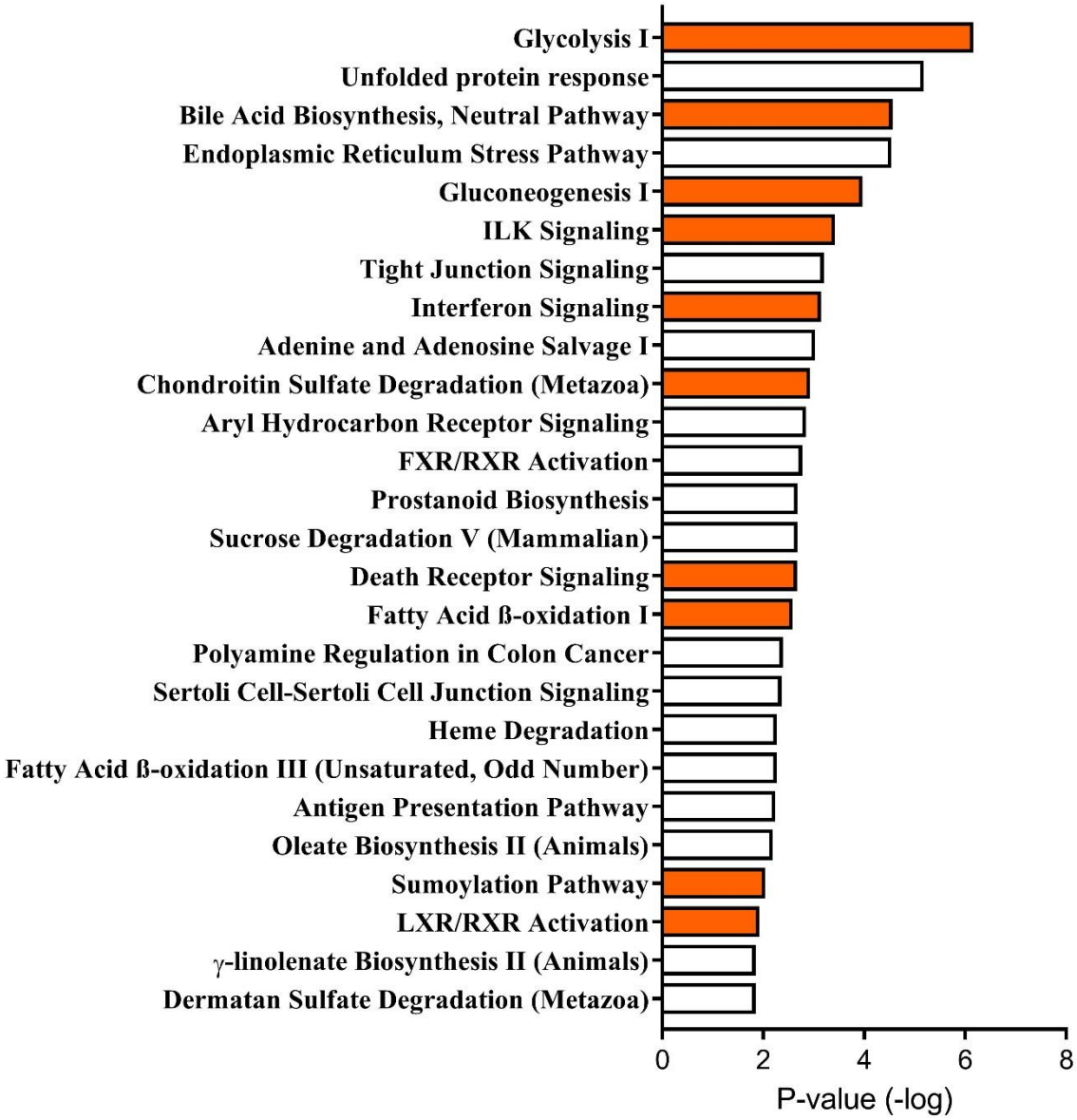
Glycolysis I
Unfolded protein response
Bile Acid Biosynthesis, Neutral Pathway
Endoplasmic Reticulum Stress Pathway
Gluconeogenesis I
ILK Signaling
Tight Junction Signaling
Interferon Signaling
Adenine and Adenosine Salvage I
Chondroitin Sulfate Degradation (Metazoa)
Aryl Hydrocarbon Receptor Signaling
FXR/RXR Activation
Prostanoid Biosynthesis
Sucrose Degradation V (Mammalian)
Death Receptor Signaling
Fatty Acid ß-oxidation I
Polyamine Regulation in Colon Cancer
Sertoli Cell-Sertoli Cell Junction Signaling
Heme Degradation
Fatty Acid ß-oxidation III (Unsaturated, Odd Number)
Antigen Presentation Pathway
Oleate Biosynthesis II (Animals)
Sumoylation Pathway
LXR/RXR Activation
γ-linolenate Biosynthesis II (Animals)
Dermatan Sulfate Degradation (Metazoa)
0
2
4
6
8
P-value (-log)

B

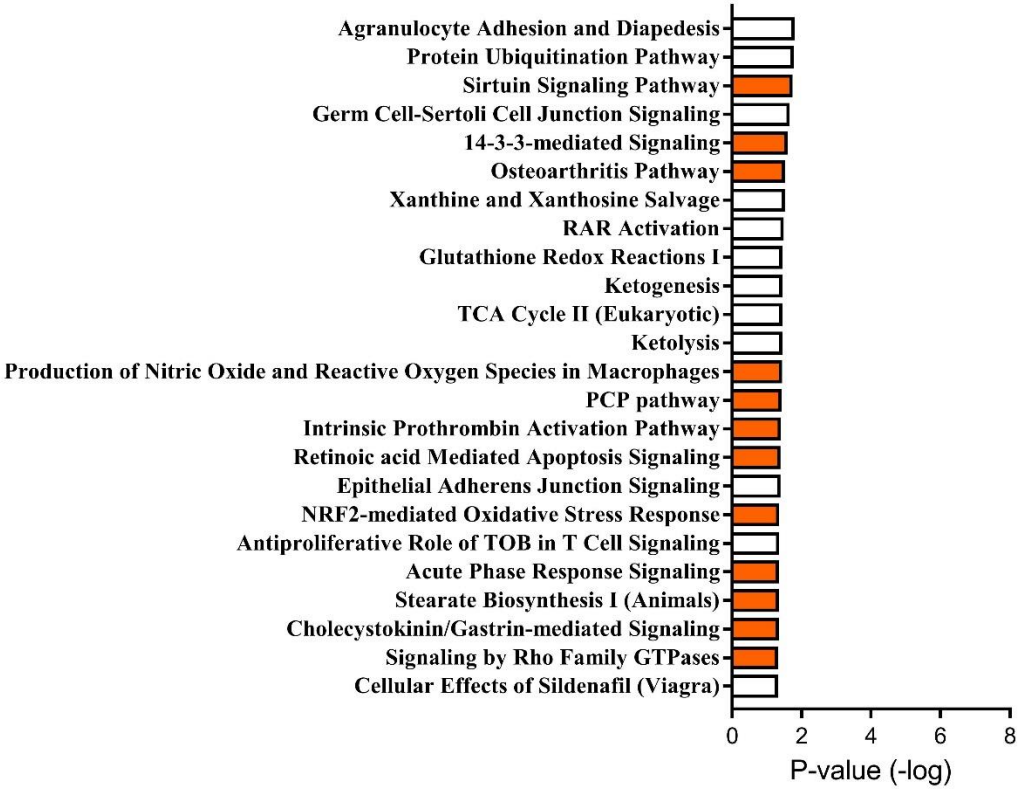

Figure 5-16. A, B - Affected canonical pathways predicted based on differentially expressed genes in oocytes from bacterial infused heifers at day 60. Pathways with significant positive z-scores are represented in orange and pathways with significant negative z-scores are represented in blue.

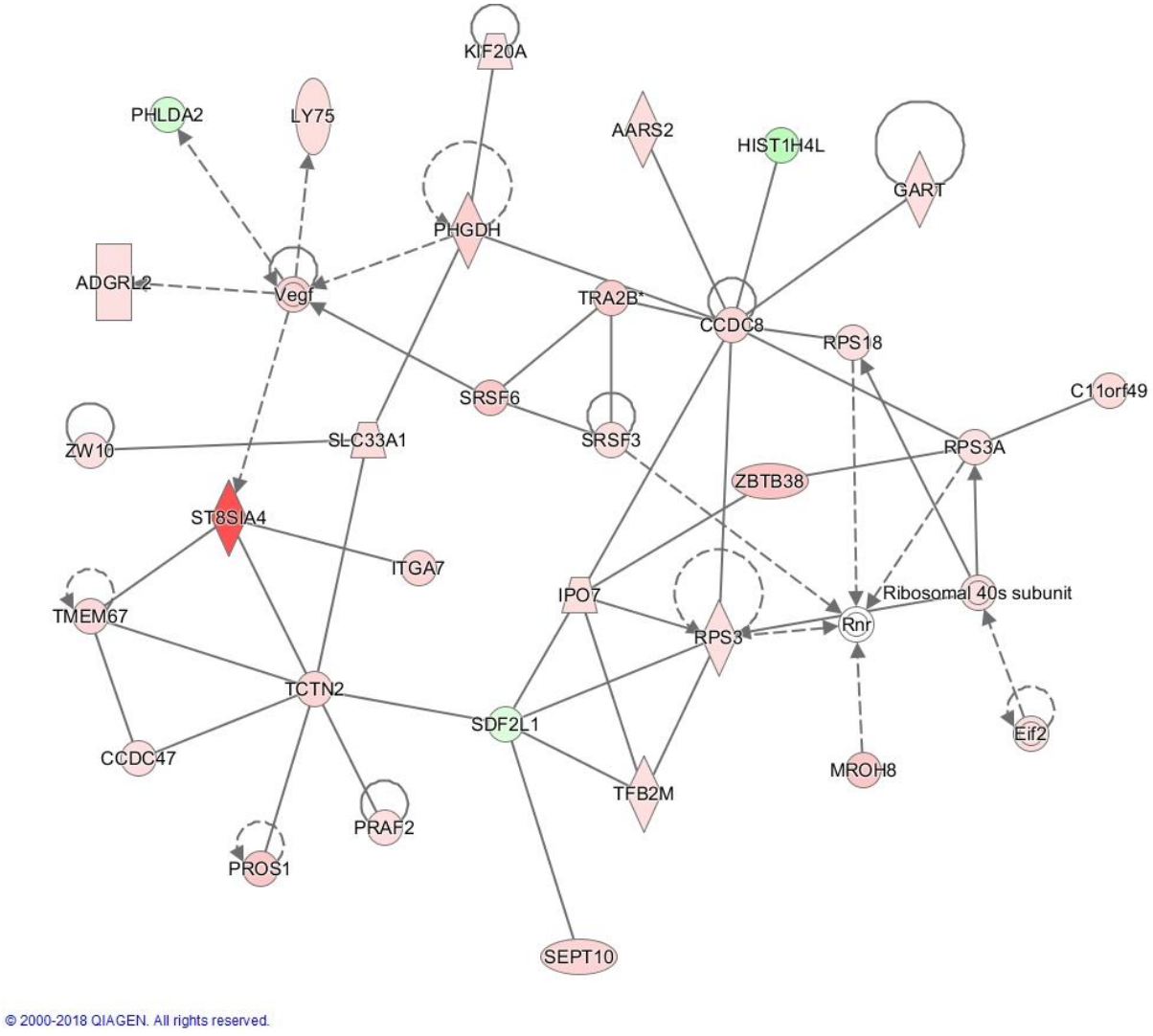

Figure 5-17. Gene network of specific differentially regulated genes in oocytes from bacterial infused heifers at day 4. Gene network in amino acid metabolism, small molecule biochemistry, developmental disorder. Genes shown in red (up) or green (down) and differentially expressed in bacteria infused heifers.

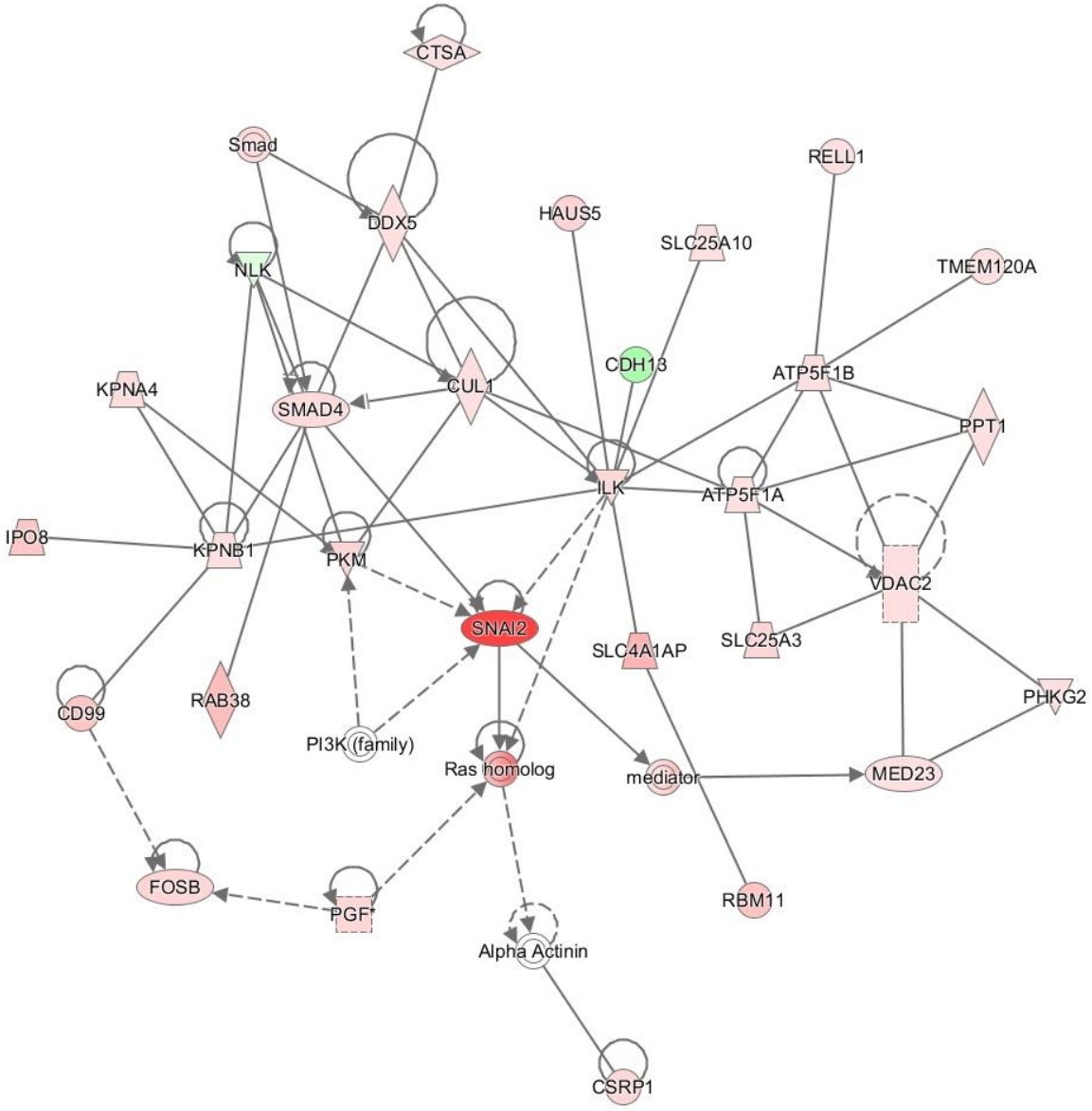

Figure 5-18. Gene network of specific differentially regulated genes in oocytes from bacterial infused heifers at day 4. Gene network in embryonic development, cancer, organismal injury and abnormalities. Genes shown in red (up) or green (down) and differentially expressed in bacteria infused heifers.

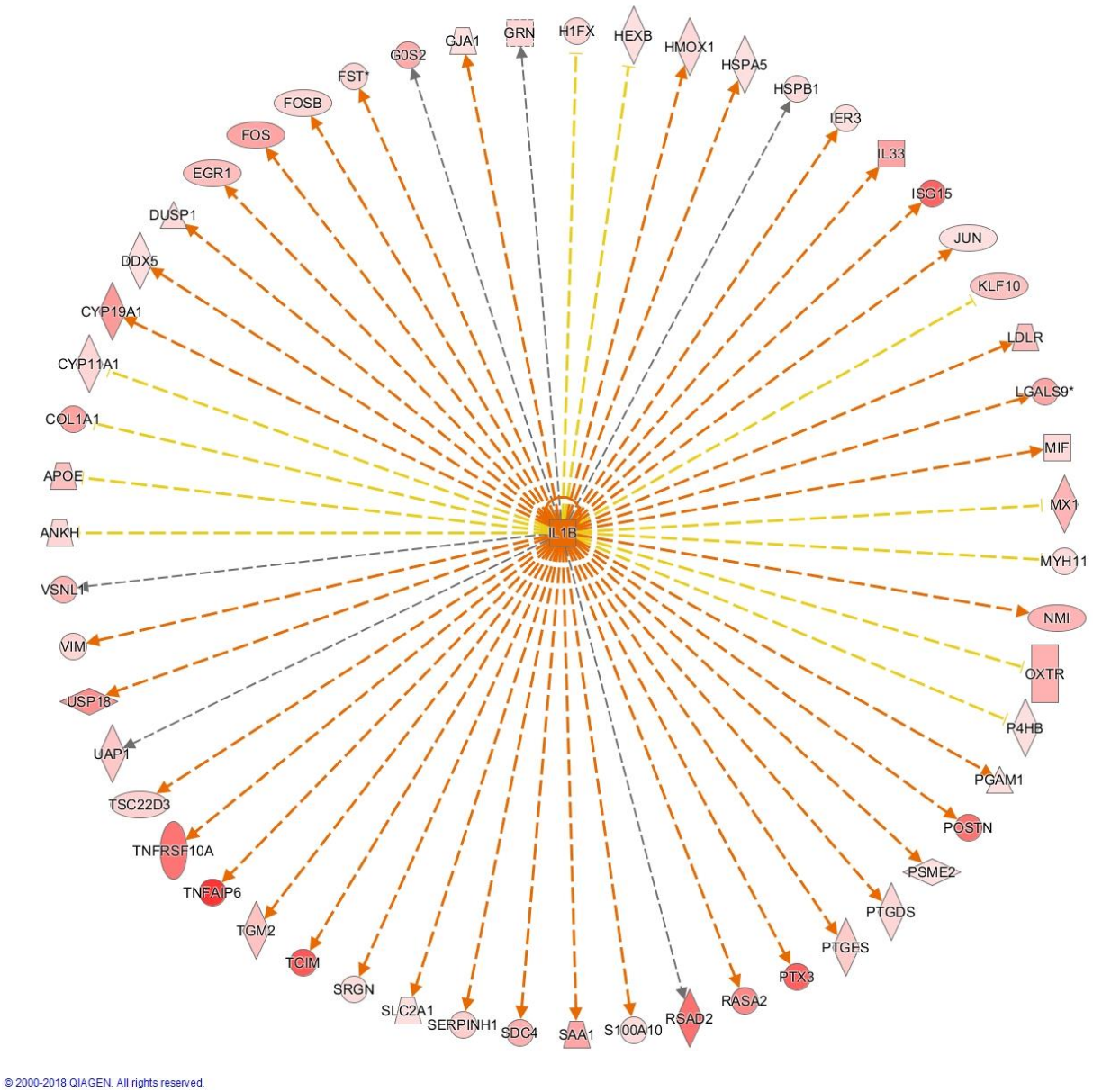

Figure 5-19. IL-1β as a predicted upstream regulator of differentially expressed genes in oocytes of bacterial infused heifers at day 4. Genes shown in red (up) or green (down) and differentially expressed in bacteria infused heifers.

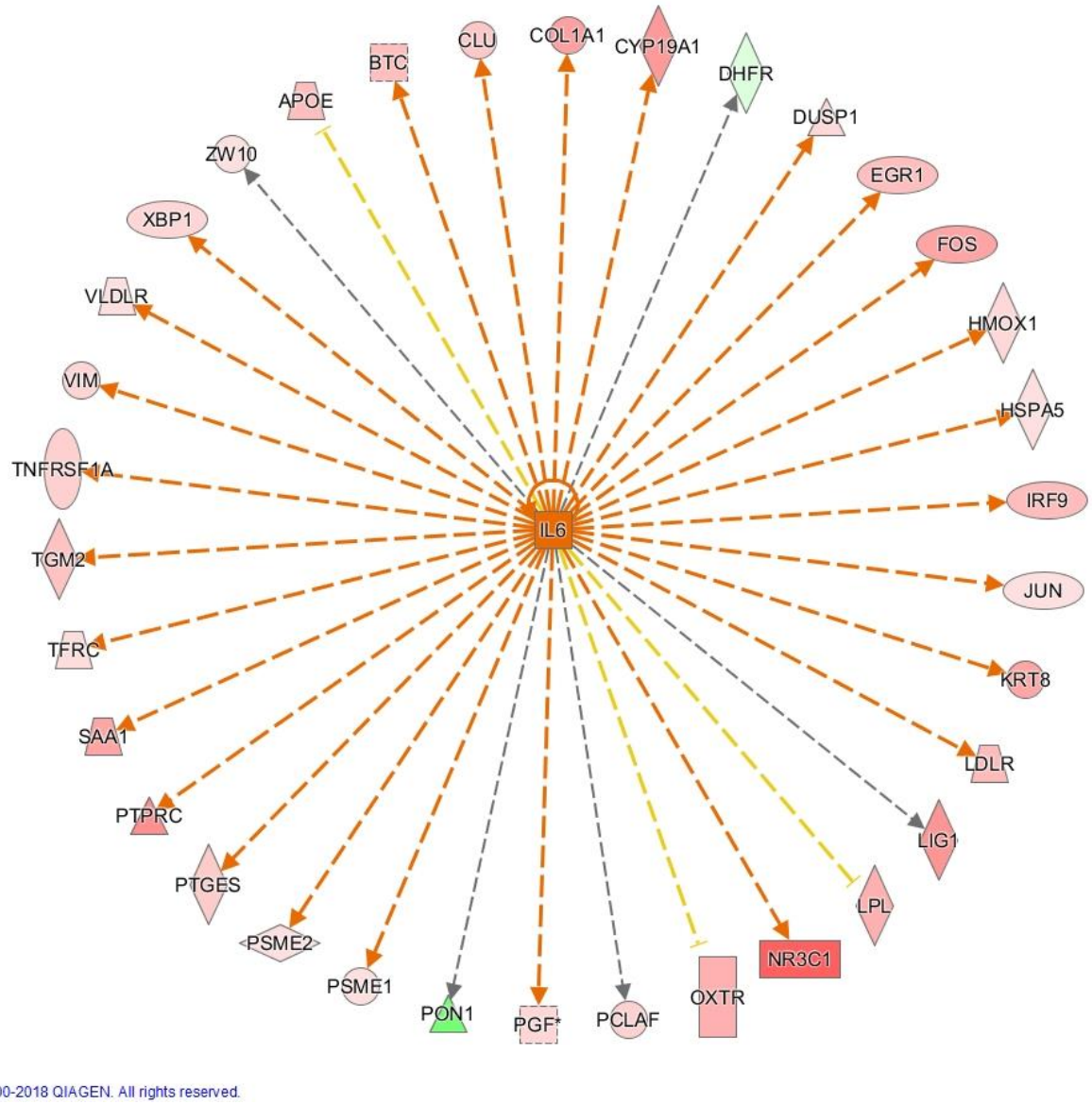

Figure 5-20. IL-6 as a predicted upstream regulators of differentially expressed genes in oocytes of bacterial infused heifers at day 4. Genes shown in red (up) or green (down) and differentially expressed in bacteria infused heifers.

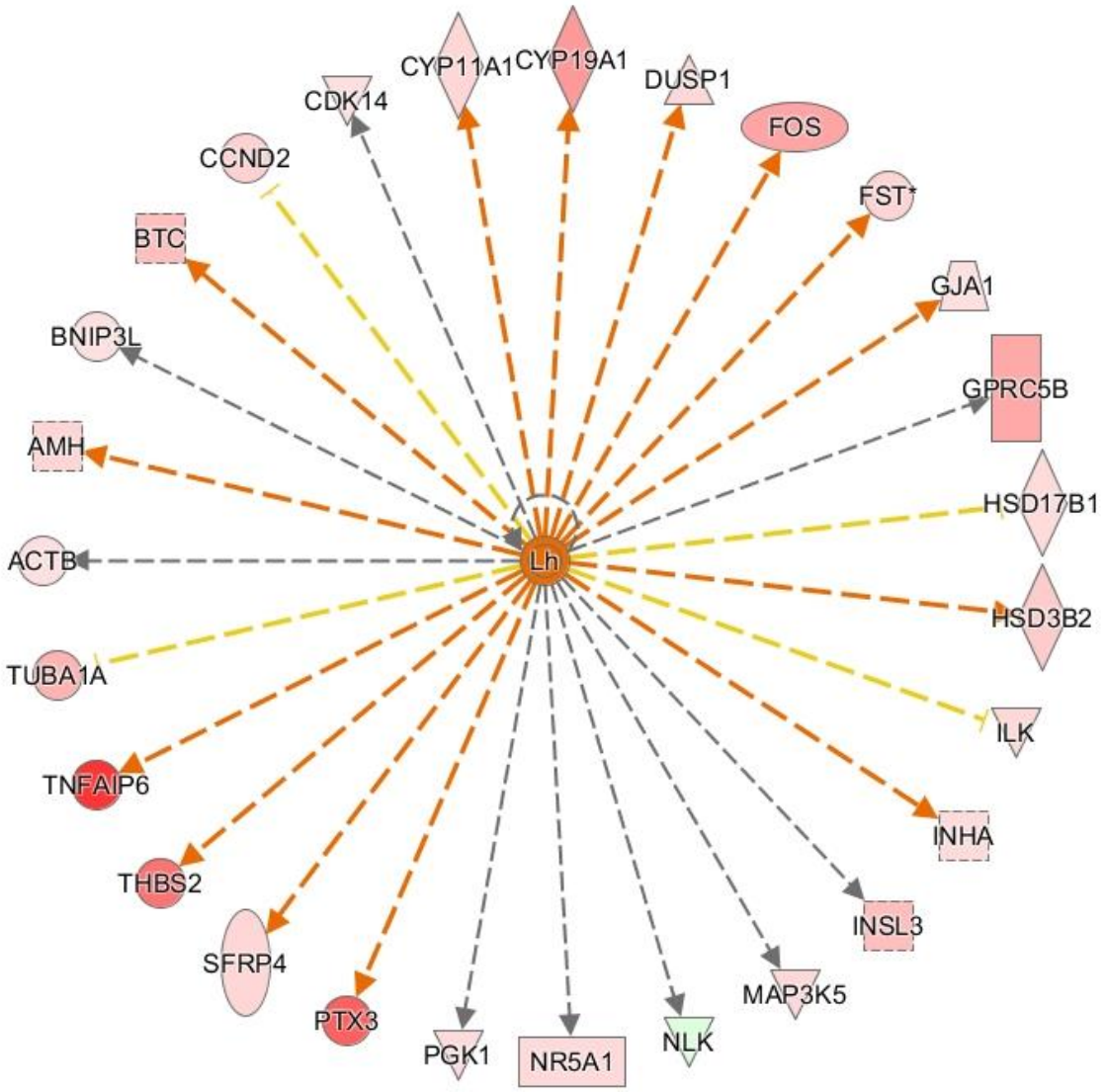

Figure 5-21. LH as a predicted upstream regulator of differentially expressed genes of oocytes in bacterial infused heifers at day 4. Genes shown in red (up) or green (down) and differentially expressed in bacteria infused heifers.

CHAPTER 6
CONCLUSIONS

The data presented here suggest that there are long term effects of uterine disease on the ovary of dairy cows. These effects may be part of the reason why dairy cows are subfertile after an episode of uterine disease. Granulosa cell transcriptome of cows with resolved metritis was altered 40 days after disease occurrence, compared to cows with no metritis. These alterations were characterized by changes to gene pathways associated with the immune response to pathogens and cell communication. Granulosa cells and the oocyte are mutually dependent on each other for appropriate development, growth and function; altering the granulosa cell profile, and subsequent follicular environment may pose a risk for the oocyte. *In vitro* we are able to access the possible mechanisms by which oocyte quality might be compromised by uterine infection and LPS accumulation in the follicle. In our system TNFα only altered expression of a few genes in oocytes and cumulus cells, while LPS altered the expression of various genes associated with epigenetic regulation of the oocyte. Potentially, altering the epigenetic machinery of the oocyte may compromise the quality of the oocyte to develop into a healthy embryo.

Finally, we successfully created an experimental, whole animal model to induce clinical endometritis in heifers. Using this model, we accessed the transcriptome of oocytes during active disease and after disease resolution. Independently of the time point, oocytes from heifers that received bacterial infusion were significantly different from control heifers. When evaluating the oocytes collected during acute disease and after resolution of disease we observed an interesting pattern of gene expression, where the oocytes aspirated during acute disease appeared to have a protective mechanism, decreasing expression of genes associated to the immune response and cellular development. Interestingly, oocytes aspirated after disease resolution had a pattern of

gene expression that resembled the pattern observed in granulosa cells of cows with resolved, spontaneous metritis.

In conclusion, this new information is compelling and needs further investigation, but suggests that uterine disease impacts the granulosa cells and oocytes present at the time of breeding after clearance of disease. Perturbations to the microenvironment of the follicle, by persistent changes to the granulosa may reduce the developmental competence of oocytes and result in long term subfertility of cows after the resolution of uterine disease.

APPENDIX A
PRIMER SEQUENCES

Table A-1. Fluidigm primer sequences

Gene symbol	RefSeq ID	Forward	Reverse
ACKR4	NM_174265.2	TACGGATCCTGGAGAAGACAAA	TACTGGTTGGCTCTGTAGCA
ACTA2	NM_001034502.1	AAGGCCAACCGGGAGAAA	ACCGCCTGAATAGCCACATA
ACTB	NM_173979.3	TGGCACCCAGCACAATGAA	GCCAATCCACACGGAGTACTT
ACVR1B	XM_002687257.5	CATGAGAACATCCTCGGGTTCA	TGCTCGTGATAGTCCGACAC
ACVR2B	NM_174495.2	GCTCATCACGGCCTTCCA	ACGTGACACAGTTCGTTCCA
ADAM10	NM_174496.2	GGAAGTACCAGATGACTGGTGTA	CCTCAGGAGTTCTGGACCATTA
ADAM17	XM_002691486.5	AAAGGGAGTACCCCGTCAAA	GTGCCAGAACCCTAGAGTCA
AJAP1	NM_001206815.1	CGGGGAGTACAAGTCCACATTTA	AGACACAAAGGCCACAGGAA
APAF1	NM_001191507.1	TGGTCTGCTGATGGTGCTAA	AACAGGCCACTGGAGTGAA
APOPT1	NM_001076459.2	ACCAACAGTTCTGGGCAGAC	GGCTTTGAGTCTTGAGCGAAC
AREG	NM_001099092.1	TGCCATGACCTTCACAGCTA	TCAGCGACACCTTCATATCCC
ATM	XM_005215785.3	TGCTTGCTGTTGTGGACTAC	CCAGCCAGAAAGCATCATCA
AY192564	AY192564.1	GCATTGCCAACCTGTTCTCC	CCCACCCATCGAAGTCTATGTAC
BAD	NM_001035459.1	GGGTCAGGGGCCTCATTA	TTCCTGCTCACTCTGCTCAA
BAK1	NM_001077918.1	GCAGACAACGCCTATGAGTAC	CAGTTGATACCGCTCTCAAACA
BMP15	NM_001031752.1	GGGCAAAAGCTCTGGAATCA	ACCAGAACTCACGAACCTCA
C1QA	NM_001014945.2	CCAGTGCATTGAAGACTGGA	CACGCTGATCACCAACCA
CACNA1G	NM_001193140.1	TACCTGGGAGACACTTGGAAC	TTCTGCAGGTCCAGCGAATA
CASP7	XM_002698509.3	ACCGGTCCTCTTTTGTCTCA	GGGGATGTTGACTGATTTCCC
CCNB1	NM_001045872.1	GGGCTCACAAAGCACATGAC	GCTGTGCTAGAGTGCTGATCTTA
CCND2	NM_001076372.1	CTCCTGGCAAAGATCACCAAC	TATTCAGCAGCACCACCTCA
CDC42EP4	NM_001046471.1	CACCTCCTTCCTCAACAGCAA	TTAGAGGACGAGGAGGAGGAC
CDK1	NM_174016.2	GCTGAATTAGCAACGAAGAAACC	CACTTCTGGCCACACTTCATTA
CREM	NM_001034710.3	CGGGAGCTGAGGCTAATGAA	CGACTCTCCAGACACTTGACATA
CXCL12	NM_001113174.1	ACTCCAAACTGCTCCCTTCA	CAATTTCGGGTCAATGCACAC
CXCL2	NM_174299.3	CCGCTCCCATGGTTAAGAAAA	ACTTCTGGAACAGCCATCCA

Table A-1. Continued

Gene symbol	RefSeq ID	Forward	Reverse
CYP11A1	NM_176644.2	TGGAGATGACCCTCTTCCTCA	GGTGTCCACGTCACCGATA
DDX4	NM_001007819.1	ACGGAACAGAGGGTTTTCCA	CACCTCTTCTGGACGATCCTAAA
DGAT2	NM_205793.2	TGGCTGGTGTTTGACTGGAA	TCGAAAGTAGCGCCACACA
DNMT1	NM_182651.2	AGAGACGTCGAGTTACATCCA	GTGTTCCTGGTCTTACTCTTCC
DNMT3A	NM_001206502.1	CCATGTACCGCAAGGCTATCTA	GCTGTCATGGCACATTGGAA
DTX3	NM_001105393.1	AACAGAGGGAATTCTGCTGTCA	TGTCCCCACTCCCTACTTGTA
ESRP1	XM_005215674.3	AAGTCGTGGATCTGGCCAAC	AGCTCCAAGTGATCCGGTCTA
ESRRB	XM_010809669.1	GAGGAGTTCGTGACGCTCAA	TTCTGGACTGCCTCCAAATCC
FGF10	NM_001206326.1	AGCCATGAACAAGAAGGGGAA	CGTTTTCCTCTATCCTCTCCTTCA
FGF4	NM_001040605.2	GTGGCCAGCCGGTTCTT	TGCACTCGTCGGTGAAGAAA
FGFR2	NM_001205310.1	AGCTGCCAGAAGATCCCAAA	GCCCAAAGCAACCTTCTCC
GAPDH	NM_001034034.2	AACGGGAAGCTCGTCATCAA	ACATACTCAGCACCAGCATCA
GATA6	XM_001253596.3	AGCAAGATGAACGGCCTCA	TGGCGCAGGACAATCCAA
GDF9	NM_174681.2	AACACTGTTCGGCTCTTCAC	ACAGCAGATCCACTGATGGAA
GJA1	NM_174068.2	CACTTGGCTTGCCTACTTCAC	GCCTAAGGCACTCCAGTCA
GREM1	NM_001082450.1	CAGCCGTACCATCATCAACC	AAAGGAGCCCTCCTCTTTCC
H2AFX	NM_001079780.2	GCTACAGCTCGGTGCTTAGAA	TCCCAGGACGAAATGAAGCAA
H2AFZ	NM_174809.2	AGCCATCCTGGAGTACCTCA	GTGACGAGGGGTAATACGCTTTA
HAS2	NM_174079.2	ACAGACAGGCTGAGGACAAC	TCCAAGGAGGAGAGAGACTCC
HDAC1	NM_001037444.2	ATGTCCGAGTACAGCAAGCA	CAGAACTCAAACAGGCCATCAAA
HDAC8	NM_001076231.2	CCGAGTCCAGCAAATCCTCA	TGTCAACTAGACCACATGCTTCA
HPSE	NM_174082.2	CTGGACTACTGCTCTTCCAAGAA	ACCAGCCTTCCTCTGGAAAC
HSD3B1	NM_174343.2	GACCAGAAGTTCGGGAGGAA	TTCAGGCACTGCTCATCCA
IGF1	NM_001077828.1	GAGTTGGTGGATGCTCTCCA	GACTGCTCGAGCCATACCC
IGF2	NM_174087.3	AGGGATGTGTCTGCCTCTAC	TGGACTGCTTCCAGATGTCA
IL6	NM_173923.2	TAAGCGCATGGTCGACAAAA	TCTCCTTGCTGCTTTCACAC
ILF3	NM_001206495.1	AACCAGGGCTGCAGTACAAA	GTCCACCTCAACTGACATGGTA
INHBA	NM_174363.2	GCAGACCTCGGAGATCATCA	GGTCACTGCCTTCTTTGGAAA
ITPR2	NM_174369.2	AGAGCTGTGGATCAGCTCAC	TGGTCTGCCCATATTCCTTCC
MAB21L2	XM_002694319.3	GGGCCTCTTTGTCCATGAATT	TGACATTGAGCAGGGTCTCT

Table A-1. Continued

Gene symbol	RefSeq ID	Forward	Reverse
MADD	NM_001193078.1	AGTGGTGAGCCACAAGTACA	CACGTACGAGAAGAGACACAAC
MAPK13	NM_001014947.1	CGTGTCCCTGACGCACATA	TTCTTGATGGCCACCTTCTCC
MOS	XM_002692654.3	GGGCTTGGAGAGGTGTCTAA	CTTGAGGTCCAAGTGCACAA
NEDD4	XM_003582720.3	CCAGTGGCTCAGAAGACGATA	AGCATCTGGTTGGTCCAAAAC
NF2	XM_002694607.4	TCTGTGCTCCTGGCTTCTTA	CAGAAATCCCCGCTTGTGAA
NLRP5	NM_001007814.2	ACTGACCAAGGTCCAAGCA	ATCACGTGGATCCTGTAGTCC
NOD2	NM_001002889.1	GTGTGTGTTTCCTCGCCAAA	GGAGCTGATGTGGTTGTTAGAC
NOTCH2	XM_002686114.4	AGGAGGAGGCGAACGAGAA	ACACAAGGCTCATAGCCATCC
NT5E	NM_174129.3	TCATGAACGCCCTGGGTTA	TGGATCAATCAGGCCTTCCA
PIK3IP1	NM_001075552.1	CGAACAATCCTCGTCAGCAA	TACAGGTGGCCGTTATCCC
PLD2	NM_001075827.1	CAGGCCATTCTGCACTTCA	GGCTGCTTTGAGACGATGTA
POLR2D	NM_001076458.2	GCGTCACAACTCATCTTTCCC	GCTTTCGATGCTCAAGAAGCA
POU5F1	NM_174580.2	AGAAGCTGGAGCCGAACC	CTGCTTTAGGAGCTTGGCAAA
PPBP	XM_002688351.3	GTGATGCTGGTTCCCTCCA	CACACAAGCAGCGAAGTTCA
PPP2R3A	XM_005201921.2	CAGGCCGATCTATCTCGATAC	CTTGTTACTGCCCCAGAGAA
PRKAR2B	NM_174649.2	TTGAGTCACTGCCATTCCTTA	TTGGTGCCTATCACGTCTAC
PTEN	XM_002698370.4	GCCAACCGATACTTTTCTCCA	GCCTCTGGATTTGATGACTCC
PTGER3	NM_181032.1	CCCTGGGTTTATCTGCTGCTA	ACCCTCCGTGTCTAGTCCATA
PTGER4	NM_174589.2	TTCATCGACTGGACCACCAA	CGAGGATGAGGAAGGAACTGAA
PTPPK	NM_001191537.1	CAGGGAGAGATGCTGTGCATA	GTTCTTAGTCTGAGCCACAGGTA
PTX3	NM_001076259.2	GCAGTGTCGGCGGAGAA	TGTCCCACTCGGAGTTCTCA
RAC1	NM_174163.2	CGTGAGTCCTGCATCATTTGAA	TGATGGGTGTGTTGGGACAA
RIPK3	NM_001101884.2	TCAAGCCCTCCAATGTCCTAC	GACTGTGAGCCTCCCTGAAA
S100A1	NM_001099042.2	GGGCAAAGAGGGAGACAAGTA	CGTTCTCATCCAGCTCCTTCA
SDHA	NM_174178.2	AGAGGGTTGACGAGTACGATTAC	TTCCTCCAGTGCTGCTCAAA
SOX17	NM_001206251.1	CAGAACCCAGATCTGCACAAC	CAGCGTCAGTGCCTTCCA
SOX2	NM_001105463.2	CCCAAGAGAACCCTAAGATGCA	CCGTCTCGGACAAAAGTTTCC
STAT1	NM_001077900.1	ATGCTGGTGCCAGAACTAA	TGGCACAACTGGGTTTCA
STAT3	NM_001012671.2	GGTGTCAGATCACATGGGCTAA	TGATGTTGTCCAGCCAGACC
TGFB1	NM_001166068.1	GCCTGCTGAGGCTCAAGTTAA	AGCGCCAGGAATTGTTGCTA

Table A-1. Continued

Gene symbol	RefSeq ID	Forward	Reverse
TJAP1	NM_001192419.1	TGCTCAAGTGCAACAAGTCC	CAGGTGTTTCCGAACCATATCC
TNF	NM_173966.3	CAAGTAACAAGCCGGTAGCC	GGCATTGGCATACGAGTCC
TNFAIP6	NM_001007813.2	GAGATGAGCTTCCAGAAGACA	GCAGTCACTGAAGCATCAC
TNFSF8	NM_001025207.1	CCTGAAAAGGGCTCCATTCAA	TGCCATCTTTGTTCCAAGACA
UBEA2A	NM_001105325.2	CCAACCTATGATGTGTCTTCCA	ATGCCAAGCAGGCTCTTCA
WEE1	NM_001101205.1	CCGGGGCTTGAGGTATATTCA	GAGGCAGCATTTGGGATTGAA
XIAP	NM_001205592.1	TCCTTGTGGACATCTGGTCAC	AGCACATGGGACACTTGTCA
YWHAZ	NM_174814.2	AACAGCAGATGGCTCGAGAA	GAAGCGTTGGGGATCAAGAAC
ZAR1	NM_001076203.1	AAGTGCCTATGTGTGGTGTGTA	CTTCTGGCATGTTCGGCAAA

Table A-2. Embryo quality primer sequences

Gene symbol	RefSeq ID	Forward	Reverse
SDHA	NM_174178.2	GGAACACTGACCTGGTGGAG	CGTCAACCCTCTCCTTGAAGT
RPL19	NM_001040516.2	ATGCCAACTCCCGCCAGCAGAT	TGTTTTTCCGGCATCGAGCCCG
HSPA1A	NM_203322.3	GACAAGTGCCAGGAGGTGATTT	CAGTCTGCTGATGATGGGGTTA
BAX	NM_173894.1	CAGGGTGGTTGGGACGG	CTTCCAGATGGTGAGCGAGG
BCL2	NM_001166486.1	GAGTTCGGAGGGGTCATGTG	ACAAAGGCGTCCCAGCC
SCL2A1	NM_174602.2	AGCGTCATCTTCATCCCAGC	AGCTTCTTCAGCACGCTCTT

APPENDIX B
MEDIUM RECIPES

Table B-1. Medium recipes

Medium	Ingredient	Concentration
IVM medium	M199 with Earle's Salts	
	L-glutamine	0.4 mM
	Sodium pyruvate	0.25 mM
	Glucose	5.5 mM
	Penicilin/Strepmicin	1 %
	Fetal calf serum	10 %
	FSH (20mg/ml Folltropin-V)	20 μg/mL
	Estradiol 17β	2 μg/mL
	ITS	1 %
HEPES-TALP	HEPES	10.0 mM
	$CaCL_2.2H_2O$	2.0 mM
	$MgCl_2.6H_2O$	0.5 mM
	$NaH_2PO_4.\ H_2O$	0.4 mM
	KCl	3.2 mM
	NaCl	114.0 mM
	$NaHCO_3$	2.0 mM
	Na-lactate	10.0 mM
	BSA, fraction V	45.4 mM
	Sodium pyruvate	20 mM
	Gentamicin	7.5ug/mL
IVF-TALP	$CaCL_2.2H_2O$	2.0 mM
	$MgCl_2.6H_2O$	0.5 mM
	$NaH_2PO_4.\ H_2O$	0.4 mM
	KCl	3.2 mM
	NaCl	114.0 mM
	$NaHCO_3$	25.0 mM
	Na-lactate	10.0 mM
	Essentially fatty acid free BSA	90.0 mM
	Sodium pyruvate	0.2 mM
	Gentamicin	0.5 μg
	Heparin	1 mg/mL
PHE	Hypotaurine	0.25 mM
	Penicillamine	0.05 mM
	Epinephrine	25 μM

Table B-1 .Continued

Medium	Ingredient	Concentration
SOF-BE2	NaCl	92 mM
	KCl	6.02 mM
	KH_2PO_4	1 mM
	$CaCL_2.2H_2O$	0.98 mM
	Sodium lactate	4.5 mM
	$NaHCO_3$	21.06 mM
	$MgCl_2.6H_2O$	0.41 mM
	Alanyl-glutamine	0.93 mM
	Sodium pyruvate	0.37 mM
	Trisodium citrate	0.4 mM
	Myo-inositol	2.56 mM
	Gentamicin sulfate	23.3 mM
	Essentially fatty acid free BSA	60.6 mM
	Non-essential amino acids (100X)	9.3 uL/mL
	Essential amino acids (50X)	18.6 uL/mL
OPU collection medium	M199 with Earle's Salts	
	BSA	0.5 %
	HEPES	20 mM
	Sodium pyruvate	2 mM
	Heparin	10 IU/mL
	Pen/Strep	1 %

LIST OF REFERENCES

Akdis, M., A. Aab, C. Altunbulakli, K. Azkur, R.A. Costa, R. Crameri, S. Duan, T. Eiwegger, A. Eljaszewicz, R. Ferstl, R. Frei, M. Garbani, A. Globinska, L. Hess, C. Huitema, T. Kubo, Z. Komlosi, P. Konieczna, N. Kovacs, U.C. Kucuksezer, N. Meyer, H. Morita, J. Olzhausen, L. O'Mahony, M. Pezer, M. Prati, A. Rebane, C. Rhyner, A. Rinaldi, M. Sokolowska, B. Stanic, K. Sugita, A. Treis, W. van de Veen, K. Wanke, M. Wawrzyniak, P. Wawrzyniak, O.F. Wirz, J.S. Zakzuk, and C.A. Akdis. 2016. Interleukins (from IL-1 to IL-38), interferons, transforming growth factor β, and TNF-α: Receptors, functions, and roles in diseases. J. Allergy Clin. Immunol. 138:984–1010.

Akira, S., S. Uematsu, and O. Takeuchi. 2006. Pathogen Recognition and Innate Immunity. Cell 124:783–801.

Albertini, D.F., C.M.H. Combelles, E. Benecchi, and M.J. Carabatsos. 2001. Cellular basis for paracrine regulation of ovarian follicle development. Reproduction 121:647–653.

Álvarez, B., C. Revilla, S. Chamorro, M. López-Fraga, F. Alonso, J. Domínguez, and A. Ezquerra. 2006. Molecular cloning, characterization and tissue expression of porcine Toll-like receptor 4. Dev. Comp. Immunol. 30:345–355.

Amos, M.R., G.D. Healey, R.J. Goldstone, S.M. Mahan, A. Düvel, H.-J. Schuberth, O. Sandra, P. Zieger, I. Dieuzy-Labaye, D.G.E. Smith, and I.M. Sheldon. 2014. Differential endometrial cell sensitivity to a cholesterol-dependent cytolysin links Trueperella pyogenes to uterine disease in cattle. Biol. Reprod. 90:1–13.

Asaf, S., G. Leitner, O. Furman, Y. Lavon, D. Kalo, D. Wolfenson, and Z. Roth. 2014. Effects of Escherichia coli-and Staphylococcus aureus-induced mastitis in lactating cows on oocyte developmental competence. Reproduction 147:33–43.

Asselin, E., P. Drolet, and M.A. Fortier. 1997. Cellular mechanisms involved during oxytocin-induced prostaglandin F2α production in endometrial epithelial cells in vitro : role of cyclooxygenase-2. Endocrinology 138:4798–4805.

Battaglia, D.F., A.B. Beaver, T.G. Harris, E. Tanhehco, C. Viguie, and F.J. Karsch. 1999. Endotoxin disrupts the estradiol-induced luteinizing hormone surge: Interference with estradiol signal reading, not surge release. Endocrinology 140:2471–2479.

Baumann, H., and J. Gauldie. 1994. The acute phase response.. Immunol. Today 15:74–80.

Beaujean, N. 2015. Epigenetics, embryo quality and developmental potential. Reprod. Fertil. Dev. 27:53–62.

Bennett, K.W., and A. Eley. 1993. Fusobacteria: new taxonomy and related diseases. J. Med. Microbiol 39:246–254.

Bicalho, M.L.S., F.S. Lima, V.S. Machado, E.B.M. Jr, E.K. Ganda, C. Foditsch, R.C. Bicalho, and R.O. Gilbert. 2016. Associations among Trueperella pyogenes , endometritis diagnosis ,

and pregnancy outcomes in dairy cows. Theriogenology 85:267–274.

Bicalho, M.L.S., V.S. Machado, G. Oikonomou, R.O. Gilbert, and R.C. Bicalho. 2012. Association between virulence factors of Escherichia coli, Fusobacterium necrophorum, and Arcanobacterium pyogenes and uterine diseases of dairy cows. Vet. Microbiol. 157:125–131.

Boby, J., H. Kumar, H.P. Gupta, M.H. Jan, S.K. Singh, M.K. Patra, S. Nandi, A. Abraham, and N. Krishnaswamy. 2017. Endometritis increases pro-inflammatory cytokines in follicular fluid and cervico-vaginal mucus in the buffalo Cow. Anim. Biotechnol. 28:163–167.

Bonnett, B.N., S.W. Martin, V.P. Gannon, R.B. Miller, and W.G. Etherington. 1991. Endometrial biopsy in Holstein-Friesian dairy cows. III. Bacteriological analysis and correlations with histological findings.. Can. J. Vet. Res. 55:168–173.

Bonnett, B.N., S. Wayne Martin, and A.H. Meek. 1993. Associations of clinical findings, bacteriological and histological results of endometrial biopsy with reproductive performance of postpartum dairy cows. Prev. Vet. Med. 15:205–220.

Bray, S.J. 2006. Notch signalling: A simple pathway becomes complex. Nat. Rev. Mol. Cell Biol. 7:678–689.

Bromfield, J., J. Santos, J. Block, R. Williams, and I. Sheldon. 2015. Mechanisms linking infection and innate immunity in the female genital tract with infertility in dairy cattle. J. Anim. Sci 93:2021–2033.

Bromfield, J.J., and I.M. Sheldon. 2011. Lipopolysaccharide initiates inflammation in bovine granulosa cells via the TLR4 pathway and perturbs oocyte meiotic progression in vitro. Endocrinology 152:5029–5040.

Bromfield, J.J., and I.M. Sheldon. 2013. Lipopolysaccharide reduces the primordial follicle pool in the bovine ovarian cortex ex vivo and in the murine ovary in vivo. Biol. Reprod. 88:1–9.

Cao, X.R., N.L. Lill, N. Boase, P.P. Shi, D.R. Croucher, H. Shan, J. Qu, E.M. Sweezer, T. Place, P.A. Kirby, J. Roger, S. Kumar, and B. Yang. 2010. Nedd4 controls animal growth by regulating IGF-1 signaling. Sci Signal. 1:1–20.

Cheong, S.H., O.G.S. Filho, V.A. Absalon-Medina, A. Schneider, W.R. Butler, and R.O. Gilbert. 2017. Uterine and systemic inflammation influences ovarian follicular function in postpartum dairy cows. PLoS One 12:1–16.

Chong, S., and E. Whitelaw. 2004. Epigenetic germline inheritance. Curr. Opin. Genet. Dev. 14:692–696.

Cloutier, J.M., S.K. Mahadevaiah, E. ElInati, A. Nussenzweig, A. Tóth, and J.M.A. Turner. 2015. Histone H2AFX links meiotic chromosome asynapsis to prophase I oocyte loss in mammals. PLoS Genet. 11:1–18.

Consortium, T. bovine genome sequencing and analysis, G. Elsik, L. Ross, and K. Worley. 2009. The genome sequence of taurine cattle: a window to ruminant biology and evolution. Science (80-.). 324:522–528.

Corcoran, D., T. Fair, and P. Lonergan. 2005. Predicting embryo quality: mRNA expression and the preimplantation embryo. Reprod. Biomed. Online 11:340–348.

Coticchio, G., M. Dal Canto, M.M. Renzini, M.C. Guglielmo, F. Brambillasca, D. Turchi, P.V. Novara, and R. Fadini. 2014. Oocyte maturation: Gamete-somatic cells interactions, meiotic resumption, cytoskeletal dynamics and cytoplasmic reorganization. Hum. Reprod. Update 21:427–454.

Cronin, J.G., M.L. Turner, L. Goetze, C.E. Bryant, and I.M. Sheldon. 2012. Toll-Like receptor 4 and MYD88-dependent signaling mechanisms of the innate immune system are essential for the response to lipopolysaccharide by epithelial and stromal cells of the bovine endometrium. Biol. Reprod. 86:1–9.

Deori, S., H. Kumar, M.C. Yadav, M. Rawat, and S.K. Srivastava. 2004. Intrauterine administration of bacterial modulins: An alternative therapy for endometritis. J. Appl. Anim. Res. 26:117–121.

Dominguez, M.H., P.K. Chattopadhyay, S. Ma, L. Lamoreaux, A. McDavid, G. Finak, R. Gottardo, R.A. Koup, and M. Roederer. 2013. Highly multiplexed quantitation of gene expression on single cells. J. Immunol. Methods 391:133–145.

Dong, J., Albertini, David F., K. Nishimori, T.R. Kumar, Naifang Lu, and M.M. Matzuk. 1996. Growth differentiation factor -9 is required during early ovarian folliculogenesis. Nature.

Drillich, M., O. Beetz, A. Pfützner, M. Sabin, H.-J. Sabin, P. Kutzer, H. Nattermann, and W. Heuwieser. 2001. Evaluation of a systemic antibiotic treatment of toxic puerperal metritis in dairy cows. J. Dairy Sci. 84:2010–2017.

Dubuc, J., T.F. Duffield, K.E. Leslie, J.S. Walton, and S.J. LeBlanc. 2010. Definitions and diagnosis of postpartum endometritis in dairy cows. J. Dairy Sci. 93:5225–5233.

Dubuc, J., T.F. Duffield, K.E. Leslie, J.S. Walton, and S.J. LeBlanc. 2011. Effects of postpartum uterine diseases on milk production and culling in dairy cows. J. Dairy Sci. 94:1339–1346. doi:10.3168/jds.2010-3758.

Duckett, C.S., F. Li, Y. Wang, K.J. Tomaselli, C.B. Thompson, and R.C. Armstrong. 1998. Human IAP-like protein regulates programmed cell death downstream of Bcl-xL and cytochrome c.. Mol. Cell. Biol. 18:608–615.

Espey, L.L. 1980. Ovulation as an Inflammatory Reaction - A Hypothesis. Biol. Reprod. 73–106.

Eswarakumar, V.P., I. Lax, and J. Schlessinger. 2005. Cellular signaling by fibroblast growth factor receptors. Cytokine Growth Factor Rev. 16:139–149.

Faast, R., V. Thonglairoam, T.C. Schulz, J. Beall, J.R.E. Wells, H. Taylor, K. Matthaei, P.D. Rathjen, D.J. Tremethick, and I. Lyons. 2001. Histone variant H2A.Z is required for early mammalian development. Curr. Biol. 11:1183–1187.

Fache, J., and A. Hamdouch. 2014. The roles of cyclin A2, B1 and B2 in early and late mitotic events. Mol Bio Cell 62:1–24.

Field, S.L., T. Dasgupta, M. Cummings, and N.M. Orsi. 2014. Cytokines in ovarian folliculogenesis, oocyte maturation and luteinisation. Mol. Reprod. Dev. 81:284–314.

Fourichon, C., H. Seegers, and X. Malher. 2000. Effect of disease on reproduction in the dairy cow: A meta-analysis. Theriogenology 53:1729–1759.

French, A.T., P.A. Knight, W.D. Smith, J.K. Brown, N.M. Craig, J.A. Pate, H.R.P. Miller, and A.D. Pemberton. 2008. Up-regulation of intelectin in sheep after infection with Teladorsagia circumcincta. Int. J. Parasitol. 38:467–475.

Galvão, K.N., L.F. Greco, J.M. Vilela, M.F. Sá Filho, and J.E.P. Santos. 2009. Effect of intrauterine infusion of ceftiofur on uterine health and fertility in dairy cows. J. Dairy Sci. 92:1532–1542.

Gilbert, R.O. 2016. Managment of reproductive disease in dairy cows. Vet. Clin. NA Food Anim. Pract. 32:387–410.

Gilbert, R.O., S.T. Shin, C.L. Guard, H.N. Erb, and M. Frajblat. 2005. Prevalence of endometritis and its effects on reproductive performance of dairy cows. Theriogenology 64:1879–1888.

Gilchrist, R.B., M. Lane, and J.G. Thompson. 2008. Oocyte-secreted factors: Regulators of cumulus cell function and oocyte quality. Hum. Reprod. Update 14:159–177.

Giuliodori, M.J., R.P. Magnasco, D. Becu-Villalobos, I.M. Lacau-Mengido, C.A. Risco, and R.L. de la Sota. 2013. Metritis in dairy cows: Risk factors and reproductive performance. J. Dairy Sci. 96:3621–3631.

Goissis, M.D., and J.B. Cibelli. 2014. Functional characterization of SOX2 in bovine preimplantation embryos. Biol. Reprod. 90:1–10.

Goldstone, R.J., M. Amos, R. Talbot, H.-J. Schuberth, O. Sandra, I.M. Sheldon, and D.G.E. Smith. 2014a. Draft genome sequence of Trueperella pyogenes, isolated from the infected uterus of a postpartum cow with metritis. Genome Announc. 2:e00194-14.

Goldstone, R.J., R. Popat, H.-J. Schuberth, O. Sandra, I.M. Sheldon, and D.G.E. Smith. 2014b. Genomic characterisation of an endometrial pathogenic Escherichia coli strain reveals the acquisition of genetic elements associated with extra-intestinal pathogenicity.. BMC Genomics 15:1075.

Hackett, J.A., R. Sengupta, J.J. Zylicz, K. Murakami, C. Lee, T.A. Down, and M.A. Surani.

2013. Germline DNA demethylation dynamics and imprint erasure through 5-hydroxymethylcytosine 9:882–886.

Haimerl, P., and W. Heuwieser. 2014. Invited review: Antibiotic treatment of metritis in dairy cows: A systematic approach.. J. Dairy Sci. 97:6649–6661.

Hansen, P.J. 1998. Regulation of uterine immune function by progesterone - Lessons from the sheep. J. Reprod. Immunol. 40:63–79.

Heinrich, P.C., J. V Castell, and T. Andus. 1990. Interleukin-6 and the acute phase response. Biochem. J. 265:621–636.

Herath, S., D.P. Fischer, D. Werling, E.J. Williams, S.T. Lilly, H. Dobson, C.E. Bryant, and I.M. Sheldon. 2006. Expression and function of toll-like receptor 4 in the endometrial cells of the uterus. Endocrinology 147:562–570.

Herath, S., S.T. Lilly, N.R. Santos, R.O. Gilbert, L. Goetze, C.E. Bryant, J.O. White, J. Cronin, and I.M. Sheldon. 2009. Expression of genes associated with immunity in the endometrium of cattle with disparate postpartum uterine disease and fertility.. Reprod. Biol. Endocrinol. 7:55.

Herath, S., E.J. Williams, S.T. Lilly, R.O. Gilbert, H. Dobson, C.E. Bryant, and I.M. Sheldon. 2007. Ovarian follicular cells have innate immune capabilities that modulate their endocrine function. Reproduction 134:683–693.

Herman, A.P., T. Misztal, K. Romanowicz, and D. Tomaszewska-Zaremba. 2012. Central injection of exogenous IL-1β in the control activities of hypothalamic-pituitary-gonadal axis in anestrous ewes. Reprod. Domest. Anim. 47:44–52.

Ibrahim, L.A., J.M. Kramer, R.S. Williams, and J.J. Bromfield. 2016. Human granulosa-lutheal cells initiate an innate immune response to pathogen-associated molecules. Reproduction 261–270.

Jeon, S.J., A. Vieira-Neto, M. Gobikrushanth, R. Daetz, R.D. Mingoti, A.C.B. Parize, S.L. de Freitas, A.N.L. da Costa, R.C. Bicalho, S. Lima, K.C. Jeong, and K.N. Galvão. 2015. Uterine microbiota progression from calving until establishment of metritis in dairy cows. Appl. Environ. Microbiol. 81:6324–6332.

Jost, B.H., and S.J. Billington. 2005. Arcanobacterium pyogenes: Molecular pathogenesis of an animal opportunist. Antonie van Leeuwenhoek, Int. J. Gen. Mol. Microbiol. 88:87–102.

Kassé, F.N., J.M. Fairbrother, and J. Dubuc. 2016. Relationship between Escherichia coli virulence factors and postpartum metritis in dairy cows.. J. Dairy Sci. 99:4656–4667.

Kim, I.-H., and H.-G. Kang. 2003. Risk factors for postpartum endometritis and the effect of endometritis on reproductive performance in dairy cows in Korea.. J. Reprod. Dev. 49:485–491.

Kobayashi, S.D., and F.R. DeLeo. 2009. Role of neutrophils in innate immunity: A systems biology-level approach. Wiley Interdiscip. Rev. Syst. Biol. Med. 1:309–333.

Langmead, B., and S.L. Salzberg. 2013. Fast gapped-read alignment with Bowtie 2. Nat. Methods 9:357–359.

Lavon, Y., G. Leitner, T. Goshen, R. Braw-Tal, S. Jacoby, and D. Wolfenson. 2008. Exposure to endotoxin during estrus alters the timing of ovulation and hormonal concentrations in cows. Theriogenology 70:956–967.

Lavon, Y., G. Leitner, E. Klipper, U. Moallem, R. Meidan, and D. Wolfenson. 2011. Subclinical, chronic intramammary infection lowers steroid concentrations and gene expression in bovine preovulatory follicles. Domest. Anim. Endocrinol. 40:98–109.

Lavon, Y., G. Leitner, H. Voet, and D. Wolfenson. 2010. Naturally occurring mastitis effects on timing of ovulation, steroid and gonadotrophic hormone concentrations, and follicular and luteal growth in cows. J. Dairy Sci. 93:911–921.

LeBlanc, S.J., T.F. Duffield, K.E. Leslie, K.G. Bateman, G.P. Keefe, J.S. Walton, and W.H. Johnson. 2002. Defining and diagnosing postpartum clinical endometritis and its impact on reproductive performance in dairy cows.. J. Dairy Sci. 85:2223–36.

Lewis, G.S. 2004. Steroidal regulation of uterine immune defenses. Anim. Reprod. Sci. 82–83:281–294.

Li, L., P. Zheng, and J. Dean. 2010. Maternal control of early mouse development. Development 137:859–870.

Lima, F.S., R.S. Bisinotto, E.S. Ribeiro, L.F. Greco, H. Ayres, M.G. Favoreto, M.R. Carvalho, K.N. Galvão, and J.E.P. Santos. 2013. Effects of 1 or 2 treatments with prostaglandin F_2 α on subclinical endometritis and fertility in lactating dairy cows inseminated by timed artificial insemination.. J. Dairy Sci. 96:6480–8.

Lima, F.S., A. Vieira-Neto, G.S.F.M. Vasconcellos, R.D. Mingoti, E. Karakaya, E. Solé, R.S. Bisinotto, N. Martinez, C.A. Risco, K.N. Galvão, and J.E.P. Santos. 2014. Efficacy of ampicillin trihydrate or ceftiofur hydrochloride for treatment of metritis and subsequent fertility in dairy cows. J. Dairy Sci. 97:5401–5414.

Liu, X., F. Xie, A.M. Zamah, B. Cao, and M. Conti. 2014. Multiple pathways mediate luteinizing hormone regulation of cGMP signaling in the mouse ovarian follicle. Biol. Reprod. 91:1–11.

Liu, Z., D.G. De Matos, H.Y. Fan, M. Shimada, S. Palmer, and J.S. Richards. 2009. Interleukin-6: An autocrine regulator of the mouse cumulus cell-oocyte complex expansion process. Endocrinology 150:3360–3368.

Liu, Z., M. Shimada, and J.S. Richards. 2008. The involvement of the Toll-like receptor family in ovulation. J. Assist. Reprod. Genet. 223–228.

Machado, V.S., M.L.S. Bicalho, R.V. Pereira, L.S. Caixeta, J.H.J. Bittar, G. Oikonomou, R.O. Gilbert, and R.C. Bicalho. 2012a. The effect of intrauterine administration of mannose or bacteriophage on uterine health and fertility of dairy cows with special focus on Escherichia coli and Arcanobacterium pyogenes. J. Dairy Sci. 95:3100–3109.

Machado, V.S., G. Oikonomou, M.L.S. Bicalho, W.A. Knauer, R. Gilbert, and R.C. Bicalho. 2012b. Investigation of postpartum dairy cows' uterine microbial diversity using metagenomic pyrosequencing of the 16S rRNA gene. Vet. Microbiol. 159:460–469. doi:10.1016/j.vetmic.2012.04.033.

Magata, F., and T. Shimizu. 2017. Effect of lipopolysaccharide on developmental competence of oocytes. Reprod. Toxicol. 71:1–7.

Martin, M. 2011. Cutadapt removes adapter sequences from high-throughput sequencing reads. EMBnet 17:10–12.

Masui, S., Y. Nakatake, Y. Toyooka, D. Shimosato, R. Yagi, K. Takahashi, H. Okochi, A. Okuda, R. Matoba, A.A. Sharov, M.S.H. Ko, and H. Niwa. 2007. Pluripotency governed by Sox2 via regulation of Oct3/4 expression in mouse embryonic stem cells. Nat. Cell Biol. 9:625–635.

Mateus, L., L. Lopes da Costa, P. Diniz, and A.J. Ziecik. 2003. Relationship between endotoxin and prostaglandin (PGE2and PGFM) concentrations and ovarian function in dairy cows with puerperal endometritis. Anim. Reprod. Sci. 76:143–154.

Matzuk, M.M. 2002. Intercellular communication in the mammalian ovary: oocytes carry the conversation. Science. 296:2178–2180.

McGinnis, L.K., S.D. Limback, and D.F. Albertini. 2013. Signaling Modalities during Oogenesis in Mammals. 1st ed. Elsevier Inc.

Moraes, J.G.N., P.R.B. Silva, L.G.D. Mendonça, A.A. Scanavez, J.C.C. Silva, and R.C. Chebel. 2017. Effects of intrauterine infusion of Escherichia coli lipopolysaccharide on uterine health, resolution of purulent vaginal discharge, and reproductive performance of lactating dairy cows. J. Dairy Sci. 100:4772–4783.

Moussa, M., J. Shu, X.H. Zhang, and F. Zeng. 2015. Maternal control of oocyte quality in cattle "a review". Anim. Reprod. Sci. 155:11–27.

Murayama, C., A. Kaji, K. Miyauchi, M. Matsui, A. Miyamoto, and T. Shimizu. 2010. Effect of VEGF (vascular endothelial growth factor) on expression of IL-8 (interleukin-8), IL-1β and their receptors in bovine theca cells. Cell Biol. Int. 34:531–536.

Nagaraja, T.G., S.K. Narayanan, G.C. Stewart, and M.M. Chengappa. 2005. Fusobacterium necrophorum infections in animals: pathogenesis and pathogenic mechanisms. Anaerobe 11:239–246.

Netea, M.G., F.L. van de Veerdonk, J.W.M. van der Meer, C.A. Dinarello, and L.A.B. Joosten. 2015. Inflammasome-independent regulation of IL-1-family cytokines. Annu. Rev. Immunol. 33:49–77.

Nibbs, R.J.B., and G.J. Graham. 2013. Immune regulation by atypical chemokine receptors. Nat. Rev. Immunol. 13:815–829.

Niwa, H., J. Miyazaki, and A.G. Smith. 2000. Quantitative expression of OCT3/4 defines differentiation , dedifferentiation or self-renewal of ES cells.. Nat Genet 24:2–6.

Opsomer, G., Y.T. Gröhn, J. Hertl, M. Coryn, H. Deluyker, and A. De Kruif. 2000. Risk factors for post partum ovarian dysfunction in high producing dairy cows in Belgium: A field study. Theriogenology 53:841–857.

Overton, M., and F. Fetrow. 2008. Economics of postpartum uterine health. Hoard`s Dairy Man 39–44.

Pan, H., and R.M. Schultz. 2011. SOX2 modulates reprogramming of gene expression in two-cell mouse embryos. Biol. Reprod. 85:409–416.

Peter, A.L., W.T.K. Bosu, and C.W. Luker. 1989. Plasma endotoxin and concentration of stable metabolites of prostacyclin, thromboxane A2, and prostaglandin E2 in postpartum dairy cows. 34:763–764.

Potter, T.J., J. Guitian, J. Fishwick, P.J. Gordon, and I.M. Sheldon. 2010. Risk factors for clinical endometritis in postpartum dairy cattle. Theriogenology 74:127–134.

Price, J.C., J.J. Bromfield, and I.M. Sheldon. 2013. Pathogen-associated molecular patterns initiate inflammation and perturb the endocrine function of bovine granulosa cells from ovarian dominant follicles via TLR2 and TLR4 pathways. Endocrinology 154:3377–3386.

Raetz, C. 1990. Biochemistry of endotoxins. Annu. Rev. Biochem. 59:129–170.

Rahman, M.M., M. Mazzilli, G. Pennarossa, T.A.L. Brevini, A. Zecconi, and F. Gandolfi. 2012. Chronic mastitis is associated with altered ovarian follicle development in dairy cattle. J. Dairy Sci. 95:1885–1893.

Regassa, F., I.M. Sheldon, and D.E. Noakes. 2002. Effect of experimentally induced metritis on uterine involution , acute phase protein response. Vet. Rec. 150:605–607.

Ribeiro, E.S., G. Gomes, L.F. Greco, R.L.A. Cerri, A. Vieira-Neto, P.L.J. Monteiro, F.S. Lima, R.S. Bisinotto, W.W. Thatcher, and J.E.P. Santos. 2016. Carryover effect of postpartum inflammatory diseases on developmental biology and fertility in lactating dairy cows. J. Dairy Sci. 99:2201–2220.

Ribeiro, E.S., F.S. Lima, L.F. Greco, R.S. Bisinotto, A.P.A. Monteiro, M. Favoreto, H. Ayres, R.S. Marsola, N. Martinez, W.W. Thatcher, and J.E.P. Santos. 2013. Prevalence of periparturient diseases and effects on fertility of seasonally calving grazing dairy cows supplemented with concentrates. J. Dairy Sci. 96:1–16.

Ricciotti and FitzGerald, G.A. 2011. Prostaglandins and inflammation. Arter. Thromb Vasc Boil 31:986–1000.

Richards, J.S. 2005. Ovulation : New factors that prepare the oocyte for fertilization 234:75–79.

Richards, J.S., Z. Liu, and M. Shimada. 2008. Immune-like mechanisms in ovulation. Trends Endocrinol. Metab. 19:191–196.

Rizos, D., F. Ward, P. Duffy, M.P. Boland, and P. Lonergan. 2002. Consequences of bovine oocyte maturation, fertilization or early embryo development in vitro versus in vivo: Implications for blastocyst yield and blastocyst quality. Mol. Reprod. Dev. 61:234–248.

Romagnani, S. 1999. Th1/Th2 Cells. Inflamm. Bowel Dis. 5:285–294.

Roth, Z., A. Dvir, D. Kalo, Y. Lavon, O. Krifucks, D. Wolfenson, and G. Leitner. 2013. Naturally occurring mastitis disrupts developmental competence of bovine oocytes. J. Dairy Sci. 96:6499–6505.

Rowson, L.E., and G.E. Lamming. 1953. Influence of ovarian hormones on uterine infection. Nature 172:156–157.

Sagirkaya, H., M. Misirlioglu, A. Kaya, N.L. First, J.J. Parrish, and E. Memili. 2006. Developmental and molecular correlates of bovine preimplantation embryos. Reproduction 131:895–904.

Santos, T.M.A., and R.C. Bicalho. 2012. Diversity and succession of bacterial communities in the uterine fluid of postpartum metritic, endometritic and healthy dairy cows. PLoS One 7.

Santos, T.M.A., L.S. Caixeta, V.S. Machado, A.K. Rauf, R.O. Gilbert, and R.C. Bicalho. 2010a. Antimicrobial resistance and presence of virulence factor genes in Arcanobacterium pyogenes isolated from the uterus of postpartum dairy cows. Vet. Microbiol. 145:84–89.

Santos, T.M.A., R.O. Gilbert, L.S. Caixeta, V.S. Machado, L.M. Teixeira, and R.C. Bicalho. 2010b. Susceptibility of Escherichia coli isolated from uteri of postpartum dairy cows to antibiotic and environmental bacteriophages. Part II: In vitro antimicrobial activity evaluation of a bacteriophage cocktail and several antibiotics. J. Dairy Sci. 93:105–114.

Scheller, J., A. Chalaris, D. Schmidt-Arras, and S. Rose-John. 2011. The pro- and anti-inflammatory properties of the cytokine interleukin-6. Biochim. Biophys. Acta - Mol. Cell Res. 1813:878–888.

Schievella, A.R., J.H. Chen, J.R. Graham, and L.L. Lin. 1997. MADD, a novel death domain protein that interacts with the type 1 tumor necrosis factor receptor and activates mitogen-activated protein kinase. J. Biol. Chem. 272:12069–12075.

Seals, R.C., M.C. Wulster-Radcliffe, and G.S. Lewis. 2002. Modulation of the uterine response to infectious bacteria in postpartum ewes. Am. J. Reprod. Immunol. 47:57–63.

Sens, A., and W. Heuwieser. 2013. Presence of Escherichia coli, Trueperella pyogenes, α-hemolytic streptococci, and coagulase-negative staphylococci and prevalence of subclinical endometritis. J. Dairy Sci. 96:6347–6354.

Sheldon, I.M., J. Cronin, L. Goetze, G. Donofrio, H.H.-J. Schuberth, and M. Veterinaria. 2009. Defining Postpartum Uterine Disease and the Mechanisms of Infection and Immunity in the Female Reproductive Tract in Cattle. Biol. Reprod. 1032:1025–1032.

Sheldon, I.M., G.S. Lewis, S. LeBlanc, and R.O. Gilbert. 2006. Defining postpartum uterine disease in cattle. Theriogenology 65:1516–1530.

Sheldon, I.M., D.E. Noakes, A.N. Rycroft, D.U. Pfeiffer, and H. Dobson. 2002. Influence of uterine bacterial contamination after parturition on ovarian dominant follicle selection and follicle growth and function in cattle. Reproduction 123:837–845.

Sheldon, I.M., and M.H. Roberts. 2010. Toll-like receptor 4 mediates the response of epithelial and stromal cells to lipopolysaccharide in the endometrium. PLoS One 5:1–10.

Sheldon, I.M., A.N. Rycroft, B. Dogan, M. Craven, J.J. Bromfield, A. Chandler, M.H. Roberts, S.B. Price, R.O. Gilbert, and K.W. Simpson. 2010. Specific strains of Escherichia coli are pathogenic for the endometrium of cattle and cause pelvic inflammatory disease in cattle and mice. PLoS One 5.

Sheldon, M., D.E. Noakes, A. Rycroft, and H. Dobson. 2001. Acute phase protein responses to uterine bacterial contamination in caftle after calving. Vet. Rec. 148:172–175.

Shimada, M., I. Hernandez-Gonzalez, I. Gonzalez-Robanya, and J.S. Richards. 2006. Induced expression of pattern recognition receptors in cumulus oocyte complexes: novel evidence for innate immune-like functions during ovulation.. Mol. Endocrinol. 20:3228–3239.

Skarzynski, D.J., M.B. Mamadou, K.M. Deptula, I. Woclawek-Potocka, A. Korzekwa, M. Shibaya, W. Pilawski, and and K. Okuda. 2003. Roles of Tumor Necrosis Factor-α in the Regulation of the Estrous Cycle in Cattle : an in vivo Study. Biol. Reprod. 1913:1907–1913.

Soto, P., R.P. Natzke, and P.J. Hansen. 2003a. Identification of possible mediators of embryonic mortality caused by mastitis: Actions of lipopolysaccharide, prostaglandin F2α, and the nitric oxide generator, sodium nitroprusside dihydrate, on oocyte maturation and embryonic development in cattle. Am. J. Reprod. Immunol. 50:263–272.

Soto, P., R.P. Natzke, and P.J. Hansen. 2003b. Actions of tumor necrosis factor-alpha on oocyte maturation and embryonic development in cattle.. Am. J. Reprod. Immunol. 50:380–388.

Spicer, L.J. 1998. Tumor necrosis factor-α (TNF-α) inhibits steroidogenesis of bovine ovarian granulosa and thecal cells in vitro: Involvement of TNF-α receptors. Endocrine 8:109–115.

Spicer, L.J., P.Y. Aad, D. Allen, S. Mazerbourg, and A.J. Hsueh. 2006. Growth differentiation factor-9 has divergent effects on proliferation and steroidogenesis of bovine granulosa cells. J. Endocrinol. 189:329–339.

Spicer, L.J., and E. Alpizar. 1994. Effects of interleukin-6 on proliferation and follicle-stimulating hormone-induced estradiol production by bovine granulosa cells in vitro: dependence on size of follicle.. Biol. Reprod. 50:38–43.

Su, Y.-Q., and J.J. Eppig. 2010. Mouse Oocyte Control of Granulosa Cell Development and Function: Paracrine Regulation of Cumulus Cell Metabolism. Semin Repro Med 27:32–42.

Subedi, K., N. Isobe, M. Nishibori, and Y. Yoshimura. 2007. Changes in the expression of gallinacins, antimicrobial peptides, in ovarian follicles during follicular growth and in response to lipopolysaccharide in laying hens (Gallus domesticus). Reproduction 133:127–133.

Sudiman, J., M.L. Sutton-McDowall, L.J. Ritter, M.A. White, D.G. Mottershead, J.G. Thompson, and R.B. Gilchrist. 2014. Bone morphogenetic protein 15 in the pro-mature complex form enhances bovine oocyte developmental competence. PLoS One 9:1–11.

Sutton, M.L., R.B. Gilchrist, and J.G. Thompson. 2003. Effect of in-vivo and in-vitro environments on the metabolism of the cumulus-oocyte complex and its influence on oocyte developmental capacity. Hum. Reprod. Update 9:35–48.

Suzuki, C., K. Yoshioka, S. Iwamura, and H. Hirose. 2001. Endotoxin induces delayed ovulation following endocrine aberration during the proestrous phase in Holstein heifers. Domest. Anim. Endocrinol. 20:267–278.

Termeer, C., F. Benedix, J. Sleeman, C. Fieber, U. Voith, T. Ahrens, K. Miyake, M. Freudenberg, C. Galanos, and J.C. Simon. 2002. Oligosaccharides of hyaluronan activate dendritic cells via Toll-like Receptor 4. J. Exp. Med. 195:99–111.

Thélie, A., P. Papillier, S. Pennetier, C. Perreau, J.M. Traverso, S. Uzbekova, P. Mermillod, C. Joly, P. Humblot, and R. Dalbiès-Tran. 2007. Differential regulation of abundance and deadenylation of maternal transcripts during bovine oocyte maturation in vitro and in vivo. BMC Dev. Biol. 7:1–13.

Tsuji, S., J. Uehori, M. Matsumoto, Y. Suzuki, A. Matsuhisa, K. Toyoshima, and T. Seya. 2001. Human intelectin is a novel soluble lectin that recognizes galactofuranose in carbohydrate chains of bacterial cell wall. J. Biol. Chem. 276:23456–23463.

Turner, M.L., J.G. Cronin, G.D. Healey, and I.M. Sheldon. 2014. Epithelial and stromal cells of bovine endometrium have roles in innate immunity and initiate inflammatory responses to bacterial lipopeptides in vitro via Toll-like receptors TLR2, TLR1, and TLR6. Endocrinology 155:1453–1465.

Del vecchio, R.P., D.J. Matsas, T.J. Inzana, D.P. Sponenberg, and G.S. Lewis. 1992. Effect of intrauterine bacterial infusions and subsequent endometritis on prostaglandin-F2-Alpha metabolite concentrations in postpartum beef cows. J. Anim. Sci. 70:3158–3162.

Werner, A., V. Suthar, J. Plöntzke, and W. Heuwieser. 2012. Relationship between bacteriological findings in the second and fourth weeks postpartum and uterine infection in dairy cows considering bacteriological results. J. Dairy Sci. 95:7105–7114.

Williams, E.J., D.P. Fischer, D.E. Noakes, G.C.W. England, A. Rycroft, H. Dobson, and I.M. Sheldon. 2007. The relationship between uterine pathogen growth density and ovarian function in the postpartum dairy cow. Theriogenology 68:549–559.

Williams, E.J., D.P. Fischer, D.U. Pfeiffer, G.C.W. England, D.E. Noakes, H. Dobson, and I.M. Sheldon. 2005. Clinical evaluation of postpartum vaginal mucus reflects uterine bacterial infection and the immune response in cattle. Theriogenology 63:102–117.

Williams, E.J., K. Sibley, A.N. Miller, E.A. Lane, J. Fishwick, D.M. Nash, S. Herath, G.C.W. England, H. Dobson, and I.M. Sheldon. 2008. The effect of Escherichia coli lipopolysaccharide and tumour necrosis factor alpha on ovarian function.. Am. J. Reprod. Immunol. 60:462–73.

Wolpe, S.D., B. Sherry, D. Juers, G. Davatelis, R.W. Yurt, and A. Cerami. 1989. Identification and characterization of macrophage inflammatory protein 2. Proc. Natl. Acad. Sci. U. S. A. 86:612–6.

Wu, L., M. Einstein, W.M. Geissler, H.K. Chan, K.O. Elliston, and S. Andersson. 1993. Expression cloning and characterization of human 17β-hydroxysteroid dehydrogenase type 2, a microsomal enzyme possessing 20α-hydroxysteroid dehydrogenase activity. J. Biol. Chem. 268:12964–12969.

Yamamoto, Y., A. Kuwahara, Y. Taniguchi, M. Yamasaki, Y. Tanaka, Y. Mukai, M. Yamashita, T. Matsuzaki, T. Yasui, and M. Irahara. 2015. Tumor necrosis factor alpha inhibits ovulation and induces granulosa cell death in rat ovaries. Reprod. Med. Biol. 14:107–115.

Yao, J.Q., and F. Yu. 2011. DEB: A web interface for RNA-seq digital gene expression analysis.. Bioinformation 7:44–5.

BIOGRAPHICAL SKETCH

Rachel graduated in veterinary medicine in 2012 and during the program she was an intern at the Department of Production Animals, more specific, at the reproduction laboratory. Although her first training was with reproductive technologies for dairy cows, Rachel shifted her interest to research and started working with applied reproduction and semen preservation in horses. The project was extremely interesting and helped discover her passion for research, as well as develop laboratory skills and the ability to work in a research team. When Rachel graduated, she aim to gain practice with applied reproduction; therefore, she joined the Equicenter – Equine Hospital and Reproduction Center as an intern. After spending only a month there, she was invited to stay as a resident at the reproductive center and gladly accepted the position. The position allowed her to grow, not only as a veterinarian, but personally as well; it gave her the capability to work with a large number of animals and manage massive responsibilities. Rachel finished the residency and started working as a field consultant, but already had her mind set on increasing her knowledge of research techniques. It was at this time that she applied for the PhD scholarship through CAPES (Brazilian sponsor) and was offered a position at the UF Animal Sciences Department, obtaining her doctorate in December 2018.

Rachel's long-term goal as a veterinarian is to combine the knowledge from applied reproduction and fieldwork, with science and research in order to improve the animals' production without decreasing their life quality and well-being. During her tenure as a PhD student, her focus was on uterine disease and inflammation, and how these variables may affect the reproductive performance of dairy cows.